Biotransformation and Toxicokinetics

of Acrylamide in Humans

Dissertation zur Erlangung des

naturwissenschaftlichen Doktorgrades

der Bayerischen Julius-Maximilians-Universität Würzburg

vorgelegt von

Eva Katharina Kopp

aus Starnberg

Würzburg 2009

Eingereicht am:...
bei der Fakultät für Chemie und Pharmazie

1. Gutachter: ....
2. Gutachter: ....
der Dissertation

1. Prüfer: ....
2. Prüfer: ....
3. Prüfer: ....
des Öffentlichen Promotionskolloquiums

Tag des Öffentlichen Promotionskolloquiums: ....

Doktorurkunde ausgehändigt am: ....

TABLE OF CONTENTS

Abbreviations

AA	Acrylamide
AA-Cys	Acrylamide-*L*-cysteine adduct (*S*-(2-carbamoylethyl-*L*-cysteine)
AAMA	Mercapturic acid of acrylamide (*N*-acetyl-*S*-(2-carbamoyl-ethyl)-*L*-cysteine)
AAMA-sulfoxide	*S*-oxide of AAMA (*N*-acetyl-*S*-(2-carbamoylethyl)-*L*-cysteine-*S*-oxide)
AA-Val	Acrylamide-*L*-valine adduct (*N*-(2-carbamoylethyl)-*L*-valine)
Accy	Accuracy
ALARA	As low as reasonably achievable
amu	Atomic mass unit
APS	Ammonium persulfate
Asp	Aspartate
AUC	Area under the concentration-over-time curve
BfR	Bundesinstitut für Risikobewertung (German Federal Institute for Risk Assessment)
BGS	Bundesgesundheitssurvey (German Federal Health Survey)
BMD	Benchmark dose
BMDL10	Benchmark dose lower limit (10%)
BVL	Bundesamt für Verbraucherschutz und Lebensmittelsicherheit (German Federal Office for Consumer Protection and Food Safety)
b.w.	Body weight
CAS	Chemical Abstracts Service
CE	Collision energy
CIR	Cosmetic Ingredient Review
c_{max}	Maximum concentration
CNS	Central nervous system

COPD	Chronic obstructive pulmonary disease
COSHH	Control of Substances Hazardous to Health
cps	Counts per second
%CV	Coefficient of variation
CXP	Collision cell exit potential
CYP	Cytochrome P450
δ	Chemical shift (NMR)
d	Doublet
dd	Doublet of doublets
DNA	Deoxyribonucleic acid
DP	Declustering potential
EFSA	European Food Safety Authority
EH	Epoxide hydrolase
EPHX1	Human gene encoding for mEH
EPHX2	Human gene encoding for sEH
ESI	Electrospray ionization
EU	European Union
FAD	Flavin adenine dinucleotide
FAD-OOH	Peroxyflavin adenine dinucleotide
FAO	Food and Agriculture Organization of the United Nations
FDA	U.S. Food and Drug Administration
FMO	Flavin-containing monooxygenase
FMO2	Human gene encoding for FMO2
GA	Glycidamide
GA-Cys	Glycidamide-*L*-cysteine adduct (rac-*S*-(2-carbamoyl-2-hydroxy-ethyl)-*L*-cysteine)
GAMA	Mercapturic acid of glycidamide (rac-*N*-acetyl-*S*-(2-carbamoyl-2-hydroxyethyl)-*L*-cysteine
GA-Val	Glycidamide-*L*-valine adduct

	(rac-*N*-(2-carbamoyl-2-hydroxyethyl)-*L*-valine)
Glu	Glutamate
GSH	Glutathione
GST	Glutathione-*S*-Transferase
GSTM1	Isoenzyme of Glutathione-*S*-Transferase
GSTP1	Isoenzyme of Glutathione-*S*-Transferase
GSTT1	Isoenzyme of Glutathione-*S*-Transferase
Hb	Hemoglobin
HILIC	Hydrophilic interaction liquid chromatography
HILIC-MS/MS	Hydrophilic interaction liquid chromatography coupled to tandem mass spectrometry
His	Histidine
HPLC	High performance liquid chromatography
Hprt	Gene encoding for hypoxanthine-guanine phosphoribosyl-transferase
HSE	Health and Safety Executive (Great Britain)
i.p.	Intraperitoneal
IS	Internal standard
iso-GA-Cys	Regioisomer of GA-Cys (rac-*S*-(1-carbamoyl-2-hydroxy-ethyl)-*L*-cysteine)
iso-GAMA	Regioisomer of GAMA (rac-*N*-acetyl-*S*-(1-carbamoyl-2-hydroxy-ethyl)-*L*-cysteine)
JECFA	Joint FAO/WHO Expert Committee on Food Additives
k_e	Coefficient of elimination
KG	Körpergewicht
LC-MS/MS	Liquid chromatography coupled to tandem mass spectrometry
LD_{50}	Median lethal dose
LOAEL	Lowest observed adverse effect level
LOD	Limit of detection

LOQ	Limit of quantification
m	Multiplet
MA	Mercapturic acid
mEH	Microsomal epoxide hydrolase
[M – H⁻]	Molecular mass following negative ionization (deprotonized anion)
MOE	Margin of exposure
MRM	Multiple reaction monitoring
MS	Mass spectrometer / mass spectrometry
MSDS	Material safety data sheet
MS/MS	Tandem mass spectrometry
m/z	Mass-to-charge ratio
NADPH	Nicotinamide adenine dinucleotide phosphate
ND	Not determined
NFCS	National Food Consumption Survey
NMR	Nuclear magnetic resonance spectrometry
NOAEL	No observed adverse effect level
NQ	Not quantified
NTP	National Toxicology Program
NVS	Nationale Verzehrsstudie (German National Food Consumption Survey)
PAGE	Polyacrylamide Gel Electrophoresis
PNS	Peripheral nervous system
ppm	Parts per million
r^2	Coefficient of correlation
ref	Reference
RP	Reversed phase
RP-LC-MS/MS	Reversed phase liquid chromatography coupled to tandem mass spectrometry

s	Singlet
SAX	Strong anion exchange
SCF	Scientific Committee on Food
S.D.	Standard deviation
sEH	Soluble epoxide hydrolase
S/N	Signal-to-noise ratio
SNFA	Swedish National Food Administration
SNP	Single nucleotide polymorphism
SPE	Solid phase extraction
t	Triplet
$t_{1/2}$	Half life
T25	Dose inducing 25% tumor-incidence
TEMED	*N,N,N,N*-Tetramethylethylenediamine
t_{max}	Time of maximum concentration
TTC	Threshold of toxicological concern
Tyr	Tyrosine
U.S.	United States of America
US EPA	U.S. Environmental Protection Agency
UV	Ultra violet
v/v	Volume/volume
WHO	World Health Organization
w/w	Weight/weight

1 Introduction

Acrylamide (AA, **Figure 1**), an industrial chemical used for more than six decades is synthesized by catalytic hydration from acrylonitrile. Today, the EU-wide output of this high-volume chemical ranges from 80 000 to 100 000 t per annum. Up to 99.9 % of AA synthesized in the EU is used for the production

Figure 1
Chemical structure of acrylamide.

of polymers. Polyacrylamides have many applications, e.g. as soil stabilizers, as grouts in sewer and tunnel construction, as flocculants for water and wastewater treatment, in paper and pulp production, and in the cosmetic industry as thickeners and film-builders. Monomeric AA is commonly used in laboratories for the preparation of polyacrylamide gels applied for electrophoretic separation of proteins or nucleic acids (*1*). Whereas polyacrylamides are generally considered non-toxic (*2, 3*), monomeric AA has been identified as a cumulative neurotoxin in rodents (*4-6*) and humans (*7-10*) with a no-observed-adverse-effect-level (NOAEL) of 500 µg/kg b.w. per day (*11*). Moreover, AA

seriously affects rodent reproduction (*12-15*) at doses exceeding 2 mg/kg b.w. per day. The AA-derived epoxide metabolite glycidamide (GA, **Figure 3**) has been demonstrated to be mutagenic in Salmonella typhimurium (*16*), in somatic cells *in vitro* (*17*) and *in vivo* (*18*) as well as in germ cells *in vivo* (*19, 20*). Based on its multisite carcinogenicity in rodents (*21, 22*), AA has been classified as a probable human carcinogen (Category 2A) by the International Agency for Research on Cancer (*23, 24*).

For decades, occupational exposure was thought to be the main source of AA exposure in humans and the risk for the general public was considered negligible. However, AA and its possible effects on human health came into the focus of public attention in 1997. During the construction of the Hallandsås tunnel in Southern Sweden, the applied AA-based grout 'Rhoca-Gil' polymerized incompletely. Large amounts of monomeric AA were released into the environment. In the following weeks, high incidences of fish mortality and neurotoxic effects in cattle were observed in the vicinity of the construction site. Workers who had been exposed to high doses of AA also exhibited signs of neurotoxicity (*1, 25*). For exposure assessment, AA-hemoglobin adducts were measured in the blood of the exposed human subjects and in a control group (*26*). Unexpectedly high levels of AA-hemoglobin adducts were detected in the control group, thus confirming the unexplained detection of AA-hemoglobin adducts previously reported in a control population (*27*). The assumption that humans could be exposed to AA via the diet was verified shortly afterwards, when relatively high concentrations of AA were detected in a variety of heat-treated carbohydrate-rich foods (*28, 29*).

National authorities were alarmed by the possible consequences of a long-term exposure of the general public to a neurotoxic, possibly reprotoxic and potentially carcinogenic substance. Initial exposure assessments estimated the average daily intake from AA-levels in foods and from nutritional habits to range from 0.3 to 0.8 µg/kg b.w. (*30*). Accordingly, neurotoxic and reprotoxic effects of AA from dietary exposure alone appeared rather unlikely. However, the epoxide metabolite GA had been demonstrated to form adducts with DNA *in vitro* as well as *in vivo* (*31*). Therefore, the risk for cancer from dietary AA

became the focus of scientific research, as it is generally assumed that genotoxic carcinogens that form DNA adducts operate by linear, non-thresholded mechanisms (*32*).

Extrapolation from tumor incidences in experimental animals to human dietary AA exposure (e.g. 1.0 µg/kg b.w. per day) suggested a comparatively high cancer risk for humans ranging from 700 to 10 000 additional cancer cases in one million people (*33, 34*). However, a large number of uncertainties are involved in these linear extrapolations, as they are based on rodent studies with AA doses exceeding the calculated mean dietary exposure by several orders of magnitude (*35*).

In January 2006, at the beginning of the work on this doctoral thesis, biotransformation and toxicokinetics of AA in humans were still unknown, and existing data was scarce and inconsistent. Therefore, the aim was to evaluate the toxicokinetic properties as well as the metabolic fate of AA in humans at doses as low as the mean daily exposure from the diet, thus improving the basis for human risk assessment.

2 Background

2.1   **Physical and Chemical Characteristics of Acrylamide**

AA (2-Propenamide, C_3H_5NO, CAS# 79-06-1) is an odorless, white, crystalline solid with a molecular weight of 71.08 g/mol. It is soluble in cold and hot water (204 g/100 g water; 25 °C), ethanol, methanol and partly soluble in acetone. AA reacts vigorously with acids or bases producing ammonia salts and acrylic acid. The solid is stable at room temperature but may polymerize violently upon melting (melting point: 84.5 °C), as well as on exposure to heat, U.V. light, oxidizers or peroxides (*36*).

Radical Polymerization. Polyacrylamide gels are routinely used in laboratories as matrices for the electrophoretic separation of proteins (polyacrylamide gel electrophoresis, PAGE). Spontaneous polymerization of AA does not readily occur at room temperature, but requires the presence of catalysts, such as *N,N,N,N*-tetramethylethylenediamine (TEMED). Under anaerobic conditions and in combination with a radical initiator, e.g.

ammonium persulfate (APS), radical polymerization of AA can be started. Cross-links may

be generated by the addition of *N,N*-methylenebisacrylamide (**Figure 2**) (*37*).
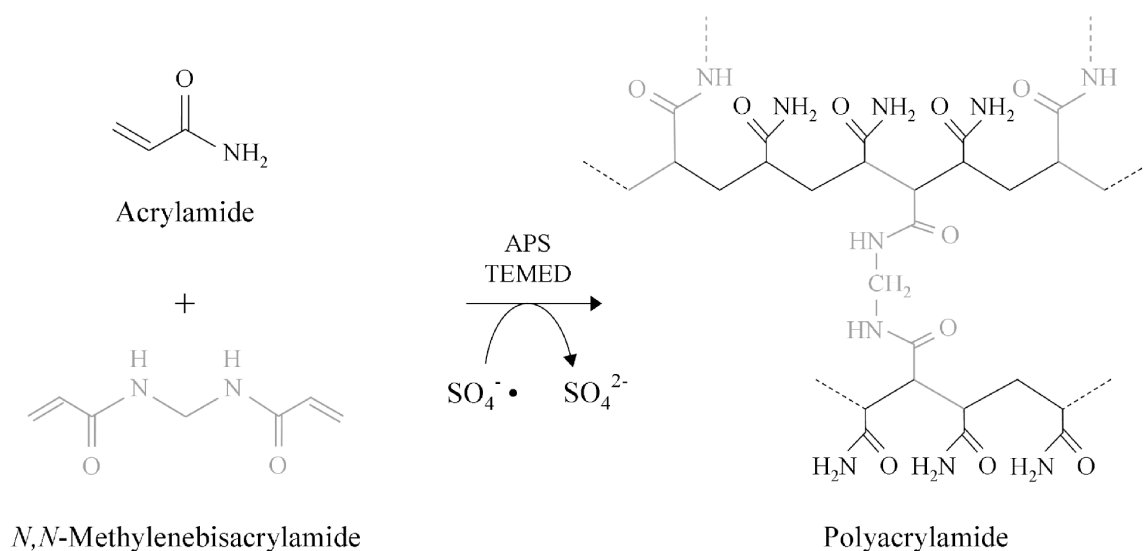
Figure 2   Mechanism of radical polymerization of acrylamide during the preparation of gels for
               polyacrylamide gel electrophoresis (PAGE).

2.2   Biotransformation and Disposition of Acrylamide

2.2.1   Biotransformation in Rodents

The metabolic conversion and elimination of AA in rodents have been thoroughly studied

after oral administration of AA in the mg/kg b.w. range (*38-41*). As a small, highly water-

soluble molecule, AA is readily absorbed and distributed throughout the organism

following oral administration (*42, 43*). According to its high reactivity towards sulfhydryl

groups, AA can directly conjugate with glutathione (GSH). After degradation by γ-

glutamyltransferase and dipeptidases and subsequent acetylation by acetyl-coenzyme A

(*44*) the resulting mercapturic acid *N*-acetyl-*S*-(2-carbamoylethyl)-*L*-cysteine (AAMA) is

excreted with urine. A major metabolic pathway in rats and mice is oxidation to the

reactive epoxide glycidamide (GA) mediated by the cytochrome P450 isoenzyme CYP 2E1 (*45*). GA can also be conjugated with glutathione and is excreted with urine after metabolic conversion to the regioisomeric mercapturic acids rac-*N*-acetyl-*S*-(2-carbamoyl-2-hydroxyethyl)-*L*-cysteine (GAMA) and rac-*N*-acetyl-*S*-(1-carbamoyl-2-hydroxyethyl)-*L*-cysteine (iso-GAMA). After administration of 50 mg/kg b.w. AA to rats, approximately 30% of the excreted metabolites are derived from GA. Following administration of the same dose to mice, 60% of all metabolites are excreted as GA-derived biotransformation products. To a small extent, GA can be detoxified via hydrolysis to glyceramide (dihydroxypropionamide) mediated by epoxide hydrolase (*39*) (**Figure 3**).

2.2.2 Biotransformation in Humans

Studies on metabolism and toxicokinetics of AA in humans, especially in the dose range similar to the daily exposure via the diet, are rare and data derived from human studies is mostly inconsistent. After administration of 0.5 – 3 mg/kg b.w. $^{13}C_3$-AA to human subjects, $^{13}C_3$-AAMA has been identified as the major urinary metabolite. Contrary to metabolism in rodents, AAMA can be oxidized to AAMA-sulfoxide in humans (*38*). The CYP 2E1 mediated epoxidation to GA (*46*) however, seems to be a minor metabolic pathway in humans. Hydrolysis to glyceramide has been reported after oral exposure to 3.0 mg/kg b.w. $^{13}C_3$-AA (*38*) (**Figure 3**).
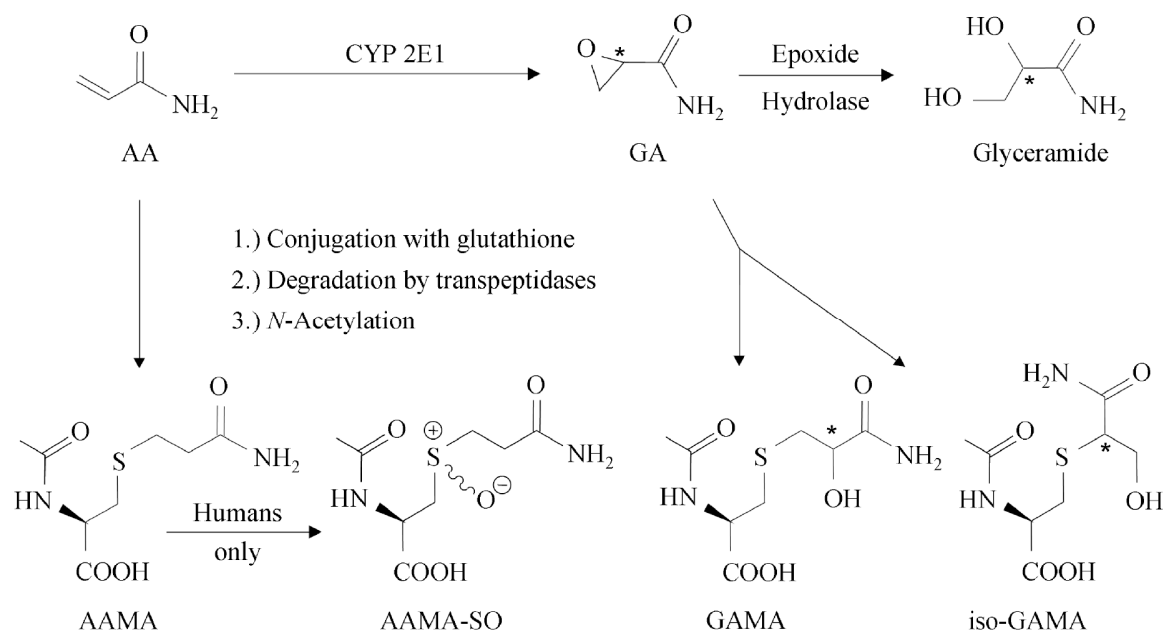
Figure 3   Biotransformation of acrylamide in rodents and humans.

2.2.3   Reactivity towards Biomacromolecules

AA is a chemically reactive α, β-unsaturated carbonyl compound. According to the Molecular Orbital Theory, α, β-unsaturated carbonyl compounds are considered to be soft electrophiles that will react most favorably with soft nucleophiles such as the sulfhydryl groups on cysteine residues in proteins (*47*). The electron deficient double-bond reacts spontaneously with nucleophiles (mostly hydroxyl-, amino-, or sulfhydryl- containing compounds) by Michael-Addition (**Figure 4**) (*48, 49*).
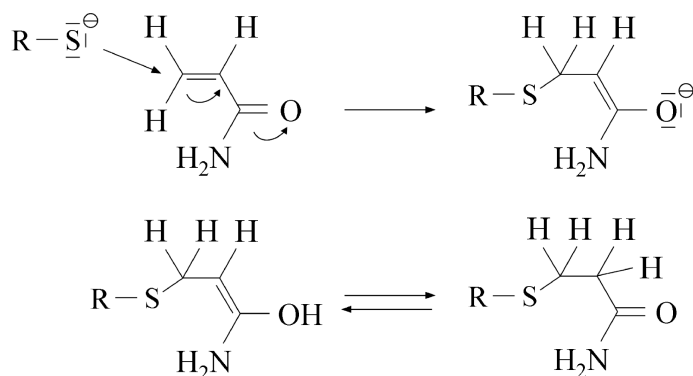
Figure 4   Michael-Addition: nucleophilic addition of an electron-rich sulfhydryl group (e.g. *L*-cysteine) to the electron-deficient α, β-unsaturated carbonyl compound acrylamide.

Michael-Addition to the thiol group of glutathione appears to be most efficient (*50*), and (after enzymatic degradation and *N*-acetylation) results in urinary excretion of mercapturic acid conjugates, thereby representing a detoxification pathway of AA (*49, 51*). AA can also bind to plasma proteins, primarily reacting with the thiol group of cysteine or the amino group of *N*-terminal valine in hemoglobin (*48, 52-54*). AA-hemoglobin adducts are essentially considered an internal dose marker for the exposure to AA. By addition to nucleophilic residues on proteins such as protamines or kinesins, AA may alter their corresponding structure and function. This mode of action has been discussed concerning AA-neurotoxicity (*55, 56*), reprotoxicity (*13*) and also potential epigenetic effects (*51*).

The epoxide metabolite GA is also a reactive electrophile that binds to glutathione (*39*) and hemoglobin (*53, 54*) according to classical nucleophilic substitution mechanisms. Compared to AA however, it acts more like a hard electrophile and therefore tends to react more readily with hard nucleophiles such as the heterocyclic amines in DNA-bases (*57*). Whereas AA only forms DNA-adducts *in vitro* (*58*), GA forms multiple adducts with DNA *in vitro* as well as *in vivo* (**Figure 5**) (*31*).
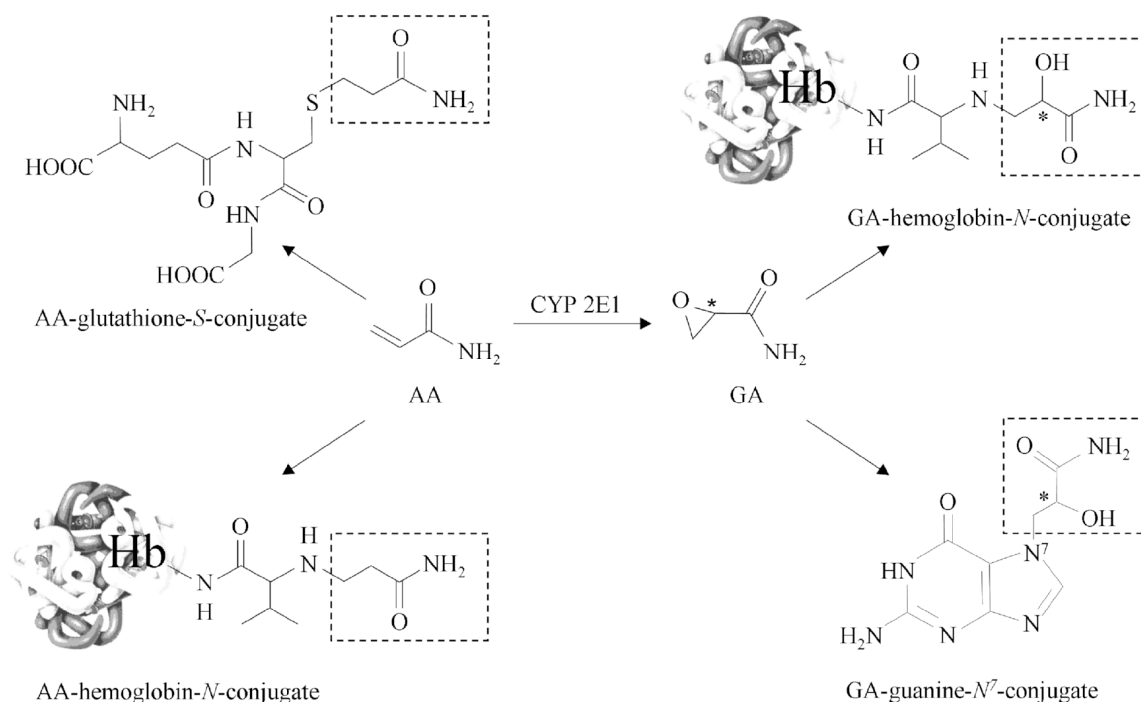
Figure 5   Schematic representation of the reactivity of acrylamide and glycidamide towards biomacromolecules. As a soft electrophile, acrylamide reacts readily with soft nucleophiles, such as glutathione, whereas glycidamide acts more like a hard electrophile and therefore forms adducts with DNA bases *in vitro* as well as *in vivo*.

2.2.4   Enzymes involved in Acrylamide Metabolism: Function, Mechanism and Polymorphism

In order to facilitate excretion via urine or bile and to prevent accumulation, xenobiotics are subjected to metabolic conversion. Basically, biotransformation of exogenous compounds can be divided into two major classes of metabolic reactions. During Phase I, substances are functionalized mainly by insertion of oxygen via oxidoreductases such as Cytochrome P450 monooxygenases (CYP) and flavin-dependent monooxygenases (FMO). The obtained redox reaction products are generally less lipophilic than the parent compounds and thus easier to excrete with urine. Additionally, many products are good substrates for Phase II reactions. Phase II reactions are characterized by conjugation of the

functionalized compound to hydrophilic endogenous substances such as GSH, glucuronic acid or sulfate, mediated by glutathione-*S*-transferases (GST), UDP-glucuronyl-transferases and sulfotransferases. The net result is an accelerated removal of the xenobiotic and its metabolites from the body. However, these metabolic reactions can lead to reactive and in some cases toxic metabolites as is the case with the CYP 2E1 mediated oxidation of AA to the mutagenic epoxide GA. **Figure 6** summarizes the detoxification/toxification pathways of AA following oral uptake with respect to the most important enzymes involved in AA biotransformation.
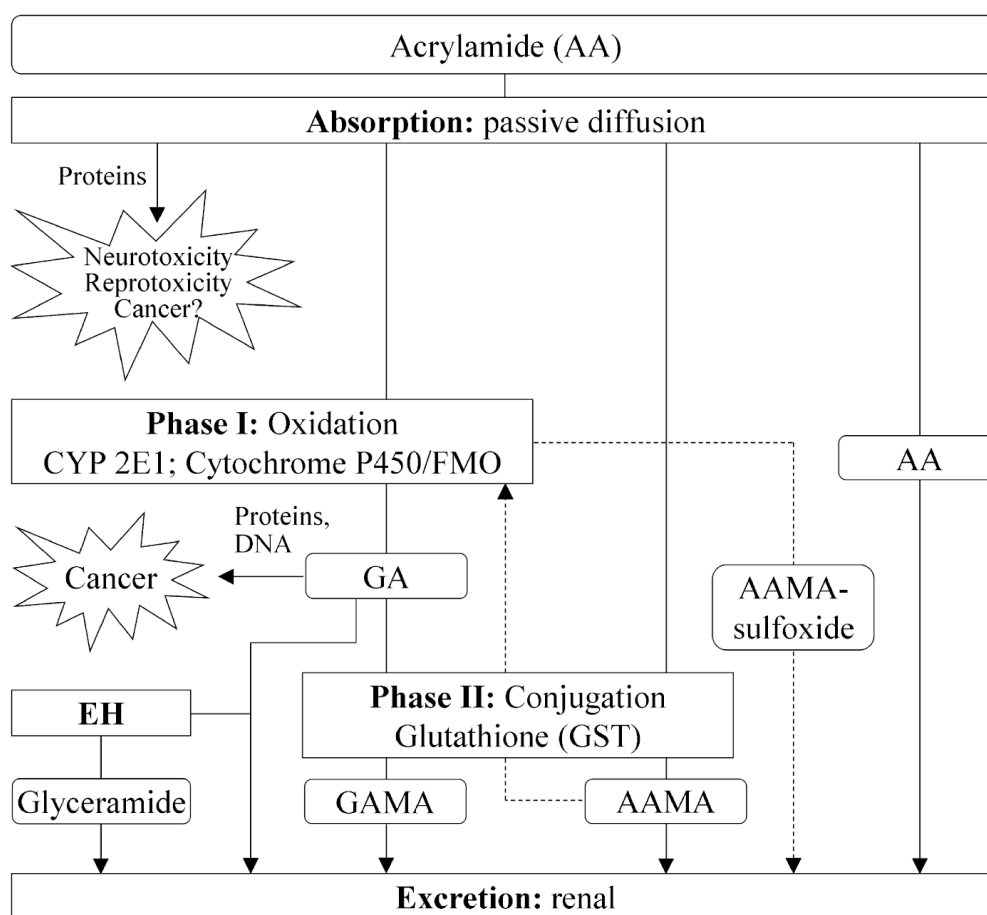
Figure 6   Schematic representation of biotransformation pathways and toxicity of acrylamide following oral administration.

Cytochrome P450. Cytochrome P540 monooxygenases (CYP) represent the largest and most important group of metabolizing enzymes in virtually all life forms. Up to now, 18 CYP-families and more than 60 isoforms have been characterized in humans. Cytochrome P450 enzymes are involved in synthesis of steroid-hormones, in oxidation of fatty acids, and in Phase I metabolism of numerous endogenous substances as well as xenobiotics. The membrane bound enzymes are mainly located in the smooth endoplasmatic reticulum membrane and some forms are found in mitochondria. They are expressed in practically all tissues with highest levels in the liver, significant activities in the small intestine wall and the lungs, and smaller activity in brain and skin (*59*).

The cytochrome P450 system consists of two coupled enzymes, the flavoprotein NADPH-cytochrome P540 reductase, which uses NADPH as cofactor and acts as an electron donor, and the hemoprotein cytochrome P450, consisting of a variable apoprotein and a heme moiety (i.e. iron-protoporphyrin IX) as prosthetic group. Oxidation of xenobiotics proceeds via complex mechanisms, which involve binding of the substrate to cytochrome P450, binding of molecular oxygen to the heme moiety, and several electron transfer steps. In short, the monooxygenase reaction can be summarized as cleavage of O_2 and insertion of one oxygen atom into the substrate XH:

$$O_2 + XH + 2e^- + 2H^+ \longrightarrow XOH + H_2O$$

or

$$O_2 + XH + NADPH + H^+ \longrightarrow XOH + H_2O + NADP^+$$
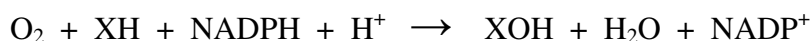
CYP 2E1. The cytochrome P450 isoenzyme CYP 2E1 is constitutively expressed in the liver and in many other tissues and may be induced by acetone, isoniazid and ethanol. CYP 2E1 metabolizes a variety of substances, in particular small compounds with a molecular weight below 100 amu (*60*). Exogenous substrates include industrial solvents (e.g. carbon tetrachloride, chloroform, vinyl chloride), alcohols (e.g. ethanol, methanol, *n*-propanol) and drugs (e.g. acetaminophen and phenobarbital) (*61*).

Physiologically, CYP 2E1 is involved in metabolism of endogenous compounds such as fatty acids and ketone bodies (postulated to be an emergency gluconeogenesis pathway during fasting) (*62*). CYP 2E1 activity can be inhibited by a number of compounds, such as the garlic constituent diallyl sulfide (*63*). Saturation of CYP 2E1 activity has been observed in mice and rats following administration of AA at doses exceeding 5 mg/kg b.w. (*54, 64-66*).

CYP 2E1 catalyzes the oxygenation of C=C bonds in alkenyl moieties, thus yielding primarily epoxides (*59*). As shown in **Figure 7**, the oxygen atom in the CYP-oxene complex binds covalently to one of the two target carbon atoms to form the two transient and interconverting intermediates. Formation of the second C–O bond generates the epoxide and liberates the (Fe^{3+})-CYP 2E1.
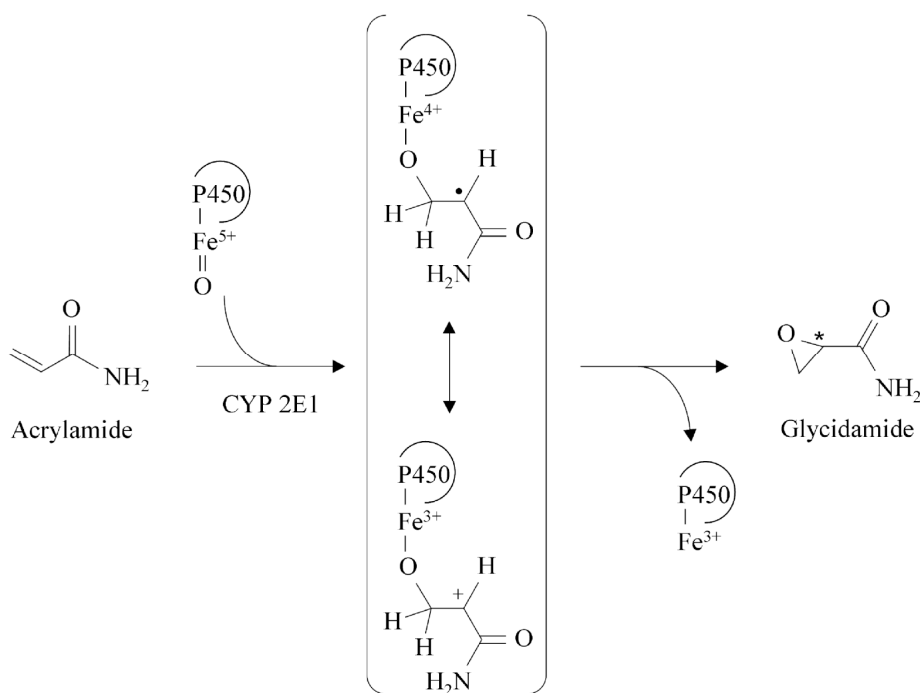
Figure 7   CYP 2E1 mediated oxygenation of acrylamide (general mechanism adapted from Testa et al., **2007** (*59*)).

Significant inter-ethnic differences exist in CYP 2E1 polymorphism (*61, 67*), but there is no clear evidence that any of these polymorphisms are related to altered function *in vivo*. The incidence of these polymorphisms has been investigated in relation to different types of cancer, alcoholic liver disease, and alcoholism. However, results are controversial and no firm conclusions can be drawn (*67-69*). An even more pronounced effect on CYP 2E1 activity has been linked to physiological and pathophysiological conditions, such as starvation (*70*), diabetes (*71*) or obesity (*71, 72*).

Until now, no significant correlation was observed concerning CYP 2E1 polymorphism and the extent of AA biotransformation to the mutagenic epoxide GA (*73*). Possible interindividual differences in the extent of CYP 2E1 mediated epoxidation of AA in humans may therefore rather be related to exogenous influences than to genetic polymorphism.

Flavin-Containing Monooxygenases. Flavin-containing monooxygenases (FMO) are membrane-bound enzymes located in the endoplasmatic reticulum with highest expression levels in the liver but also substantial activities in lungs, kidneys, and small intestine. FMOs catalyze some of the reactions mediated by CYPs, sometimes in parallel, often yielding the same metabolites. They are flavin adenine dinucleotide (FAD) containing flavoproteins without a heme moiety. In contrast to CYPs, they receive their reducing equivalents directly from their cofactor NADPH without an electron-transfer chain. FMOs show relatively low substrate specificity and preferentially oxygenize soft nucleophiles such as basic amines and sulfides as well as selenium- or phosphor-containing substrates (*59, 74*).

Oxygenation of the sulfur in AAMA may be catalyzed by CYP as well as by FMO. The observed lack of AAMA-sulfoxide in rodents following administration of AA however, may be explained by notable species differences in enzyme expression/activity and substrate specificity reported for FMO (*75*) as well as for CYP (*76*).

The mechanism of FMO mediated oxygenation of soft nucleophiles is represented in **Figure 8**. In the first step of the catalytic cycle, FAD undergoes 2-electron reduction by NADPH. The reduced flavin reacts rapidly with molecular oxygen to form the peroxyflavin. This activated state is considered to be the predominant form of the enzyme to exist in the cell. In contrast to the CYP monooxygenase system, binding of the substrate to FMO is not required and has no effect on the reaction velocity. As a result, any chemical containing a soft nucleophile that gains access to the peroxyflavin intermediate is a potential substrate (*77*). The nucleophilic attack on FAD-OOH by the substrate results in one atom of molecular oxygen to be transferred to the substrate and one atom to form water (*74, 78*).
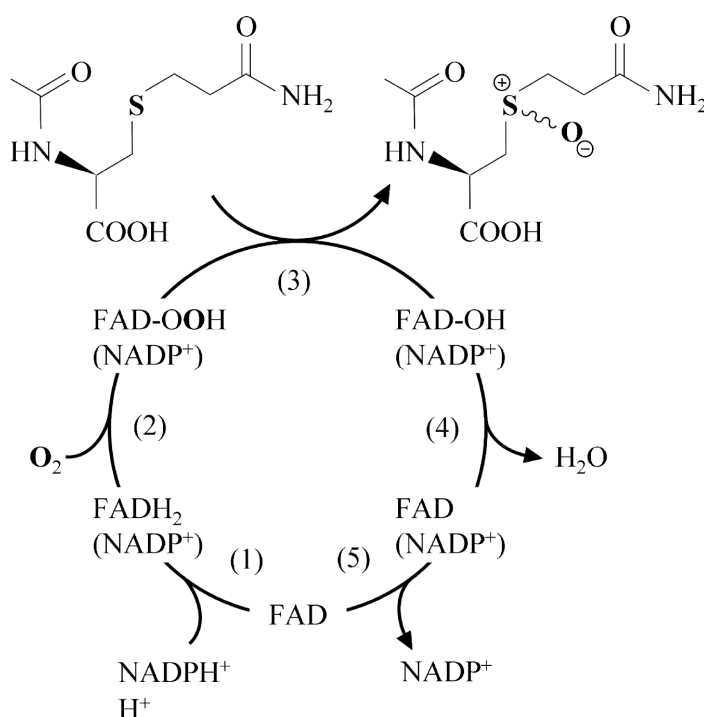
Figure 8   Schematic representation of the catalytic cycle of FMO during sulfoxidation of AAMA. (general mechanism adapted from Ziegler et al., **1993** (*75*)).

Five isoforms of FMO (FMO1 – FMO5) have been detected in humans. Whereas FMO1 is expressed primarily in fetal liver, adult kidney and intestine, FMO2 is the major FMO isoenzyme expressed in lungs of most mammalian species, except of most humans. FMO3

is the dominant isoenzyme in adult human liver and FMO4 and FMO5 are thought to be of minor relevance concerning metabolism of exogenous chemicals due to their limited substrate specificity and relatively low expression levels in most tissues (*74*). FMO1, FMO2 and FMO3 exhibit genetic polymorphisms (mostly single nucleotide polymorphisms (SNP)) in humans. For example, a SNP in the *FMO2* gene results in absence of functional FMO2 in Caucasians and Asians. Functional *FMO2* alleles could only be determined with frequencies ≤13% and ≤7% in African-Americans and Hispanic-Americans, respectively (*76*). Genetic polymorphism leading to FMO3 deficiency results in a disease known as trimethylaminuria or 'fish-odor syndrome' caused by absent metabolism of endogenous trimethylamine (*77*). Possible consequences of FMO polymorphisms concerning the extent of *S*-oxidation of AAMA during AA metabolism in humans have not been elucidated yet.

Glutathione-S-Transferases. The main route of detoxification of AA and GA is conjugation to the tripeptide glutathione (*γ*-glutamyl-cysteinyl-glycine, GSH). Due to their reactivity towards sulfhydryl groups, AA and GA may readily react with GSH directly or mediated by glutathione-*S*-transferase (GST). GSTs are a large and diverse group of enzymes present in the cytoplasm, in the endoplasmatic reticulum, in mitochondria, and in peroxisomes (*79*). GSH and the GSTs represent the major chemical protection against reactive xenobiotics and reactive intermediates produced during biotransformation of endogenous and exogenous compounds (e.g. products of lipid peroxidation, reactive oxygen species and radiation damage) (*79, 80*).

A main element in the catalytic mechanism of GSTs is the acidity of the thiol group in GSH, which is increased significantly by assistance of a neighboring tyrosine residue via donation of an H-bond (**Figure 9**). This increased thiol acidity is translated into increased nucleophilicity of the respective thiolate anion towards reactive electrophiles. Additionally, the reactivity of the substrate is increased by polarization of its electrophilic center, thus facilitating nucleophilic addition of GSH.
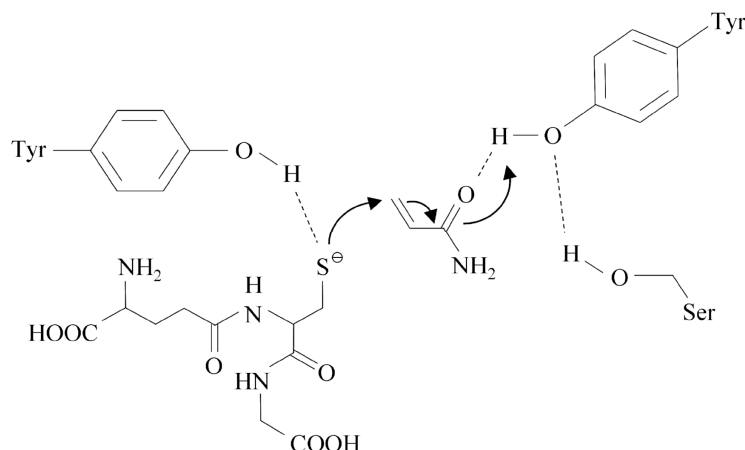
Figure 9 Simplified representation of GST mediated nucleophilic addition of GSH to acrylamide (general mechanism adapted from Testa et al, **2008** (*79*)).

Once formed, GSH conjugates are extensively processed in the body through stepwise enzymatic degradation. The first step is cleavage of the glutamyl residue by *γ*-glutamyltranspeptidase (**Figure 10**). *γ*-Glutamyltranspeptidases are membranal enzymes present in the liver, kidneys and other organs. The resulting cysteinylglycine-*S*-conjugate loses its glycyl moiety by action of various dipeptidases. Subsequently, the cysteine-*S*-conjugate is *N*-acetylated by cysteine-*S*-conjugate *N*-acetyltransferase, a microsomal enzyme mainly present in the kidney. The resulting mercapturic acid (MA) is a major urinary excretion product of the GSH biotransformation pathway. *N*-acetylation of cysteine conjugates is reversible due to the involvement of various amidases (*79, 81*).

In humans, the isoenzymes GSTT1, GSTM1 and GSTP1 are polymorphic, with decreased (heterozygotes) or absent (homozygotes) enzyme activity in individuals bearing the null genotype. Absence of GSTM1 activity ($35 - 62\%$ in Caucasians (*76*)), for example, has been associated with an increased risk for cancer in smokers (*82, 83*). Additionally, species differences in GST activity have been reported. For instance, mice are much less susceptible to adverse effects (i.e. liver-tumors) mediated by aflatoxin B_1 compared to rats. Much higher levels of aflatoxin B_1-GSH-conjugates were detected in mice compared to rats and humans, indicating a more effective detoxification of this carcinogenic compound (*84*).
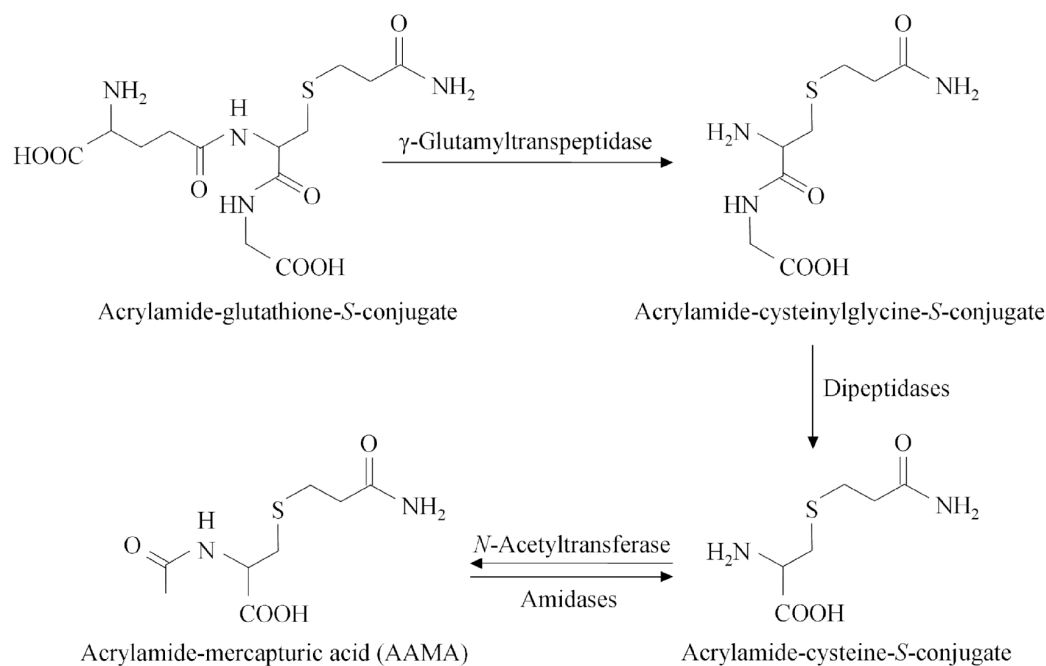
Figure 10   Metabolic processing of the acrylamide-glutathione-*S*-conjugate to the urinary excreted mercapturic acid AAMA.

No significant correlations were detected in *in vitro* studies concerning the effectiveness of different GST isoenzymes (GSTT1, GSTM1 and GSTP1) and the influence of polymorphisms on the detoxification of AA and GA in human blood. Conjugation of AA and GA to GSH in blood therefore seems to be more or less independent of GST, indicating a nonenzymatic mechanism for GSH conjugation (*85*). However, in a recent *in vivo* study in humans, significantly increased background concentrations of both, AA-Hb and GA-Hb were observed for individuals with the GSTT1 null genotype and the GSTM1 null genotype, respectively (*73*).

Epoxide Hydrolases. The mutagenic epoxide GA has been reported to be detoxified by hydrolysis to the diol compound glyceramide via epoxide hydrolase (*38, 39*). Epoxide hydrolases (EH) are a class of enzymes that cleave oxiran derivatives to yield the corresponding diols. They can be diverted into membrane-bound microsomal EH (mEH),

mainly located in the liver and encoded for by the human gene *EPHX1*, and soluble EH (sEH), located in the liver, lung and placenta, encoded for by human *EPHX2* (*86*). EHs play important physiological roles, as e.g., vitamin K_1 oxide reductase or cholesterol epoxide hydrolase (*86, 87*). Additionally, mEHs are of utmost significance in molecular toxicology, being involved in the detoxification of reactive arene oxides (*88*). The overall reaction catalyzed by EHs is the addition of an H_2O molecule to an epoxide. In detail, the reaction involves a catalytic triad consisting of a nucleophile (Asp226/mEH, Asp333/sEH), a general base (His431/mEH, His523/sEH) and a charge relay acid (Glu376/mEH, Asp495/sEH). First, an ester intermediate is formed by nucleophilic attack of aspartate at the oxiran ring (**Figure 11**). Meanwhile, histidine and an acidic amino acid (Asp or Glu) build a charge relay system that activates a water molecule via proton abstraction. Finally, the ester intermediate is hydrolyzed, yielding a diol. Additional essential participants in this catalytic reaction are two tyrosines (Tyr299 + Tyr374/mEH, Tyr382 + Tyr465/sEH) that form hydrogen bonds to the oxygen atom in the epoxide ring of the substrate, thereby increasing its electrophilicity and optimizing its position for the nucleophilic attack of aspartate (*86-88*).

It has been shown, that the activity of the enzyme mEH is affected by two polymorphisms. A substitution of Tyr113 to His113 in exon 3 corresponds to a 40% decrease in enzyme activity, whereas a substitution of His139 to Arg139 in exon 4 corresponds to a 25% increase in enzyme activity (*89*). Polymorphisms of EH have been associated with pre-eclampsia in pregnant women (*90*), elevated risk for a whole range of different cancer types (e.g. lung cancer and ovarian cancer) (*91, 92*), and COPD (chronic obstructive pulmonary disease) (*93*).

However, in an *in vitro* study in human blood, no significant influence of EH on the detoxification rate determined via measurements of GA-hemoglobin adducts was observed (*85*). Also, attempts to determine the influence of the different genotypes of mEH on the ratio GA-Hb/AA-Hb in humans yielded inconsistent results (*73*).
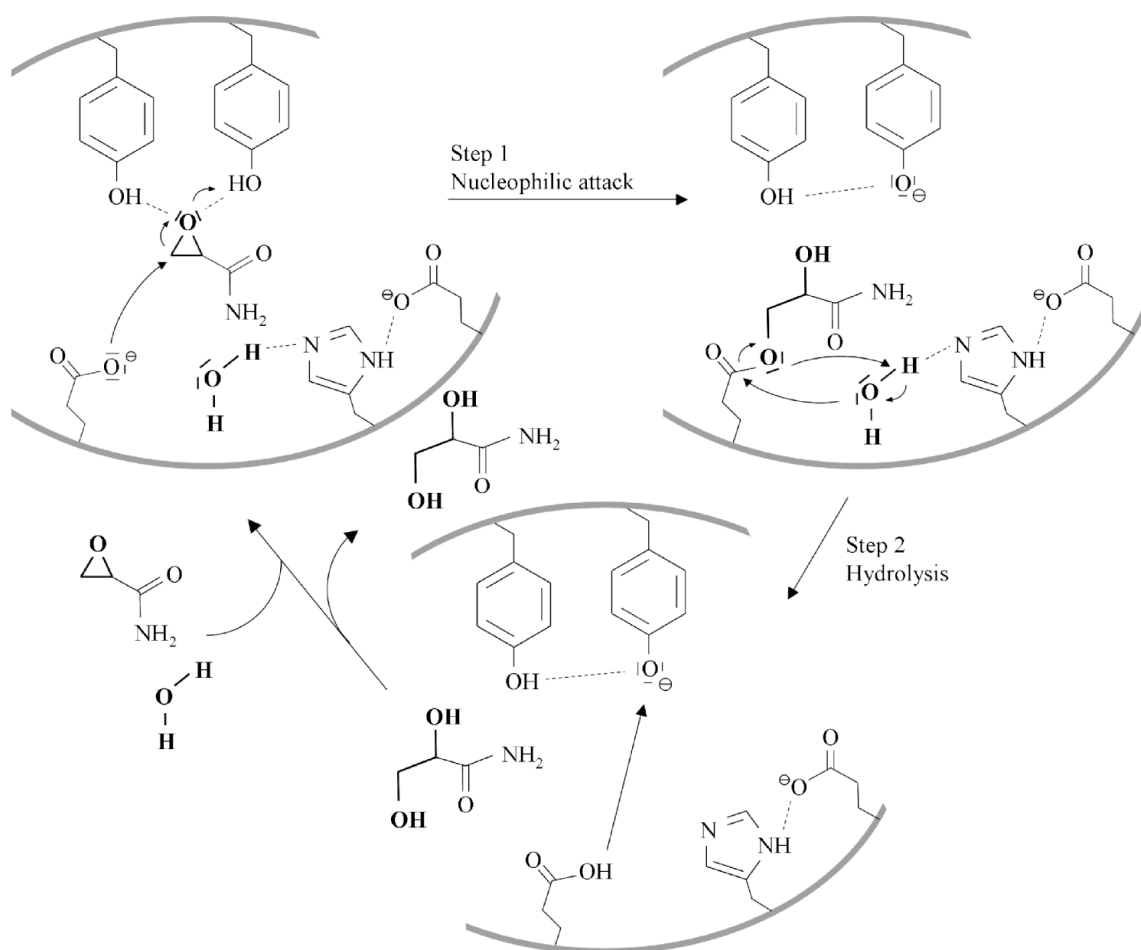
Figure 11   Enzymatic mechanism of epoxide hydrolase mediated hydrolysis of glycidamide to glyceramide (general mechanism adapted from Arand et al., **2005** (*88*)).

2.3   Acrylamide Toxicity

2.3.1   Acute Toxicity

Upon contact, inhalation or ingestion, AA causes irritation of the skin, eye irritation, irritation of the respiratory tract and mucous membranes as well as irritation of the digestive tract including nausea and vomiting. AA can be absorbed through the skin. It affects the central nervous system as well as the peripheral nervous system. Symptoms of acute intoxication include changes in motor activity, numbness, paresthesia, ataxia, tremor, convulsions, confusion, memory loss and hallucinations (*36*). The LD_{50} values for acute toxicity following oral and dermal exposure in rodents and rabbits are summarized in **Table 1.**

Table 1
LD_{50} values for acute toxicity of acrylamide in rats, mice and rabbits.

Species	LD_{50} (mg/kg b.w.) *oral*	LD_{50} (mg/kg b.w.) *dermal*
Mouse	107	-
Rat	124	400
Rabbit	150	1680

2.3.2   Neurotoxicity

AA is a cumulative neurotoxin in rodents as well as in humans (*94*). So far, neurotoxicity is the only adverse effect of AA confirmed in humans occupationally exposed to AA. General symptoms of AA neurotoxicity in humans are a characteristic skin peeling of the hands followed by ataxia, skeletal muscle weakness and numbness of hands and feet

(*8, 26*). In experimental animals, intoxication at 5 – 50 mg/kg b.w. per day produced neurological deficits such as hind-limb foot splay, ataxia (gait abnormalities), and skeletal muscle weakness (decreased fore- and hind-limb grip strength) (*11, 95*). Experimental AA intoxication is also associated with neurogenic autonomic dysfunction, for example urinary retention, baroreceptor dysfunction, and impaired vasomotor control (*96, 97*). On the basis of a subchronic (90 days exposure) study of peripheral nerve damage in rats, a NOAEL of 0.5 mg/kg b.w. has been established (*11*). In double-blind studies in factory workers, no neurotoxicity was found in workers exposed to less than 3.0 mg/kg b.w. per day as determined by biomonitoring (*98*).

The mother compound AA itself is considered responsible for neurological symptoms, although an additive effect of GA has also been discussed (*99*). AA neurotoxicity has been characterized as central-peripheral distal axonopathy (*4, 5*). The primary effect however, seems to be nerve terminal damage which subsequently leads to synaptic dysfunction. Degeneration of axons in the central nervous system (CNS) as well as the peripheral nervous system (PNS) is considered a consequence of these primary lesions (*7, 100*). Also, neurotoxicity seems to be exposure-rate dependent. Acute high dose intoxication results in mainly CNS damage (neurodegeneration of cerebellar Purkinje cells and terminalopathy), whereas lower dose-rate exposure produces axon degeneration in PNS and CNS (*100*). There is some evidence, that neurotoxicity is mediated via direct reaction of AA with nucleophilic sites at the nerve terminal, e.g. regulatory nerve terminal proteins or microtubule-based motor proteins, thus inhibiting neurotransmission (*7, 55, 101, 102*).

2.3.3   Reproductive Toxicity

AA has been extensively tested in rodents for effects on a variety of reproductive parameters. Whereas females seem resistant to the reproductive effects of AA, male reproductive capacity is strongly affected by AA (*15, 103, 104*). Observed effects include dominant lethal mutations in germ cells, degeneration of testicular epithelial tissue, and impaired fertilization (*13, 105*). As a result, reduced litter sizes and decreased body

weights were observed in the pups. A direct correlation between neurotoxicity and male reproductive effect has been proposed (*15, 106*). In experimental animals, a NOAEL of 2.0 mg/kg b.w. has been determined for reproductive toxicity (*12*).

It has been demonstrated that reproductive toxicity is not only induced by AA, but also by GA, which exerts clastogenic effects on spermatids (*20, 105, 107*). Thus, the fundamental mechanisms of action for AA reprotoxicity appear to be

(1) AA and/or GA binding to spermatid protamines, resulting in dominant lethality (from induced clastogenesis) and effects on sperm morphology,

(2) AA binding to the motor proteins kinesin and dyneine, leading to distal axonopathy, and therefore hindlimb weakness, resulting in adverse effects on mating, and

(3) kinesin inhibition during spermiogenesis by direct interaction with AA or GA leading to decreased sperm motility (*13, 56*).

2.3.4   Carcinogenicity

Cancer in Humans. There are a number of epidemiological studies concerning the possible carcinogenicity of AA in humans. Two different cohorts of occupationally exposed factory workers have been studied over several decades (*108-112*). Although workers were exposed to comparably high amounts of AA for many years, no statistically significant excess mortality due to cancer of any specific site was reported.

To evaluate possible cancer risk from dietary AA, several cohort cancer incidence studies with unintentionally exposed human subjects have been conducted (*113-119*). Most studies revealed no significant association between levels of dietary AA and cancer. Only weak associations were found between dietary AA and renal cell cancer risk (*118*). Additionally, some association was found between AA-hemoglobin adduct levels and incidence of

estrogen receptor positive breast cancer (*117*) as well as between AA intake and other endocrine tumors (endometrial and ovarian) in postmenopausal women (*120*).

However, results of these studies should be interpreted with caution, as these studies, as with most epidemiological studies, are limited by size of cohort, poor characterization of exposures, confounding factors (e.g. cigarette smoke or additional exposure to other carcinogens), and limited statistical power to detect small increases in a particular response.

Cancer in Rodents. AA treatment in both rats and mice resulted in an organ-specific tumorigenicity. Administration of AA via different routes, e.g. orally, topically or systemically, increased the incidence of lung and skin adenomas and carcinomas in mice (*121*). Treatment of Fischer 344 rats with AA at levels of 0.1 – 2.0 mg/kg b.w. per day for two years induced scrotal mesotheliomas, thyroid adenomas and/or adenocarcinomas, mammary gland tumors, uterine adenocarcinomas, clitoral gland adenomas, and oral papillomas (*21, 22*).

The sites for cancer found in rats suggest a hormone-related cause and disruption of hormone levels or activity by AA has been proposed as the underlying mechanism for some of the tumors observed. However, the available data supporting such a mode of action is limited or inadequate. Moreover, results from rats may not be transferred to humans directly, especially as rats lack circulating proteins that bind hormones and act as a hormone reservoir. Thus, rats are substantially more sensitive to perturbations in hormone physiology than humans (*122, 123*). In a recent study in male Fischer 344 rats, no evidence could be found for hormone dysregulation as a possible mechanism for AA-induced thyroid cancer, suggesting that the carcinogenic effects of AA are based on its genotoxicity rather than endocrine disruption (*124*). However, additional data are needed to resolve why mostly hormonally responsive tissues were susceptible to AA carcinogenicity in the chronic rat bioassays, whereas GA-DNA adducts have been observed in a much wider array of tissues including liver, lung and kidneys (*125*).

Genotoxicity of Acrylamide. AA has been shown to be a clastogenic agent, inducing chromosomal aberrations, micronuclei, sister chromatid exchanges, polyploidy, aneuploidy and other mitotic disturbances in mammalian cells in the absence of metabolic activation (*126-129*). AA induces somatic and male sperm cell chromosomal aberrations as measured in the mouse bone marrow micronucleus assay, dominant lethal test, mouse spot test, and heritable translocation test (reviewed in (*130*)). It produces chromosome damage in somatic cells. No apparent gene mutations were observed *in vitro* as determined in bacterial as well as mammalian cell mutagenicity assays (*130, 131*). The epoxide GA however, was positive in the Salmonella typhimurium mutagenicity test (Ames Test) with and without metabolic activation (*16*). Mutation assays *in vivo* have demonstrated that oral administration of AA or GA increases mutant frequencies in lymphocyte *Hprt* and liver *cII* genes of adult Big Blue mice by inducing primarily G:C → T:A transversions (*18*).

Mechanisms of Acrylamide Carcinogenicity: DNA-adducts. Formation of DNA-adducts is a key element in the multi-stage process of carcinogenesis (*32*). DNA-adducts that are not repaired by DNA repair mechanisms may cause mispairing during DNA replication, thus giving rise to mutations. Specific mutations in crucial genes, e.g. oncogenes or tumor suppressor genes, may eventually trigger tumorigenesis.

In vitro incubation of AA with calf thymus DNA over a prolonged period (40 days) showed a slow direct reactivity of AA towards DNA (*58*). The resulting DNA-alkylation products in order of decreasing abundance were *N1*-(2-carboxyethyl)-adenine, *N3*-(2-carboxyethyl)-cytosine, *N7*-(carbamoylethyl)-guanine, *N6*-(2-carboxyethyl)-adenine, and *N1*-(2-carboxyethyl)-guanine (**Figure 12**). *In vitro* incubation of AA with DNA in the presence of *S9* liver extracts (*31*) as well as *in vivo* treatment of mice and rats with AA, predominantly induced formation of *N7*-(2-carbamoyl-2-hydroxyethyl)-guanine (*N7*-GA-Gua), a GA derived DNA-adduct (*31, 65*) which may lead to G:C → T:A transversions. Additionally, *N3*-(2-cabamoyl-2-hydroxyethyl)-adenine and *N1*-(2-carboxy-2-hydroxy-ethyl)-adenine were identified as minor adducts in mice treated with a single i.p. dose of

AA (**Figure 12**). No adducts derived from AA directly were observed *in vivo*. Consistent with the pervasive presence of AA in the treated animals (*43*), GA-DNA-adducts were evenly distributed in different organs, i.e. liver, lung and kidney (*31, 65, 132*). This is in line with the low molecular weight and high water solubility of AA and GA, which allows them to pass easily through various biological membranes.

Mechanisms of Acrylamide Carcinogenicity: Non-Genotoxic Effects. An alternative mechanism discussed for carcinogenicity mediated by AA and GA, is binding to kinesin proteins of the mitotic/meiotic spindle, thus modifying chromosome segregation and polarization (*56*). In addition, AA was found to produce oxidative stress in rodents (*133*). Reactive oxygen species can lead to mutagenic oxidative DNA lesions and strand breaks (*134*). Deletions observed in mouse lymphoma cells following AA treatment were similar to those observed by compounds causing oxidative damage (*131*). It therefore appears likely, that the mode of action for AA is a combination of DNA damage, interference with mitosis and meiosis, and oxidative stress.
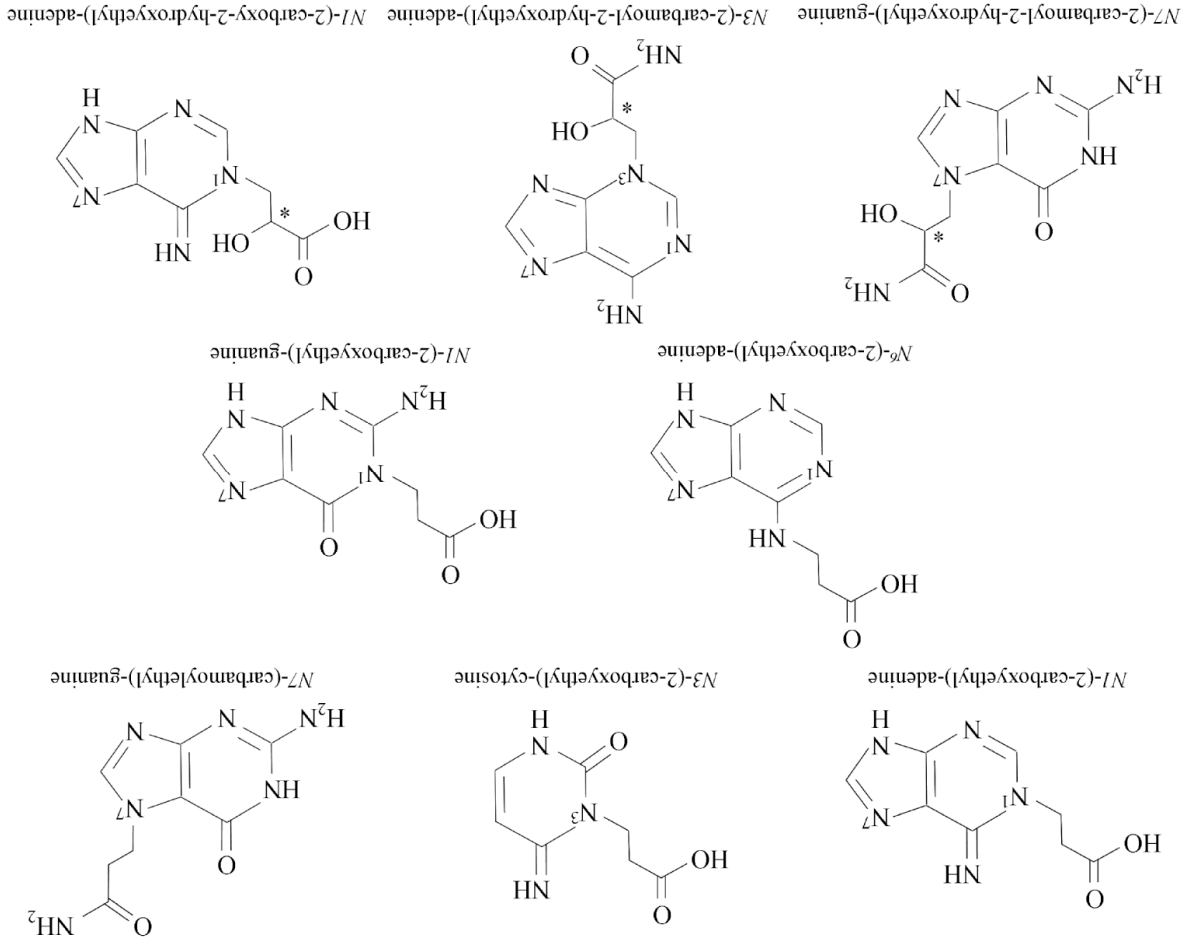
Figure 12 Chemical structures of the major DNA-adducts of acrylamide (*in vitro*) and glycidamide (*in vitro* and *in vivo*). *N7*-(2-carbamoyl-2-hydroxyethyl)-guanine (*N7*-GA-Gua) is the predominant glycidamide-derived DNA adduct.

2.4   Human Exposure to Acrylamide

Humans can be exposed to AA via oral or inhalational routes and also by dermal absorption (*12*). Whereas exposure to AA residues in drinking water seems negligible (maximum: 0.25 µg AA in 2 L drinking water per day), exposures from water, cosmetics, diet, occupational exposure and cigarette smoke are cumulative (*1*). AA can pass the transplacental barrier (*135, 136*), and AA-hemoglobin adducts were detected in neonatal blood (*137*). Additionally, infants may be exposed to AA due to the carry-over into breast milk (*138*). Latest research suggested that AA may also be formed *in vivo* (*139*).

2.4.1   Biomarkers of Exposure

Hemoglobin Adducts of Acrylamide and Glycidamide. Due to their reactivity towards biomacromolecules, AA and GA readily conjugate with hemoglobin (Hb) in red blood cells (*53, 54*). Adducts formed by reaction with the *N*-terminal amino acid *L*-valine (**Figure 13**) can be measured via GC-MS or LC-MS/MS after modified Edman degradation (*53, 140, 141*).

N-(2-carbamoylethyl)-*L*-valine   *N*-(2-carbamoyl-2-hydroxyethyl)-*L*-valine
(AA-Val)   (GA-Val)
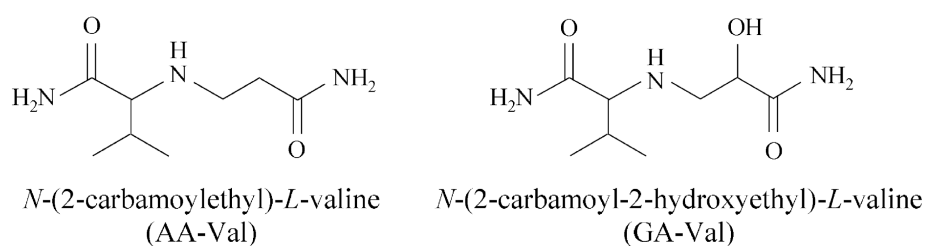
Figure 13   Valine adducts of acrylamide and glycidamide derived from the respective Hb-adducts following enzymatic hydrolysis or Edman degradation.

Since hemoglobin has a long and well-defined life-span *in vivo* (about 65 days in rats and 120 days in man (*98*)), the Hb-adduct levels of AA and GA are convenient parameters for long-term exposure to AA. The Hb-adduct approach has been used during the last 15 years for the biomonitoring of AA exposure in factory workers (*8, 27, 142*). Initially, Hb-adducts were mainly used for correlation of AA exposure to signs of neurotoxicity. By monitoring the internal dose of AA via Hb-adduct measurements however, the possible role of diet as a source of AA in otherwise non-exposed control groups was discussed for the first time (*25, 143*). Results from a number of biomonotoring studies in humans with respect to occupational exposure to AA as well as smoking status are summarized in **Table 2**.

Hb-adducts have proven useful in monitoring exposure to genotoxic agents, in order to determine the dose of toxic compound which escapes detoxification and reaches its target protein or DNA (*144*). GA-hemoglobin adducts are considered as biomarkers for DNA-adduct formation, as a linear correlation between these two markers was determined *in vivo* in mice and rats. AA-hemoglobin adducts on the other hand, are significantly correlated to the urinary excretion of the mercapturic acid of AA (AAMA) and are therefore considered as a measure for the internal dose of AA (*41*).

Urinary Biomarkers. Measurement of metabolites excreted with urine is a convenient, non-invasive method for biomonitoring exposure to xenobiotics. In rodents as well as in humans, AA is metabolized via conjugation to glutathione, with the resulting mercapturic acids (MA) excreted in urine. Another metabolic pathway of toxicological interest is epoxidation to the mutagenic metabolite GA, which is also excreted as mercapturic acid (**Chapter 2.2**). A number of studies analyzing AAMA and GAMA in human urine and correlating the mercapturic acid excretion to AA intake via diet or smoking have been performed over the last years (*38, 145-152*). Quantification of these urinary biomarkers from spot-urine samples however, is only suitable for short-term biomonitoring, as these compounds are excreted quite rapidly (*153, 154*).

Table 2
Levels of hemoglobin adducts of acrylamide and glycidamide in humans with occupational exposure to acrylamide as well as in smokers and nonsmokers.

Exposure	AA-Val (pmol/g globin)	GA-Val (pmol/g globin)	Reference
Control (n = 10)	< 10	$< 10 \times 10^3$	(*142*)
Exposed workers [a, d] (n = 41)	$300 - 34 \times 10^3$	$1.6 \times 10^3 - 32 \times 10^3$	
Control (n = 8)	24 – 49	–	(*27*)
Exposed workers [b] (n = 22)	24 – 116	–	
Smokers (n = 10)	27 – 148	–	
Control (n = 18)	20 – 70	–	(*26*)
Exposed workers [c, d] (n = 210)[a]	$< 80 - 17.7 \times 10^3$	–	
Nonsmokers (n = 24)	11 – 50	–	(*155*)
Smokers (n = 38)	16 – 294	–	
Nonsmokers (n = 25)	12 – 50	–	(*156*)
Smokers (n = 47)	13 – 294	–	
Nonsmokers (n = 5)	20 – 40	26	(*157*)
Nonsmokers (n = 13)	7 – 31	9 – 23	(*158*)
Smokers (n = 16)	25 – 199	22 – 119	
Nonsmokers (n = 10)	18 – 34	–	(*137*)
Nonsmokers (n = 70)	20 – 100	–	(*159*)
Smokers (n = 72)	30 – 430	–	
Men (n = 70)	27 – 453	27 – 240	(*141*)
Women (n = 26)	31 – 325	36 – 239	
Nonsmokers (n = 60)	18 – 51	–	(*148*)
Smokers (n = 60)	18 – 210	–	
Nonsmokers (n = 52)	9 – 70	12 – 47	(*160*)
Smokers (n = 16)	16 – 163	15 – 62	
Men (n = 29)	10 – 119	13 – 57	
Women (n = 39)	9 – 163	12 – 62	
Nonsmokers (n = 44)	18 – 66	7 – 46	(*161*)
Smokers (n = 6)	99 – 211	29 – 99	
Men (n = 94)	20 – 610	7 – 399	(*162*)
Women (n = 67)	4 – 364	7 -260	
Nonsmokers, Women (n = 296)	14 – 148	23 – 157	(*163*)

[a] Workers employed in the synthesis of AA and in the production of polyacrylamides.
[b] Laboratory personnel working with PAGE.
[c] Tunnel workers handling AA-containing grouts (Hallandsås tunnel).
[d] Neurotoxicity observed in workers with increased exposure to AA
   (LOAEL (AA-Val) = 6×10^3 pmol/g globin).

2.4.2   Workplace Exposure

Occupational exposure to AA occurs during the production or processing of AA, during grouting and during laboratory preparation of polyacrylamide gels. The main routes of exposure are dermal absorption of AA monomer from solution and inhalation of dry monomer or aerosols of AA solution (*164*). Although a maximum allowable concentration for AA cannot be assigned (*165*) due to the proposed non-threshold mode of action concerning carcinogenicity, a workplace exposure limit of 0.3 mg/m³ (*166*) (resp. 0.03 mg/m³ (*36, 167*)) has been established. Several exposure assessments in workers employed in the AA producing or processing industry were performed using Hb-adducts as biomarkers of exposure (**Table 2**). In laboratory personnel working with PAGE, the AA burden was relatively low, corresponding to an uptake of AA from approximately 3 cigarettes per day (*27*). This finding was confirmed by inhalation exposure evaluations resulting in mean workplace exposures of approximately 0.01 mg/m³ AA for PAGE workers (*168*). In factory workers and tunnel construction workers (Hallandsås) however, exposures were extremely high (up to 153 mg/m³), inducing neurotoxicity in a number of cases (*8, 26, 142*). From these studies, a lowest observed adverse effect level (LOAEL) of 6×10^3 pmol AA-Val/g globin for development of peripheral neuropathy could be derived.

2.4.3   Exposure to Acrylamide Residues from Polyacrylamides

Approximately 99.9% of AA produced in the EU is used in the production of polymers. Whereas the release of free monomeric AA by degradation of polymers is reported to be unlikely, monomeric AA may be present in polyacrylamides due to incomplete polymerization during production. The residual content of AA in polymers produced in the EU is kept below 0.1% (w/w) to avoid classification as a Category 2 carcinogen under the Dangerous Preparations Directive (88/379/EEC). For polymers used in the preparation of drinking water, the maximum permitted amount of free AA in the polymer is 0.025% (w/w) (*1*).

Drinking Water. A major part of the produced polymers is used as flocculants in the treatment of municipal drinking water and waste water. Due to its excellent solubility in water, free AA is readily released. In drinking water, the maximum content of AA has been limited to 0.125 µg/L. Accordingly, the maximum daily intake from drinking water has been estimated to approximately 0.0036 µg/kg b.w. in adults (*1*).

Cosmetics. Another possible source of exposure to residual AA in polyacrylamides are cosmetic products. AA polymers are used as thickeners in soap and various other cosmetic formulations, such as pre-shave lotions and hair grooming preparations (*1*). Polyacrylamide is used in concentrations ranging from 0.05% to 2.8%. Residual levels of AA in the polyacrylamides used, can range from <0.01% to 0.1% (*169*). Whereas polymers do not penetrate the skin due to their size, approximately 4.5% of the applied AA is absorbed through human skin (*147*). As AA uptake via the skin is relatively slow, AA content in leave-on formulations has been limited to 0.1 ppm and to 0.5 ppm in other cosmetic products (*169*).

2.4.4 Smoking

AA is a constituent of cigarette smoke (>1 – 2 µg/cigarette) (*170, 171*) and elevated Hb-adduct levels (2 – 3 times the background level) have been reported in smokers (*27, 148, 158, 162, 172*) (**Table 2**). It has been estimated that one cigarette raises the AA-Hb adduct level by 3.4 pmol/g globin (*156*). Smokers also excrete more AA-derived metabolites in urine compared to the non-smoking population (3 – 4 times). Therefore, smoking status can be correlated directly to elevated levels of Hb-adducts as well as urinary excreted metabolites of AA (*155*).

2.4.5   Dietary Exposure

Exposure to AA via the diet is the most prevalent source of AA in the general population. AA is ubiquitous in the human diet. About 38% of our caloric uptake is provided from food known as a source of AA (*173*). Foods with the highest concentrations of AA are potato products such as French Fries and chips. Also, very high contents were detected in gingerbread (**Table 4**). Although in coffee, AA concentrations are relatively low, it is a major contributor to AA exposure in adults, due to the high amounts consumed (*174*). Daily dietary intakes of AA were estimated from food consumption surveys and median concentrations of AA in the most common foodstuffs (**Table 3**).

Children and adolescents tend to eat more AA on a per body weight basis. This may be due to a combination of children's higher caloric intake relative to body weight as well as their higher consumption of certain AA-rich foods, such as French fries and potato crisps. Accordingly, intakes 1.5 to 2 times the daily exposure in adults have been estimated for children and adolescents with possible worst-case scenarios of up to 6.9 µg/kg b.w. per day (*175*).

Table 3
Estimated daily intakes of acrylamide with the diet.

Exposure Assessment	Age group	Daily Intake (µg/kg b.w.)	
		Mean	95th percentile *90th percentile
WHO/FAO (**2002**) (*30*)		0.3 – 0.8	
FDA (**2002**) (*176*)		0.7	
BfR, Germany (**2003**) (*175*)	4 – 6	1.2	
	15 – 18	1.1	3.4
	25+	0.6	
SNFA, Sweden (**2003**) (*177*)	18 – 74	0.45	1.03
NFCS, Netherlands (**2003**) (*178*)	1 – 97	0.4	1.2
	1 – 6	1.0	1.7
SNT, Norway (**2003**) (*34*)	males	0.49	1.01*
	females	0.46	0.86*
	9, boys	0.36	0.72*
	9, girls	0.32	0.61*
	13, boys	0.52	1.35*
	13, girls	0.49	1.2*
	16 – 30, males	0.53	
	16 – 30, females	0.50	
FDA (**2003**) (*176*)	2+	0.37	0.81*
	2 – 5	1.0	2.15*
FDA (**2004**) (*176*)	2+	0.43	0.92*
	2 – 5	1.06	2.31*
FDA (**2006**) (*176*)	2+	0.44	0.95*
	2 – 5	1.07	2.33*

2.5   Formation of Acrylamide in Food

In early 2002, the Swedish National Food Administration reported that a group of Swedish scientists had detected high levels of AA in various baked, fried or grilled foods (*179*). Until then, AA had only been known as a probably carcinogenic industrial chemical. Consequently, this finding caused major concern and led to numerous studies to help understand how AA is formed in food. Subsequent research in many European countries as well as in the United States revealed that AA is generated primarily in carbohydrate-rich foods prepared at elevated temperatures (*28, 29, 180*). Median levels of AA in food groups known to be major sources of AA in the Western diet are summarized in **Table 4**. It is apparent that the level of AA can vary broadly even within the same product group or product type. Reasons for this variation in industrially processed foods are yet unknown, but may be due to varying levels of AA precursors in the natural raw materials. However, an even higher variation of AA content is to be expected from home-prepared foods.

Table 4
Acrylamide levels in selected food groups (*181*).

Food Group	n[a]	Minimum Acrylamide (µg/kg)	Maximum Acrylamide (µg/kg)	Median Acrylamide (µg/kg)
Crisp bread	131	21	3383	311
Cereals	81	3	149	28
Fine biscuits	92	20	1556	50
Gingerbread	369	6	3779	319
Potato chips	158	70	2233	394
French fries	409	5	1846	227
Coffee, roasted	90	15	515	195

[a] Number of tested products.

Maillard Reaction. The basic mechanism of AA-formation in starch-containing foods is a non-enzymatic browning reaction known as Maillard Reaction between amino acids and reducing sugars (*180, 182*). Asparagine, a major amino acid in potatoes and cereals is a crucial participant in the formation of AA by this pathway, as it already has an amino group attached to a chain of two carbon atoms (*183*). During high temperature heating, the amino group of asparagine and the carbonyl group of reducing sugars (fructose or glucose) form an asparagine-*N*-glycosyl-conjugate which is dehydrated to the corresponding Schiff´s base (*180, 183, 184*). Decarboxylation, either directly (Path **I**), via intramolecular cyclization to oxazolidine-5-one (Path **Ia**) (*184*), or via the zwitterionic Schiff´s base (Path **Ib**) to the azomethine ylide, and further deamination eventually yield AA (*185*) (**Figure 14**). Low water content as well as elevated temperatures with an optimum between 120 °C and 170 °C promote the formation of AA by this pathway (*182*).

Additional Routes of Acrylamide Formation. In addition to the generation of AA via Maillard browning, other routes of formation have been investigated. Low levels of AA were detected in foods with negligible content of carbohydrates, e.g. grilled or fried meat, or foods that were not prepared under heating, such as canned black olives or prune juice. For meat, formation from the dipeptide carnosine (*N-β*-alanyl-*L*-histidine) (*186*) or via *β*-oxidation products of fatty acids (e.g. acrolein) (*187*) was discussed. During the processing of black olives, the methods of preservation and darkening seemed to have the most pronounced effect on AA content (*188*). Yet, the precise mechanism of AA formation in olives or prune juice is still unclear.

Formation of Glycidamide in Food. Recently, GA, the genotoxic metabolite of AA, was also detected in potato chips and French fries (*189*) at very low concentrations ranging from 0.3 to 1.5 µg/kg. As a possible way of formation, epoxidation of AA by linoleic acid hydroperoxides from sunflower oil was discussed.
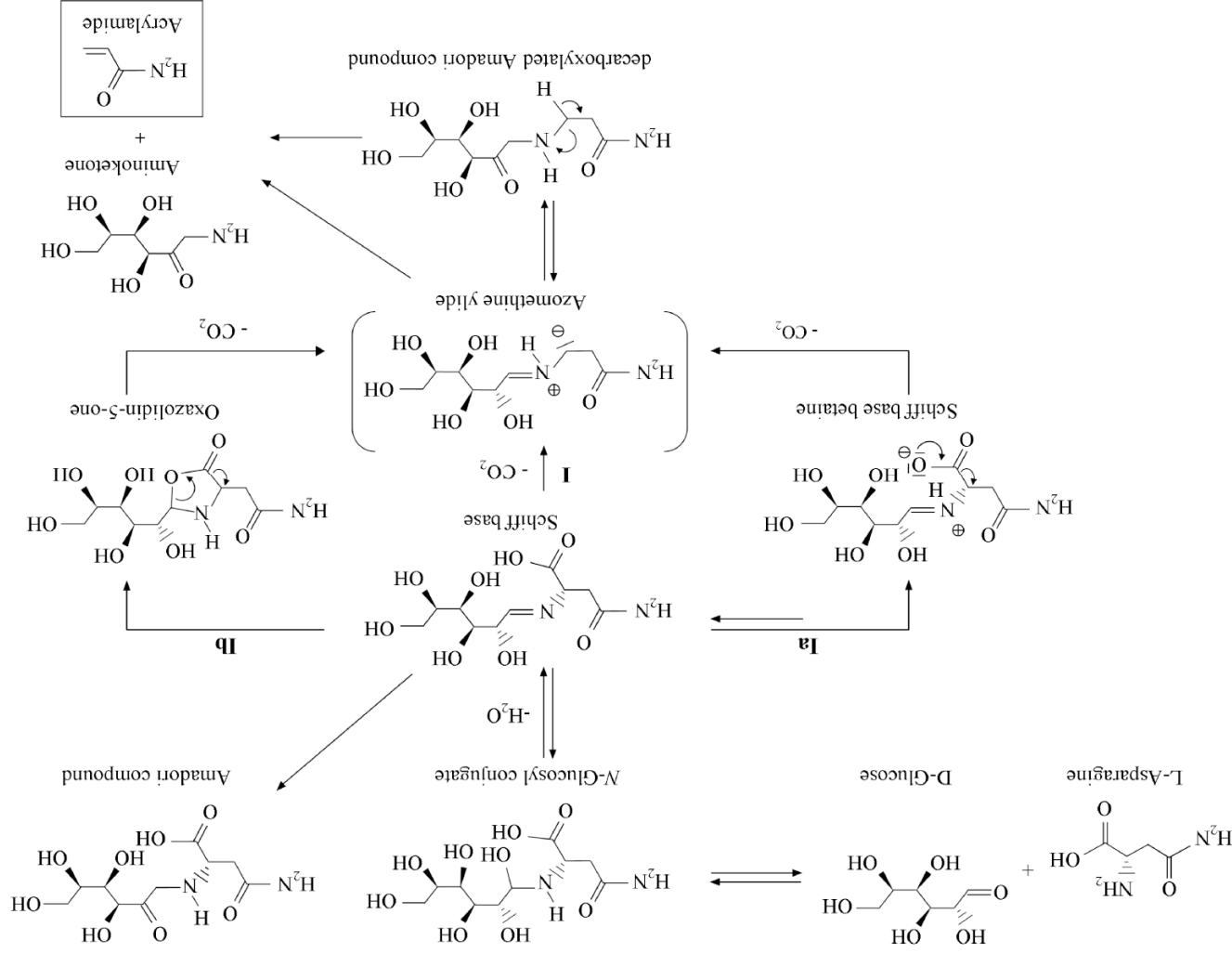
Figure 14 Mechanistics of acrylamide formation in carbohydrate-rich food according to Stadler et al., 2004 (185).

Reduction of Acrylamide Content in Food. Unavoidable substances considered to be genotoxic carcinogens, such as AA, are unwanted in foods and are usually dealt with via the ALARA principle (as low as reasonably achievable). According to the ALARA principle, the exposure to AA should be reduced to a minimum (*164, 190*). In the last years, several approaches to reduce AA content in industrially prepared foodstuffs have been promoted (*191*). In Germany, 'Signal Values' have been introduced for each food group known as a source of dietary AA (*181*). Under this mitigation regimen, food processing companies are encouraged to reduce the amount of AA in their products under a certain level, which is defined anew every year as the lowest value of the upper 10th percentile for each food group. A Signal Value higher than 1000 µg/kg is automatically set to 1000 µg/kg. If individual values exceed the Signal Value, the food control authorities contact the food producers and enter in the so-called 'minimization-dialogue' with the aim to reduce the levels found via changing ingredients and/or processing conditions.

However, products of the Maillard Reaction are responsible for much of the tastiness, odor and color generated during baking and roasting. Browned crispy crusts in foods like French fries, potato chips, crackers, cereals and toasted bread tend to have the highest levels of AA (*192*). Reduction of temperature and heating time may reduce the amount of AA formed during preparation of food, but will inevitably lead to a loss of flavor. For some foods, especially for coffee, which is one of the major sources of dietary AA in Western societies (*34*), this would result in a loss of the major characteristics of the product itself, since the roasting step cannot be fundamentally changed.

2.6 Risk Assessment

2.6.1   Human Risk Assessment of Genotoxic Carcinogens

General Strategies for Risk Assessment. Risk assessments serve as the foundation of regulatory decisions on whether to take actions to reduce (or otherwise manage) a toxicological risk or not. Chemical risk assessment follows a specific paradigm composed of four steps (*35*). The first step, *hazard identification* aims at determining the specific properties of a substance, i.e. its potential to cause harm in experimental animals or humans. The required toxicity data can be obtained either from experimental systems, such as *in vitro* assays or *in vivo* animal experiments, or from epidemiological studies in humans. The next step is the *dose-response assessment*. The purpose of dose-response assessments is to describe the relationship between the administered dose and the response in the exposed population. The third step of the risk assessment process is *exposure assessment*. Exposure assessments are generally based on measured data from biomonitoring studies and/or the use of theoretical exposure models. The likelihood of human exposure, the magnitude and duration, as well as the potential routes of exposure are determined. The final step is *risk characterization*, which involves comparing the quantitative or qualitative information on human exposure to the dose-response relationship for the critical effect, or when possible, a qualitative evaluation of the probability that an effect will occur at any given exposure.

Risk Classification of Carcinogenic Substances. Carcinogens can generally be divided into those for which a threshold can be determined and those for which, for various reasons, a threshold cannot be established. The threshold paradigm implies that some exposure can be tolerated by an organism with substantially no initiation of a toxic response. The identification of practical biological 'thresholds' experimentally or via dose-response modeling may allow the determination of an exposure level that correlates to an acceptable level of risk. Carcinogens operating by non-threshold mechanisms on the other

hand, are historically considered to have no safe level of exposure (*32*). It is assumed that even a small number of molecular events (i.e. DNA-adducts leading to mutations) can evoke changes in a single cell that can result in uncontrolled cellular proliferation. Hence, in terms of risk assessment, the NOEL or NOAEL found in a study of carcinogenicity represents the limit of detection in the respective bioassay rather than an estimate of a possible threshold (*193*). The traditional approach of using a NOAEL to define a tolerable daily intake is therefore not appropriate for DNA-reactive substances. As a result, for unavoidable contaminants that are considered undesired in foods, the ALARA principle is applied, which states that the intake level should be as low as reasonably achievable (*164, 190, 193*). However, ALARA provides non-quantitative advice based solely on hazard identification and does not take into account either carcinogenic potency or human exposure.

Apart from ALARA, more recent approaches are customarily used for risk characterization of genotoxic carcinogens (*194*):

(1) TTC (threshold of toxicological concern) if adequate cancer dose-response data are lacking,

(2) low-dose extrapolation of data from rodent carcinogenicity bioassays, and

(3) MOE (margin of exposure), representing the ratio between a reference dose on the dose-response curve from animal bioassays or epidemiological studies and the estimated human exposure.

The TTC approach is only used if there is no biological data available. As an alternative, risk estimates are based on data from structurally related carcinogens, assuming similar genotoxic potential (*195*).

For linear extrapolation to risk at low doses, mathematical models are fitted to carcinogenicity data in test animals to create quantitative risk estimates at doses several orders of magnitude below the lowest experimental dose. Simple linear extrapolation from either a selected incidence within the experimental range (e.g. LOAEL) or from a derived

incidence (e.g. BMDL10 or T25, see below) as well as more complex mathematical models are commonly used by risk assessment authorities. A calculated lifetime risk of cancer of one in a million (1×10^{-6}) or one in a hundred thousand persons (1×10^{-5}) associated to the level of exposure has been defined as a low risk (*194*). In using this approach, it must be taken into account that, as the applied mathematical models are in most cases highly conservative, linear extrapolation results in an upper bound estimate of risk rather than an accurate estimate.

Recently, the margin of exposure (MOE) approach has been suggested most appropriate for risk assessment of substances that are both genotoxic and carcinogenic (*193, 196*). The MOE is based on available animal dose-response data (i.e. the dose leading to tumor formation in experimental animals), without extrapolation, and on human exposures. It represents a helpful means for classification of genotoxic carcinogens and is used to determine the level of priority for risk management actions. For calculations of a MOE, a suitable reference point in the dose-response data in animal experiments must be determined via mathematical modeling. For this purpose, generally, a benchmark dose (BMD) close to the bottom end of the observed effect range or limit of quantification is chosen that leads to a 10% increase in tumor incidence over background in the experimental species. By using the lower limit of the 95% confidence interval (BMDL10), uncertainties and statistical errors in the available dose-response data are taken into account. Another possible reference point on the dose-response curve is the T25 value, which is the chronic dose that will give rise to tumors in 25% of the animals above background at specific tissue site (*197*). The T25 is determined by linear extrapolation from the lowest dose giving a statistically significant increase in tumors (the critical dose). It is generally agreed, that a MOE above 10 000 based on a BMDL10 from an animal study is a value for which a low concern arises for the public health and which poses a low priority for risk management actions (*196*). An advantage of the MOE approach is that it is not based on extrapolations outside the dose range tested in animal models. As a simple ratio, the magnitude of the MOE reflects the possible magnitude of the risk, but does not attempt to define an actual risk level.

2.6.2   Human Risk Estimations for Acrylamide Toxicity

Hazard Identification. Potential hazards to human health associated with exposure to AA include neurotoxicity, reprotoxicity and carcinogenicity (*51*). The NOAELs for neurotoxicity and reprotoxicity have been determined in rodent bioassays to be 0.5 mg/kg b.w. (*11*) and 2.0 mg/kg b.w. (*12*) AA, respectively. Considering estimated daily intake levels of approximately 0.4 µg/kg b.w. via food (*176*), these effects do not appear to be relevant as possible human health hazards from dietary AA. In contrast, due to expected non-threshold mechanisms, genotoxicity and carcinogenicity are commonly acknowledged as the pivotal effects for AA risk assessment in humans (*198*).

Most of the available data indicate that the major genotoxic effects that lead to tumors from exposure to AA are clastogenicity, involving covalent modifications of proteins by AA and GA, and mutagenicity produced by GA via direct alkylation of DNA (*12, 17, 31, 126, 132*). Support for the genetic damage in somatic and germ cells of mice treated with AA being dependent upon metabolism of the parent compound to GA by CYP 2E1 comes from studies with CYP 2E1-null mice where in comparison to CYP 2E1 wild-type mice no increase in micronuclei or germ cell mutations could be observed following administration of AA (*20, 199*). In Big Blue mice, similar mutation spectra were found following administration of AA or GA (*18*). *In vivo* micronuclei measurements following i.p. administration of AA or GA to rats and mice indicated equal potency of GA to increase micronucleus frequency, whether its *in vivo* dose results from direct administration of GA or from metabolism from AA. (*200, 201*).

In two 2-year drinking water bioassays, increased incidences of thyroid tumors in male and female rats, scrotal sac mesotheliomas in male rats, and mammary gland tumors in female rats were detected, with the mammary gland tumors in female rats being the most sensitive end-point at a daily dose of 0.5 mg/kg b.w.(*21, 22*).

Although evidence from available human epidemiological studies is judged to be limited to inadequate, risk assessors consistently agree that the carcinogenic effects observed in rodents are relevant to human exposure to AA. (*1, 24, 30, 34, 193, 196, 202, 203*).

Dose-Response Assessment. Due to the lack of consistent epidemiological data, as well as adequate human and animal biomarker data, dose-response relationships for AA risk assessment are established on the basis of animal studies (*35*). In terms of a conservative risk assessment, the development of mammary gland fibroadenomas in female rats is generally chosen as the critical endpoint (*204*).

BMDL10 and T25 values can be derived from the dose-response curve. The T25 value for AA has been estimated by linear extrapolation to be 0.65 mg/kg b.w. per day. Using a number of different mathematical models (*193*), BMDL10 values varying from 0.31 to 0.62 mg/kg b.w. have been calculated (*205*). For risk evaluations, the more conservative lower end of this range of values is favored.

Exposure Assessment. Based on measurements of AA in different foodstuffs and on food consumption data, the daily dietary intake for adults was determined to range from 0.3 to 0.8 µg/kg b.w. AA (**Table 3**).

Various exposure data have been applied for risk assessment, thereby reflecting different exposure levels. Daily doses ranging from 0.41 µg/kg b.w. AA to 4.0 µg/kg b.w. were chosen to represent the life-long intake in average consumers up to high consumers (**Table 5**) (*193, 205*).

Risk Characterization – Margin of Exposure Assessment. In order to quantitatively characterize the risk for human exposure to AA, margins of exposure were determined on the basis of different AA intake levels (**Table 5**). As has been mentioned above, a MOE above 10 000 is considered safe. However, the MOE for AA is relatively low for a compound that is genotoxic and carcinogenic. Therefore, it has to be concluded that dietary exposure AA poses a human health concern (*193*).

Table 5
Comparison of margins of exposure for acrylamide at different exposure levels in humans.

Reference	T25 (mg/kg b.w)	BMDL10 (mg/kg b.w)	Human Exposure (µg/kg b.w)	MOE	
				T25	BMDL10
JECFA, **2005** (*193*)		0.30	1.00		300
			4.00		75
O´Brien et al., **2006** (*205*)	0.65	0.31	0.41	1600	760
			0.42	1600	740
			0.43	1500	720
			0.92	710	340
			2.31	280	130

T25: chronic daily dose, which will give rise to tumors in 25% of the animals above background. Calculated by linear extrapolation from the lowest dose giving a statistically significant increase in tumors (critical dose).

BMDL10: the 95% lower confidence interval of a benchmark dose (BMD) for a 10% increase in tumor incidence in test animals. Determined by fitting dose-response data to various mathematical models.

MOE: ratio between a dose leading to tumor formation in experimental animals (e.g. T25 or BMDL10) and the human intake.

Risk Characterization – Linear Extrapolation of Risk to Low Doses. Quantitative lifetime cancer risk estimates for human dietary exposure to AA may be obtained by linear extrapolation from rodent cancer data. Usually, T25 and BMDL10 are used as points of departure. **Table 6** summarizes the cancer risk estimates calculated by different risk assessment agencies. In general, a daily intake of 1.0 µg/kg b.w. AA (unit risk) over a period of 70 years was assumed. The obtained lifetime cancer risks range between 700×10^{-6} and $10\,000 \times 10^{-6}$, which corresponds to 700 to 10 000 additional cancer cases in one million people, thereby exceeding the tolerable cancer risk of 1×10^{-6} to 1×10^{-5} (*194*) by several orders of magnitude.

Table 6
Human lifetime cancer risk estimates for dietary exposure to acrylamide.

Reference	Lifetime Cancer Risk
US EPA, **1985** (*206*)	5500×10^{-6}
WHO, **1985** (*207*)	700×10^{-6}
Granath et al., **2001**(*33*)	$10\,000 \times 10^{-6}$
Sanner et al., **2001**(*197*)	5000×10^{-6}
Dybing et al., **2003** (*34*)	$1\,600 \times 10^{-6}$

2.6.3   Gaps and Limitations in Human Risk Assessment of Acrylamide

Generally, risk assessments are subjected to a number of uncertainties evolving from extrapolations from experimental data to actual human risk. An example of a risk assessment principle that may lead to uncertainties is that for dose extrapolation. In order to identify a small risk in a population with significant biological variability, a very large study is needed. It has been estimated, that epidemiological studies cannot reliably detect excess relative risks about 10% or smaller (*203*). In experimental systems on the other hand, the study design can be adjusted to increase the probability to detect rare effects by increasing the applied doses. Consequently, toxicity data generated by standard bioassays or animal studies are usually obtained from exposures that are significantly higher than those relevant to human risk assessment.

Another example for a commonly applied risk assessment principle is species extrapolation. Extrapolation from experimental animal data to human risk is a critical step in the risk assessment process, as both qualitative (e.g. nature of the response) and quantitative (e.g. magnitude of the response) species differences have been shown to exist. A possible way to address this problem is the use of simple conversion factors (*35*).

Due to the lack of consistent human data regarding toxicodynamics and toxicokinetics of AA at low doses, risk assessment for AA carcinogenicity in humans is based on extrapolation from rodent studies with exposures in the mg/kg b.w. range. It must be taken into consideration however, that a cancer risk determined by linear extrapolation from animal data represents an upper bound on the risk for rodents rather than a mathematical estimate of the real risk in humans (*205*). It has also been criticized that the use of low-dose linear extrapolation over several orders of magnitude does not necessarily reflect the underlying biological processes. There is potential for significant non-linearity in the intake-response relationship outside the observed dose range. Since cellular protective mechanisms such as detoxification processes, cell cycle arrest, DNA repair, and apoptosis may be operative at low doses, linear extrapolation may overestimate the actual risk arising from exposures as low as those derived from the human diet (*34*).

3 Objectives

Precise knowledge of biotransformation and toxicokinetics of a potential carcinogen is crucial for risk assessment, especially, if formation of reactive intermediates is involved. To elucidate whether and to what extent chemicals are transformed into electrophilic metabolites, measurement of GSH-adducts or corresponding mercapturic acids excreted in urine is a convenient means (*208*). Therefore, the first part of this thesis was devoted to the development and validation of a highly sensitive and specific analytical method for the simultaneous detection and quantification of the hydrophilic mercapturic acid metabolites of AA. The analytical method was intended to be suitable for quantification of AAMA, GAMA and AAMA-sulfoxide from exposures to AA as low as those expected from the diet.

Following the demonstration of applicability of the analytical method by measurement of background exposures to AA in smokers and nonsmokers, a major aim was to estimate the daily dietary exposure in humans via biomonitoring. Compared to previous exposure calculations on the basis of AA levels in foods and dietary habits, measurement of urinary

biomarkers may result in a more realistic estimate because it directly reflects the internal dose of AA (*209, 210*).

Risk assessment for AA in humans is generally based on results from animal studies with doses exceeding the mean dietary intake by several orders of magnitude. As a result, major uncertainties evolve from extrapolation of animal data down to human exposures (*35*). There have been some findings suggesting differences in AA biotransformation in humans and rodents (*211*). Therefore, the most important objective of this work was to evaluate possible inter-species differences in biotransformation and toxicokinetics of AA after administration of doses similar to the daily exposure from food. For this purpose, studies in rats and humans with single oral administration of $^{13}C_3$-labelled AA at low doses were planned.

The obtained results may improve the basis for risk assessment of human dietary exposure to AA and help to avoid high-dose to low-dose as well as inter-species extrapolation.

4 Analytical Method Development

4.1 Introduction

4.1.1 Analysis of Acrylamide-derived Metabolites in Urine

Several methods for LC-MS/MS quantification of AA-derived metabolites in urine based on Reverse Phase (RP) chromatography have been published over the last 4 years (*146, 148-150, 153*). Apart from one method, where online sample-workup is applied (*149*), time-consuming sample preparation prior to LC-MS/MS analysis is needed. However, neither of these methods is suitable for the analysis of AAMA-sulfoxide or glyceramide, the hydrolysis product of GA. This is due to insufficient retention of the highly hydrophilic substances on RP column material. At the relatively low urinary metabolite concentrations derived from dietary exposure to AA, interferences such as ion suppression from the urinary matrix, especially close to, or in, the void volume of the analytical column, have crucial influence on the detection of analytes. Accordingly, AAMA-sulfoxide has only been determined in human urine following administration of

0.5, 1 and 3 mg/kg b.w. AA, and glyceramide could only be detected by ^{13}C-NMR following exposure to 3 mg/kg b.w. ^{13}C$_3$-AA (*147*). These doses however, are approximately 1000 to 6000 times higher than the median dietary exposure.

4.1.2   Hydrophilic Liquid Interaction Chromatography

Hydrophilic Liquid Interaction Chromatography (HILIC) has been introduced more than 30 years ago as an analytical separation technique mainly for carbohydrates (*212, 213*). Due to difficulties during application, e.g. major retention time shifts and insufficient availability of HILIC phases, and particularly because of the rapid advance of Reversed Phase (RP) technology, HILIC fell into oblivion for at least two decades. With the emergence of new research fields like metabonomics and proteomics at the beginning of the 21st century, a need for analytical methods for very polar substances (e.g. proteins or urinary metabolites) arose, and HILIC came into the focus of scientific attention again (*214*). Due to the ability to separate polar analytes, HILIC technology has recently been used for metabonomic screening studies in human and rat urine (*215-217*). Quantitation of single analytes in urine with HILIC-MS/MS however, still requires sample preparation procedures such as solid phase extraction due to interferences of polar matrix components (*218, 219*).

HILIC Retention Mechanistics. HILIC is a separation technique utilized for chromatography of highly hydrophilic analytes. In contrast to RP chromatography, polar column materials are used in combination with mobile phases with relatively high content of organic solvent (e.g. acetonitrile, $\geq 60\%$) and low content of water or buffers (e.g. ammonium acetate buffer). Accordingly, HILIC is often referred to as 'Reversed-RP'. Retention is mediated by distribution of the analytes between a water-enriched, quasi-stationary phase attracted by the polar column material, and the rest of the solvent (**Figure 15**). The high content of acetonitrile in the mobile phase and the application of

volatile salts for the preparation of buffers, such as ammonium acetate, make HILIC an almost ideal chromatography technique for electrospray ionization-mass spectrometry (ESI-MS) (*214*).
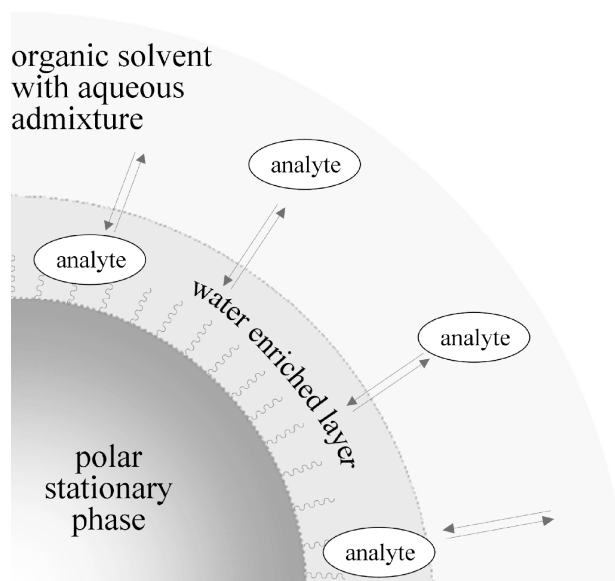
Figure 15   HILIC-principle. Retention of polar analytes by separation between a water-enriched layer and the mainly organic solvent.

Retention capabilities of HILIC material increase with hydrophilicity and polarity of the analytes. Also, an increasing concentration of organic solvent in the mobile phase increases retention (*220*). These characteristics are the complete opposite to those observed with RP (*217*). In RP chromatography, retention is largely mediated by van-der-Waals forces between the relatively unpolar stationary phase (e.g. C-8 or C-18 bonded silica) and the analytes. Thus, more hydrophobic compounds are preferentially retained, and retention of polar analytes is increased with decreasing admixture of organic solvent. The orthogonality of retention of AAMA and GAMA on RP and HILIC columns is demonstrated in **Figure 16.**

HILIC Separation of AAMA, GAMA and AAMA-sulfoxide. For the separation of AAMA, GAMA, iso-GAMA and AAMA-sulfoxide, a Zic-HILIC column (3.5 µm, 2.1 mm × 150 mm, SeQuant AB, Umeå, Sweden) was chosen as analytical column. The zwitterionic sulfoalkylbetaine stationary phase offers the possibility of a very selective separation of charged analytes by weak electrostatic interactions with the column surface (*221*).
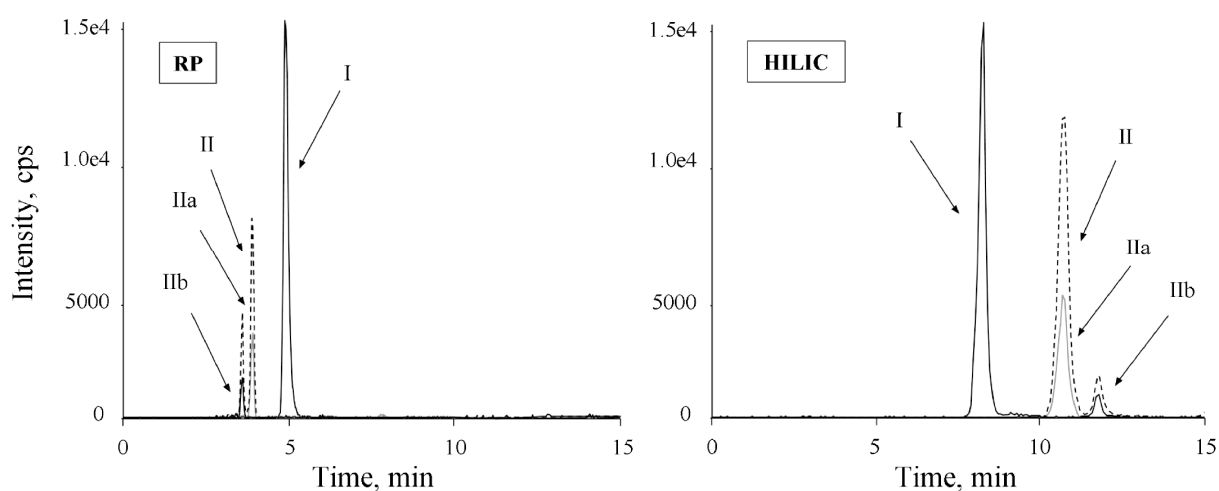
Figure 16   Orthogonality of HILIC compared to RP. Retention of AAMA (**I**), GAMA (**II***; **IIa**) and iso-GAMA (**IIb**) (standards dissolved in acetonitrile) on a Reprosil-Pur C18-Aq column (3 µm, 150 × 2 mm, Dr. Maisch, Ammerbuch, Germany) (**RP**); mobile phase: 98% formic acid 0.1% in water, 2% methanol; flow rate: 200 µL/min and on a Zic-HILIC column (3.5 µm, 2.1 mm × 150 mm, SeQuant AB, Umeå, Sweden) (**HILIC**); mobile phase: 80% acetonitrile, 20% ammonium acetate buffer, pH 6.9, 20 mM; flow rate: 200 µL/min.
* This mass transition accounts for both GAMA and iso-GAMA.

LC-MS measurements in urine are often complicated due to interferences with coeluting matrix-components. To avoid complex and time-consuming sample preparation steps such as solid phase extraction, an online clean-up method was developed. A Stability BS-C17 trap column (5 µm, 3 mm × 33 mm, Dr. Maisch, Ammerbuch, Germany) was applied. The RP/SAX (reverse phase/strong anion exchange) column material consists of quaternary ammonium groups embedded in carbon chains with altogether 17 carbon atoms (*222*). Due

to the positive charge of the material, a HILIC-like mode of retention could be observed when a mobile phase with high content of acetonitrile and very low admixture of ammonium acetate buffer was used. With decreasing water content in the mobile phase, retention and separation of the hydrophilic substances increased immensely (**Figure 17**). Compared to the Zic-HILIC column however, a different pattern of retention could be observed. Instead of AAMA, iso-GAMA and GAMA were eluted first from the column. This effect was desired, as, due to this weak orthogonality, a larger amount of confounding substances from the urine matrix could be eliminated compared to the application of a trap column with exactly the same retention performance as the analytical column (*223*).
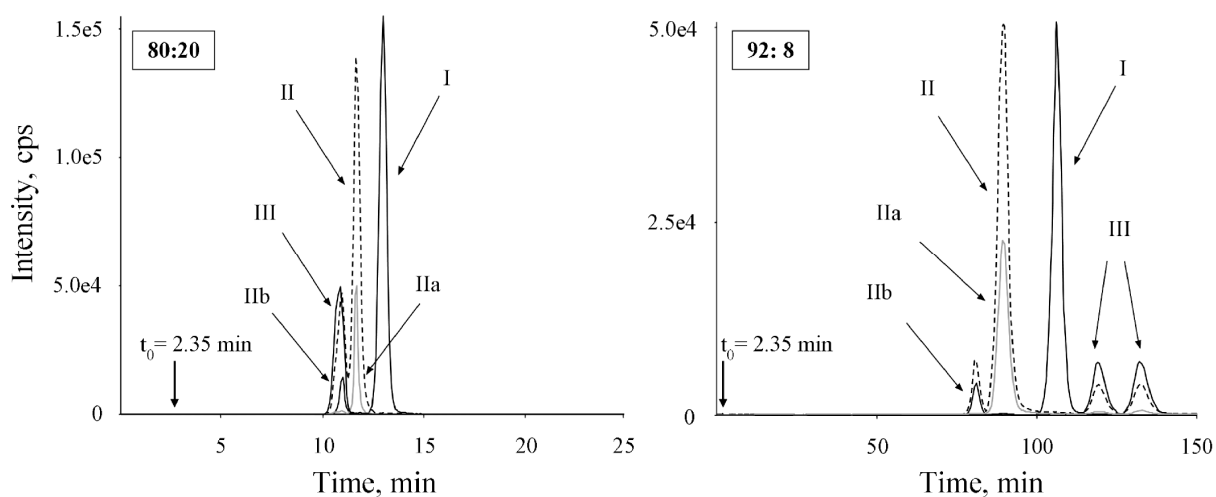
Figure 17   Retention of AAMA (**I**), GAMA (**II***; **IIa**), iso-GAMA (**IIb**) and AAMA-sulfoxide (**III**) (standards dissolved in acetonitrile) on a Stability BS-C17 analytical column (5 µm,150mm × 2mm, Dr. Maisch, Ammerbuch, Germany) depending on water content in the mobile phase. Mobile phases consisted of 80% acetonitrile and 20% ammonium acetate buffer, pH 6.9, 20 mM (left hand side) and of 92% acetonitrile and 8% ammonium acetate buffer, pH 6.9, 20 mM (right hand side), respectively. t_0 represents the void volume of the column.
* This mass transition accounts for both GAMA and iso-GAMA.

4.1.3   Electrospray Ionization

An API 3000 mass spectrometer equipped with an electrospray ionization (ESI) source (Applied Biosystems) was used for MS/MS analysis of the urinary metabolites of AA and $^{13}C_3$-AA. ESI is the preferred method of ionization for polar substances at atmospheric pressure (*224*). The solvent flow from the LC system is lead through a charged metal capillary. According to the applied voltage, analytes form ions either in anion or cation form. An aerosol, a mist of small charged droplets (electrospray) is formed. A heated (400 °C) stream of nitrogen (nebulizer gas) helps to evaporate the neutral solvent. Eventually, as the analyte molecules are forced closer together, the droplets break up in a process called Coulomb fission or Coulomb explosion. This process repeats until the analytes are free of solvent and lone ions remain. Ions are then transferred into the high vacuum region of the mass spectrometer for analysis (**Figure 18**). ESI represents a soft ionization technique useful for the MS analysis of polar biomolecules.
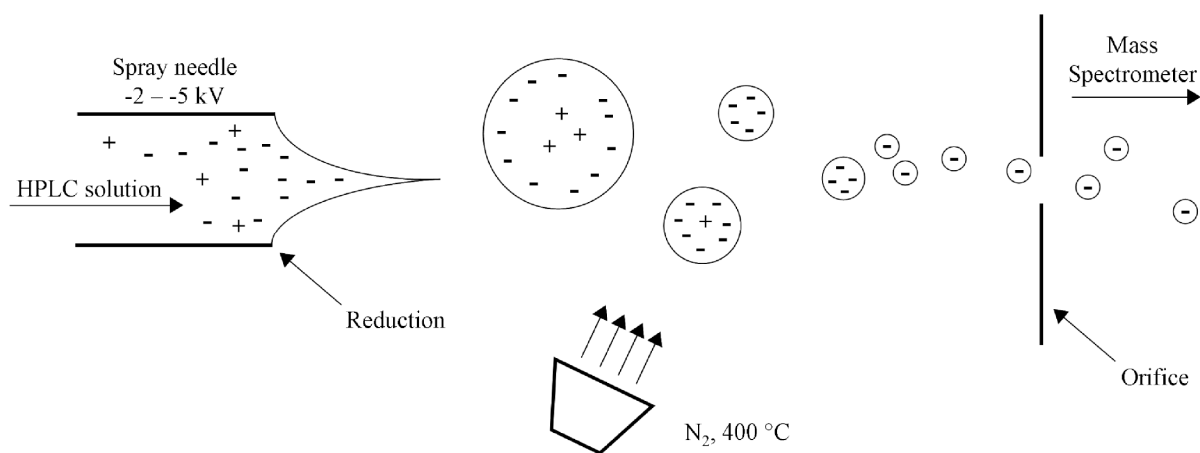
Figure 18   Schematic illustration of the negative electrospray ionization process (adapted from Cech and Enke, **2001** (*224*)).

4.1.4   Multiple Reaction Monitoring Mode

Analytes were detected in a triple-quadrupole mass spectrometer run in the multiple reaction monitoring mode (MRM). In this configuration, the first (Q1) and the third (Q3) quadrupole act as mass analyzers (filters). The second quadrupole (Q2) is used as 'collision cell', where the precursor ions are collided with inert gas (argon or nitrogen) to give substance-specific fragments (**Figure 19**). The desired analytes are selected by their mass-to-charge ratios (*m/z*) in Q1. If the charge is ±1, then *m/z* is equal to the molecular weight of the ion or fragment of interest. After collision induced fragmentation in Q2, specific product ions are detected in Q3. Using MRM, highly specific analysis of substances in mixtures of multiple compounds can be achieved.
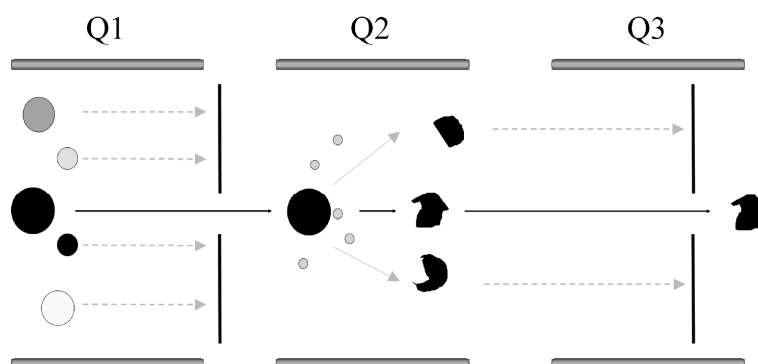
Figure 19   Multiple reaction monitoring. The first quadrupole (**Q1**) filters the precursor ion that undergoes collision with nitrogen in **Q2**, resulting in a specific fragment analyzed in **Q3**.

Figure 20 shows the substance-specific fragmentation of AAMA determined by MS/MS. The mass trace *m/z* 233 → 104 gave the highest relative response in the mass spectrum and was therefore chosen for quantification. The neutral loss of 129 amu resulting from the cleavage between the sulfur and the carbon atom in the *N*-acetyl-*L*-cysteine moiety during negative electrospray ionization has been reported to be common in all mercapturic acids (*225*). Similar fragmentation was observed for all other mercapturic acids determined

during this work. For the deuterated standards, fragmentation resulted in a neutral loss of 131 amu, correspondingly.
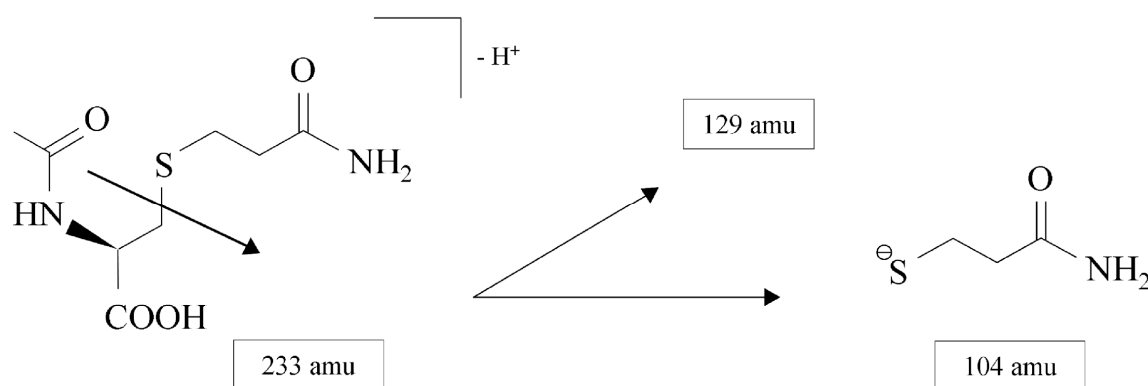
Figure 20   Specific MRM-fragmentation of AAMA following negative ESI-ionization and collision with nitrogen. The *L*-cysteine moiety is lost as a neutral fragment (129 amu). The specific mass transition *m/z* 233 → 104 is used for quantification of AAMA via HILIC-MS/MS.

4.2   Materials and Methods

4.2.1   Instrumentation

Identification and purification of synthesis products was performed with an HPLC system consisting of a quaternary solvent pump (Agilent Technologies, Waldbronn, Germany) and an autosampler (Agilent Series 1100, Agilent Technologies) coupled to a QTRAP 2000 mass spectrometer (Applied Biosystems, Darmstadt, Germany) with a TURBO-Ionspray source. An electrical valve (Valco Valve) was used for automated sample clean-up. ^{1}H-NMR (600 MHz) and ^{13}C-NMR (150 MHz) spectra were recorded on a DMX 600 or on an AMX 400 spectrometer (Bruker Biospin GmbH, Rheinstetten, Germany). For HPLC-MS/MS measurements, an HPLC system consisting of two binary solvent pumps (Agilent

Technologies) and an autosampler (Agilent Technologies) coupled to an API 3000 mass spectrometer equipped with an electrospray ionization (ESI) source (Applied Biosystems) was used. An electrical valve (Valco Valve) was applied to control the solvent flow from the two different pumps during the HILIC-MS/MS measurements of urine samples. Analyst software 1.4.1 and 1.4.2 (Applied Biosystems) was used for data acquisition and quantification. The centrifuge used was an Eppendorf Centrifuge 5403 (Hamburg, Germany). For freeze-drying of synthesis solutions, an Alpha 1 – 4 LSC Freeze Dryer (Martin Christ Gefriertrocknungsanlagen GmbH, Osterode, Germany) was applied.

4.2.2   Chemicals

Water, methanol and acetonitrile were purchased from Roth (Karlsruhe, Germany). $^{13}C_3$-AA (chemical purity >98%, isotope enrichment >99%) was purchased from CK Gas Products Ltd. (Hook, Hampshire, UK). GA (chemical purity >98%) was purchased from Toronto Research Chemicals Inc. (North York, Ontario, Canada). All other chemicals were from Sigma/Fluka (Taufkirchen, Germany) in the highest purity available and all solvents used were HPLC grade.

4.2.3   Synthesis of Glyceramide

Glyceramide was synthesized from GA by acidic hydrolysis according to Sugiyama et al. (*226*). Formic acid (15 µL, 18.3 mg, 397 µmol) was added to a solution of GA (170 mg, 1.95 mmol) in water (3.25 mL). The solution was stirred for 5 hours at 74 – 82 °C and for another 18 hours at room temperature. The yield of the oily product was 60% (123 mg, 1.17 mmol).

4.2.4   Synthesis of AAMA, $^{13}C_3$-AAMA and $^2H_3$-AAMA

Synthesis of the mercapturic acids of AA and $^{13}C_3$-AA was performed in two steps. In the first step, the cysteine-*S*-conjugates *S*-(2-carbamoylethyl)-*L*-cysteine (AA-Cys) and $^{13}C_3$-*S*-(2-carbamoylethyl)-*L*-cysteine ($^{13}C_3$-AA-Cys) were synthesized according to Calleman et al. (*53*). *L*-cysteine (600 mg, 4.95 mmol) and triethylamine (700 µL, 5.05 mmol) were dissolved in water (10 mL). After addition of AA (500 mg, 7.03 mmol) or $^{13}C_3$-AA (500 mg, 6.76 mmol), the solution was stirred at room temperature for 2.5 hours. Following addition of 100 mL acetone and subsequent washing with 3×40 mL acetone, white solid products were obtained. AA-Cys and $^{13}C_3$-AA-Cys were dried under vacuum. Yield was 97% (921 mg, 4.80 mmol) for AA-Cys and 96% (860 mg, 4.41 mmol) for $^{13}C_3$-AA-Cys.

In the second step, AA-Cys and $^{13}C_3$-AA-Cys were acetylated with acetic anhydride according to Kellert et al. (*149*) using acetic acid as solvent instead of water. $^2H_3$-AAMA was synthesized analogous to AAMA using $^2H_6$-acetic anhydride and $^2H_3$-acetic acid. AA-Cys (20 mg, 104 µmol) or $^{13}C_3$-AA-Cys (20 mg, 103 µmol) was suspended in acetic acid (2 mL) or $^2H_3$-acetic acid (2 mL). While the suspension was stirred on an ice bath, acetic acid anhydride (50 µL, 529 µmol) or $^2H_6$-acetic anhydride (50 µL, 500 µmol) was added drop-wise. Afterwards, the ice bath was removed and the now clear solution was stirred at room temperature over night. The solvent was removed by repeated addition of water and subsequent freeze-drying. Yields of the solid white products were 70% (17.0 mg, 73 µmol) for AAMA, 70% (17.1 mg, 72 µmol) for $^{13}C_3$-AAMA and 72% (17.6 mg, 74 µmol) for $^2H_3$-AAMA.

4.2.5   Synthesis of AAMA-sulfoxide, $^{13}C_3$-AAMA-sulfoxide and $^2H_3$-AAMA-sulfoxide

AAMA, $^{13}C_3$-AAMA and $^2H_3$-AAMA were transformed into sulfoxides by oxidation with hydrogen peroxide (H_2O_2) as described by Werner et al. (*227*). AAMA (23.4 mg, 0.1 mmol), $^{13}C_3$-AAMA (23.7 mg, 0.1 mmol) or $^2H_3$-AAMA (23.7 mg, 0.1 mmol) was

dissolved in acetic acid and stirred at 16 °C (melting point of acetic acid) under the stepwise addition of a 30% solution of H_2O_2 (11.3 µL, 0.11 mmol). After 60 min, the ice-bath was removed and stirring of the mixtures was continued at room temperature over night. The solvent was removed by repeated addition of water and subsequent freeze-drying. Yields of the solid white products were 85% (21.3 mg, 85 µmol) for AAMA-sulfoxide, 83% (21.0 mg, 83 µmol) for $^{13}C_3$-AAMA-sulfoxide, and 87% (22.0 mg, 87 µmol) for $^2H_3$-AAMA-sulfoxide, respectively.

4.2.6   Synthesis of $^{13}C_3$-Glycidamide

$^{13}C_3$-GA was synthesized by oxidation of $^{13}C_3$-AA with dimethyldioxirane. In the first step, dimethyldioxirane was prepared according to Adam et al. (*228*). Sodiumhydrogencarbonate (60 g, 714 mmol) was added to a mixture of water (250 mL) and acetone (200 mL, 158 g, 2.72 mol). The suspension was stirred at 0 – 5 °C (ice-bath) and Oxone® (2 $KHSO_5 \cdot KHSO_4 \cdot K_2SO_4$; 120 g, 657 mmol) was added over a period of 10 min. The ice bath was removed and the evolving gas was distilled by means of a water-jet vacuum pump (80 – 140 mbar). The condensate was collected in a cooled (-78 °C; acetone/dry ice) round bottom flask. Distillation was continued for approximately 2 hours. The yellow liquid was stored over molecular sieve 3 Å at -20 °C.

As described by Paulsson et al. (*201*), $^{13}C_3$-AA was oxidized with dimethyldioxirane in acetone to give $^{13}C_3$-GA. To a solution of dimethyldioxirane in acetone (75 mL) a solution of $^{13}C_3$-AA (500 mg, 6.76 mmol) in dichlormethane (20 mL) was added, and the mixture was stirred for 24 hours at room temperature. After checking the progress of the reaction via mass spectrometry, another 75 mL of the dimethyldioxirane solution were added and stirring was continued for another 24 hours. Then, after the progress of the reaction was checked again, the solvent was removed under vacuum (100 mbar). The oily residue was covered with *n*-pentane and stored for 4 days at -20 °C for crystallization. Subsequently, the *n*-pentane layer was removed and the solid crystals were dried under vacuum (100 mbar). For further clean-up, the solid was dissolved in acetone and all undissolved

particles were removed by filtration. Then, the solvent was removed under vacuum (100 mbar). The yield of the white solid was 80% (487 mg, 5.41 mmol).

4.2.7   Synthesis of GAMA, $^{13}C_3$-GAMA and $^2H_3$-GAMA

Analogous to the synthesis of AAMA, synthesis of the mercapturic acids of GA and $^{13}C_3$-GA was performed in two steps. In the first step, the regioisomeric cysteine conjugates *S*-(1-carbamoyl-2-hydroxyethyl)-*L*-cysteine and *S*-(2-carbamoyl-2-hydroxyethyl)-*L*-cysteine (summarized as GA-Cys) as well as $^{13}C_3$-*S*-(1-carbamoyl-2-hydroxyethyl)-*L*-cysteine and $^{13}C_3$-*S*-(2-carbamoyl-2-hydroxyethyl)-*L*-cysteine (summarized as $^{13}C_3$-GA-Cys) were synthesized (*53*). *L*-cysteine (60 mg, 495 µmol) and triethylamine (70 µL, 505 µmol) were dissolved in water (2 mL). After addition of GA (50 mg, 575 µmol) or $^{13}C_3$-GA (50 mg, 556 µmol), the solution was stirred at room temperature for 2.5 hours. Following addition of 10 mL acetone and subsequent washing with 3×5 mL acetone, white solid products were obtained. GA-Cys and $^{13}C_3$-GA-Cys were dried under vacuum. Yield was 94% (89.6 mg, 431 µmol) for GA-Cys and 97% (93.9 mg, 445 µmol) for $^{13}C_3$-GA-Cys.

In the second step, GA-Cys and $^{13}C_3$-GA-Cys were acetylated with acetic anhydride according to Kellert et al. (*149*) using acetic acid as solvent instead of water. $^2H_3$-GAMA was synthesized analogous to GAMA using $^2H_6$-acetic anhydride and $^2H_3$-acetic acid. GA-Cys (20 mg, 96.2 µmol) or $^{13}C_3$-GA-Cys (20 mg, 94.8 µmol) were suspended in acetic acid (2 mL) or $^2H_3$-acetic acid (2 mL). While the suspension was stirred on an ice bath, acetic anhydride (50 µL, 529 µmol) or $^2H_6$-acetic anhydride (50 µL, 500 µmol) was added drop-wise. Afterwards, the ice bath was removed and the now clear solution was stirred at room temperature over night. The solvent was removed by repeated addition of water and subsequent freeze-drying. Yields of the solid white products were 93% (22.4 mg, 89.5 µmol) for GAMA, 90% (21.6 mg, 85.3 µmol) for $^{13}C_3$-GAMA and 98% (23.7 mg, 94.3 µmol) for $^2H_3$-GAMA.

4.2.8   Purification and Characterization of Synthesis Products

With the exception of $^{13}C_3$-GA and glyceramide, all synthesized chemicals (endproducts) were purified by HPLC (Reprosil-Pur C18 Aq, 5 µm, 150 mm × 4.6 mm, Dr. Maisch, Ammerbuch, Germany). The compounds were dissolved in water at concentrations of approximately 1 mg/ml and samples of 50 - 100 µl were injected in a series of separations. One-sixth of the total flow of 0.75 ml/min (isocratic elution with a mixture of 98% of water containing 0.1% formic acid and 2% of acetonitrile) was split into the mass-spectrometer. By monitoring the specific mass transitions (**Table 7**) for the compounds to be isolated, fractions were collected. An electrical valve (Valco Valve) was applied to automatize the procedure.

The synthetic products were characterized by mass spectrometry in the negative ion mode after direct infusion. The declustering potential was set to -20 V and collision energy and cell exit potential were set to -30 V and -15 V, respectively.

AAMA; *m/z (%)*:	233 (89) [M – H⁻], 162 (10), 128 (1), 104 (100), 58 (12)
$^{13}C_3$-AAMA; *m/z (%)*:	236 (100) [M – H⁻], 162 (5), 107 (67), 60 (15)
$^2H_3$-AAMA; *m/z (%)*:	236 (94) [M – H⁻], 165 (13), 104 (100), 58 (14)
GAMA; *m/z (%)*:	249 (100) [M – H⁻], 128 (23), 120 (87), 75 (11), 73 (8)
$^{13}C_3$-GAMA; *m/z (%)*:	252 (79) [M – H⁻], 128 (11), 123 (100), 77 (13), 75 (11)
$^2H_3$-GAMA; *m/z (%)*:	252 (100) [M – H⁻], 131 (23), 120 (86), 75 (12), 73 (12)
AAMA-sulfoxide; *m/z (%)*:	249 (100) [M – H⁻], 178 (36), 120 (17), 116 (38), 49 (44)
$^{13}C_3$-AAMA-sulfoxide; *m/z (%)*:	252 (100) [M – H⁻], 178 (15), 116 (21), 49 (24)
$^2H_3$-AAMA-sulfoxide; *m/z (%)*:	252 (100) [M – H⁻], 181 (41), 120 (15), 119 (49), 49 (49)
Glyceramide; *m/z (%)*:	104 (100) [M – H⁻], 74 (30), 57 (6), 42 (4)

The compounds (except for glyceramide) were also characterized by ^{1}H-NMR and ^{13}C-NMR spectroscopy. Chemical shifts were determined in ppm, according to the δ-scale. $^2H_4$-methanol was used as solvent and as internal standard with a chemical shift of δ = 3.31

ppm and $\delta = 49.05$ ppm for the ^{1}H-NMR and ^{13}C-NMR measurements, respectively. Spectra were recorded at 23 °C. Purity of all compounds was determined to be >96%.

^{1}H-NMR <u>AAMA</u> (600 MHz, ^{2}H$_4$-methanol): δ = 2.08 (3H, s, CH_3), 2.50 (2H, t, SCH$_2$CH_2), 2.82 (2H, t, SCH_2CH$_2$), 2.88 (1H, dd, CHCH_2S), 3.06 (1H, dd, CHCH_2S), 4.60 (1H, dd, CHCH$_2$S) ppm.

^{13}C-NMR <u>AAMA</u> (150 MHz, ^{2}H$_4$-methanol): δ = 21.60 (*C*H$_3$), 27.18 (CH$_2$S*C*H$_2$CH$_2$), 32.80 (*C*H$_2$SCH$_2$CH$_2$), 34.74 (CH$_2$SCH$_2$*C*H$_2$), 53.06 (NH*C*H), 172.36 (*C*O), 174.11 (*C*O(O)H), 177.45 (*C*(O)NH$_2$) ppm.

^{1}H-NMR <u>GAMA</u> (600 MHz, ^{2}H$_4$-methanol): δ = 1.99 (3H, s, CH_3), 2.77 – 2.85 (1H, m, SCH_2CHOH), 2.91 – 2.99, (2H, m, SCH_2CHOH, CHCH_2S), 3.12 – 3.21 (1H, m, CHCH_2S), 4.18 – 4.28 (1H, m, SCH$_2$CHOH), 4.59 – 4.63 (1H, m, NHCHCH$_2$) ppm.

^{13}C-NMR <u>GAMA</u> (150 MHz, ^{2}H$_4$-methanol): δ = 21.66 (*C*H$_3$), 32.96 and 33.07 (S*C*HC(H)COOH), 50.0 and 50.3 (S*C*H), 61.59 and 61.63 (*C*H$_2$OH), 53.54 and 53.63 (SCH*C*(H)COOH), 174.11 (CH$_3$*C*O), 174.55 and 174.58 (*C*O$_2$H), 177.78 (*C*ONH$_2$) ppm.

^{1}H-NMR <u>iso-GAMA</u> (600 MHz, ^{2}H$_4$-methanol): δ = 1.97 (3H, s, CH_3), 2.91-2.92 (1H, m, SCHCH_2OH), 2.93-3.03 (2H, m, CHCH_2S, SCHCH_2OH), 3.12-3.17 (1H, m, CHCH_2S), 4.27-4.28 (1H, m, CHCH$_2$S), 4.46-4.50 (1H, m, SCHC(O)NH$_2$) ppm.

^{13}C-NMR <u>iso-GAMA</u> (150 MHz, ^{2}H$_4$-methanol): δ = 21.66 (*C*H$_3$), 33.67 and 33.53 (CH*C*H$_2$S), 35.85 and 36.05 (S*C*H$_2$CHOH), 53.06 and 53.12 (*C*HCH$_2$S), 70.38 and 70.41 (*C*HOHC(O)NH$_2$), 174.11 (CH$_3$*C*O), 174.55 and 174.58 (*C*O$_2$H), 177.78 (*C*(O)NH$_2$) ppm.

^{1}H-NMR <u>AAMA-sulfoxide</u> (600 MHz, ^{2}H$_4$-methanol): δ = 1.96 (3H, s, CH_3), 2.71 (2H, m, CH_2CONH$_2$), 3.04 (1H, m, SCH_2CH$_2$), 3.07 (2H, m, SCH_2CH$_2$, CHCH_2S), 3.35 (1H, m, CHCH_2S), 4.21 (1H, m, NCHCH$_2$) ppm.

^{13}C-NMR <u>AAMA-sulfoxide</u> (150 MHz, ^{2}H$_4$-methanol): δ = 21.70 (*C*H$_3$), 27.66 (CH$_2$S*C*H$_2$CH$_2$), 47.60 (*C*H$_2$SCH$_2$CH$_2$), 50.54 (CH$_2$SCH$_2$*C*H$_2$), 52.89 (NH*C*H), 171.0 (*C*O), 173.36 (*C*(O)OH), 174.06 (*C*(O)NH$_2$) ppm.

As the diastereomers of GAMA and iso-GAMA as well as the diastereomers of AAMA-sulfoxide were not measured separately, multiplets (m) were observed in the ^{1}H-NMR-spectra for the signals of the L-cysteine and AA/GA-derived protons. In the ^{13}C-NMR spectra, pairs of peaks for the L-cysteine and AA/GA-derived carbons were observed, consistent with the occurrence of pairs of diastereomers. In comparison with the unlabeled standards, the ^{2}H$_3$-labeled standards showed no signal for the L-cysteine methyl-group at $\delta = 2.08$ ppm, $\delta = 1.99$ ppm, $\delta = 1.97$ ppm, or $\delta = 1.96$ ppm (3H, s, CH_3) in the ^{1}H-NMR-spectra due to the H $\rightarrow$ ^{2}H exchange.

4.2.9   Liquid Chromatography

The Stability BS-C17 trap column (5 µm, 3 mm × 33 mm, Dr. Maisch, Ammerbuch, Germany) was preconditioned for 60 min with a mixture of 80% ACN and 20% ammonium acetate buffer (20 mM, pH 6.9) at a flow rate of 1.0 ml/min and subsequently equilibrated to 90% ACN and 10% ammonium acetate buffer for 45 min.

An electrical valve (Valco Valve) was applied to control the flow of the solvents from two pumps into two different columns (**Figure 21**). In the first step, the autosampler (Agilent Series 1100, Waldbronn, Germany) introduced the sample (100 µl) into the system and pump 1 (Agilent Series 1100, Waldbronn, Germany) delivered the mobile phase, consisting of 10% ammonium acetate buffer (20 mM, pH 6.9) and 90% acetonitrile at a flow rate of 1.0 ml/min to load the sample onto the trap column (**Figure 21A**). Sample loading and elimination of matrix components were completed after 3 min. Then, the valve switched to the eluting position and pump 2 (Agilent Series 1100) flushed the trapped analytes at 0.4 ml/min in the reverse direction from the trap column to the analytical column (**Figure 21B**). The applied solvent mixture consisted of 14% ammonium acetate buffer and 86% acetonitrile. After 6 min, the valve was switched back to loading position to prevent transfer of trapped matrix components to the analytical column (**Figure 21A**).

The trap column was flushed with 10% ammonium acetate buffer and 90% acetonitrile for another 10 min, and analysis was completed after 25 min.

(A) Loading Position
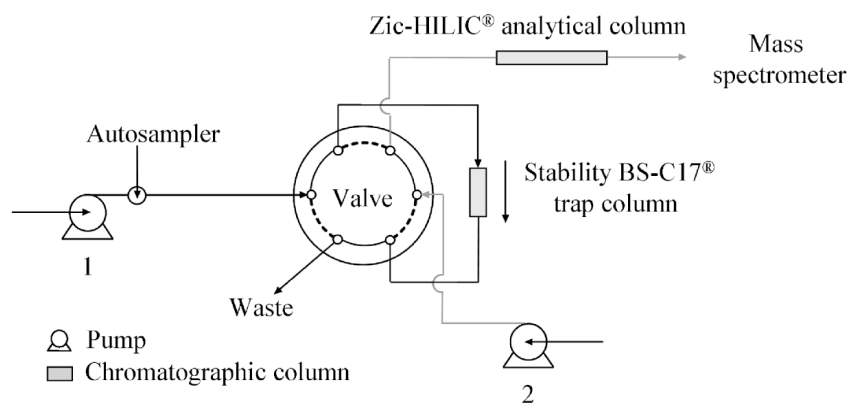
(B) Eluting Position
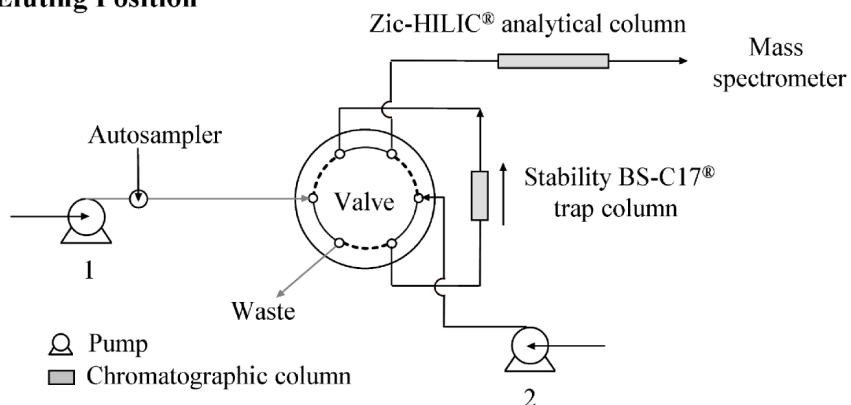
Figure 21   Column switching liquid chromatography assembly for online clean-up of urine samples and analysis of AAMA, GAMA and AAMA-sulfoxide in human and rat urine.

4.2.10 Mass Spectrometry

For the mercapturic acids of AA, highest relative responses were obtained with negative ionization. Therefore, an ion spray voltage of -3 100 V was applied. Source temperature was 400 °C. Nitrogen was used as curtain and collision gas. Focusing potential was set to -200 V and entrance potential to -10 V. For each transition analyzed by MRM, a dwell time of 100 msec was applied. Analyte specific acquisition parameters were obtained by infusion of standards using the quantitative optimization function of the Analyst 1.4.1 software (Applied Biosystems) (**Table 7**). At least two transitions were monitored for each analyte and MRMs with the highest relative response and specificities were used for quantification.

4.2.11 Calibration Curves and Quantification

For the quantification of AAMA, AAMA-sulfoxide and GAMA in urine of humans unintentionally exposed to AA from the diet or from cigarette smoke, calibration samples were prepared in human urine as matrix with concentrations of $^{13}C_3$-AAMA, $^{13}C_3$-GAMA and $^{13}C_3$-AAMA-sulfoxide ranging from 0.5 to 1 000 µg/L. Samples were prepared and analyzed in duplicate according to the methods described. Calibration curves were calculated by linear regression and weighted 1/x using the Analyst 1.4.2 software (Applied Biosystems). Due to an identical response for ^{13}C-labeled and ^{12}C-analytes, background AAMA, GAMA and AAMA-sulfoxide contents in human urine were calculated from the linear regression coefficients obtained with the ^{13}C-labeled compounds (*229*).

Table 7
MS/MS-transitions, declustering potentials (DP), collision energies (CE) and cell exit potentials (CXP) used for the detection of AAMA and $^{13}C_3$-AAMA, GAMA and $^{13}C_3$-GAMA as well as AAMA-sulfoxide and $^{13}C_3$-AAMA-sulfoxide in human and rat urine, respectively.

Transition $[M - H]^- \rightarrow$	Compound	DP (V)	CE (V)	CXP (V)
233.2 → 104.0	AAMA (quantifier)	-26	-24	- 5
233.2 → 58.0	AAMA (qualifier)	-26	-52	- 7
236.2 → 107.0	$^{13}C_3$-AAMA (quantifier)	-21	-18	-15
236.2 → 162.0	$^{13}C_3$-AAMA (qualifier)	-26	-52	- 7
236.2 → 104.0	$^2H_3$-AAMA (internal standard)	-16	-22	- 5
249.2 → 120.0	GAMA^a (quantifier)	-26	-22	- 7
249.2 → 128.0	GAMA (qualifier)	-26	-18	- 7
249.2 → 75.0	GAMA (qualifier)	-26	-48	- 1
249.2 → 73.0	iso-GAMA (qualifier)	-26	-48	-11
252.2 → 123.0	$^{13}C_3{}^b$-GAMA (quantifier)	-21	-24	-11
252.2 → 77.0	$^{13}C_3$-GAMA (qualifier)	-26	-48	- 1
252.2 → 75.0	$^{13}C_3$-iso-GAMA (qualifier)	-26	-48	-11
252.2 → 120.0	$^2H_3{}^c$-GAMA (internal standard)	-21	-24	- 9
249.2 → 116.0	AAMA-sulfoxide (quantifier)	-16	-22	- 9
249.2 → 178.0	AAMA-sulfoxide (qualifier)	-16	-14	- 9
252.2 → 116.0	$^{13}C_3$-AAMA-sulfoxide (quantifier)	-21	-24	- 9
252.2 → 178.0	$^{13}C_3$-AAMA-sulfoxide (qualifier)	-16	-14	- 9
252.2 → 119.0	$^2H_3$-AAMA-sulfoxide (internal standard)	-21	-22	- 9

[a] This transition accounts for GAMA and iso-GAMA as well. Both metabolites are quantitated together as GAMA.
[b] This transition accounts for both $^{13}C_3$-GAMA and $^{13}C_3$-iso-GAMA.
[c] This transition accounts for both $^2H_3$-GAMA and $^2H_3$-iso-GAMA.

4.2.12 Method Validation

The method was characterized for dynamic range, limit of detection (LOD, defined by a signal-to-noise ratio S/N ≥3), and limit of quantification (LOQ, S/N ≥10). LODs and LOQs were determined by analysis of urine by adding increasing concentrations of $^{13}C_3$-AAMA, $^{13}C_3$-GAMA and $^{13}C_3$-AAMA-sulfoxide. For intraday and interday precision and accuracy, urine samples (26.5 mg/dL creatinine) were spiked with three different concentrations (5 µg/L, 50 µg/L and 500 µg/L) of $^{13}C_3$-labeled analytes, split into aliquots (500 µL) and stored at -20 °C. To assess intraday precision and accuracy, the three concentrations were prepared and measured in triplicate. For interday precision and accuracy, determinations of the three concentrations were performed on three different days with new samples prepared each day from the frozen aliquots. Additionally, quality control samples (n = 50) were analyzed continuously along with the analyses. Each quality control sample was prepared individually from the same urine sample. The samples were analyzed for AAMA, GAMA and AAMA-sulfoxide on 9 different days, thus providing further data on long-term stability of the analytical method.

4.2.13 Human Study: Smokers vs. Nonsmokers

To confirm that the established method is suitable for the detection of background exposure in smoking and nonsmoking human subjects, students and PhD students (age 22 to 31) of the local university were asked to donate spot urine samples. 67 smokers (22 male and 45 female) with a self-reported cigarette consumption of more than 5 cigarettes per day, and 67 nonsmokers (21 male and 46 female) were randomly chosen to participate in the study. Spot urine samples were collected between 9:00 a.m. and 1:00 p.m.. Samples were aliquoted (5 × 2 mL) and stored at -20 °C until analysis. One aliquot (200 µL) of each sample was analyzed for content of creatinine at the local Laboratory for Clinical Chemistry. In accordance with the Declaration of Helsinki, the study was performed with

informed consent, and the study protocol was reviewed and approved by the local Institutional Review Board.

4.2.14 Sample Preparation

Frozen human urine samples were thawed, vortexed and diluted with an equal volume of acetonitrile. To remove precipitated proteins and salts, samples were centrifuged for 10 min at 4 °C and 1 400 × g followed by addition of the internal standards (IS) at a final concentration of 30 µg/L of each standard. The IS-solution was prepared by dissolving $^2H_3$-AAMA, $^2H_3$-GAMA and $^2H_3$-AAMA-sulfoxide in water at a concentration of 3 000 µg/L.

4.2.15 Analysis of Creatinine

All urine samples (aliquots of 200 µL) were analyzed for content of creatinine at the local Laboratory for Clinical Chemistry. Quantitation of creatinine was performed with a 'Cobas Integra' system creatinine plus ver. 2 (Roche Diagnostics, Mannheim, Germany).

4.3   Results and Discussion

4.3.1   Synthesis of Glyceramide

Glyceramide (2,3-dihydroxypropanamide) was synthesized from GA according to Sugiyama et al. (*226*). Acidic hydrolysis catalyzed by formic acid gave the highest yield (*60%*) compared to a range of other organic acids (e.g. acetic acid) recommended by Sugiyama et al. (**Figure 22**).
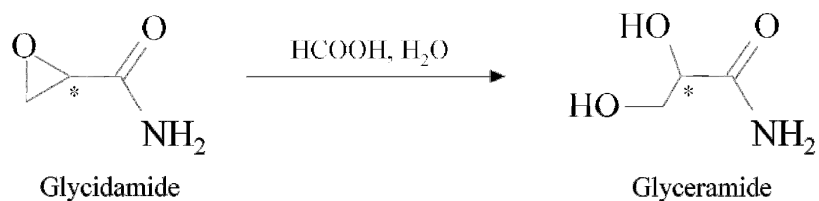
Figure 22   Acidic hydrolysis of glycidamide to glyceramide catalyzed by formic acid.

4.3.2   Synthesis of AAMA, $^{13}C_3$-AAMA and $^2H_3$-AAMA

AAMA, $^{13}C_3$-AAMA and $^2H_3$-AAMA were prepared in a double-stage synthesis. First, the *L*-cysteine-*S*-conjugates   *S*-(2-carbamoylethyl)-*L*-cysteine   (AA-Cys)   and $^{13}C_3$-*S*-(2-carbamoylethyl)-*L*-cysteine ($^{13}C_3$-AA-Cys) were synthesized according to Calleman et al. (*53*) (**Figure 23**). Yields were 96% and 97%, respectively. Because the cysteine-*S*-conjugates were too hydrophilic for preparative purification and separation via HPLC, AA-Cys and $^{13}C_3$-AA-Cys were employed directly in the following synthesis step.
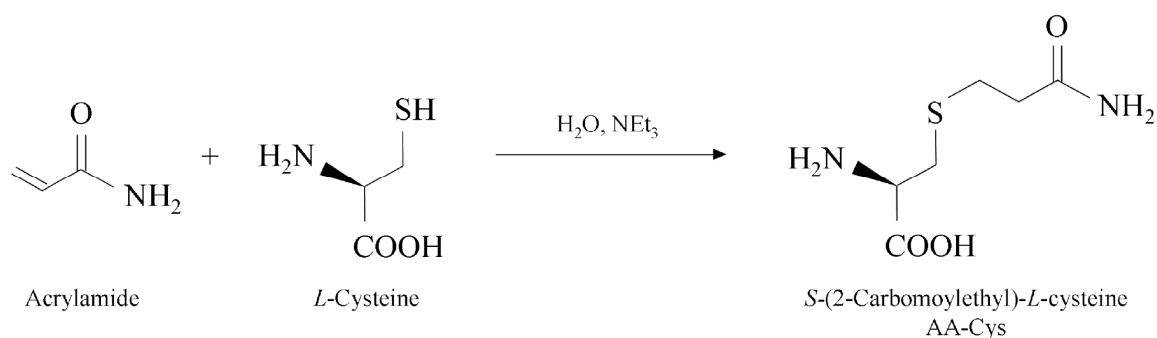
Figure 23   Synthesis of *S*-(2-carbamoylethyl)-*L*-cysteine (AA-Cys).

The *L*-cysteine-*S*-conjugates were acetylated by reaction with acetic anhydride or $^2H_6$-acetic anhydride according to Kellert et al. (*149*) to give AAMA, $^{13}C_3$-AAMA and $^2H_3$-AAMA (**Figure 24**). However, acetic acid ($^2H_3$-acetic acid) was used as solvent instead of

water to prevent premature hydrolysis of acetic acid anhydride. Yields were 70 and 72% compared to the employed quantity of AA-Cys and $^{13}C_3$-AA-Cys, respectively.
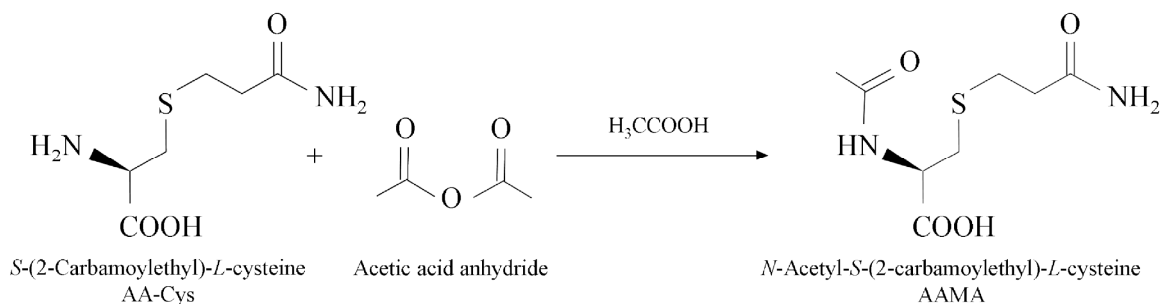
Figure 24 *N*-Acetylation of the *L*-cysteine-*S*-conjugate of acrylamide (AA-Cys). For the preparation of ^{2}H-labeled AAMA, $^2H_6$-acetic anhydride was used.

4.3.3   Synthesis of AAMA-sulfoxide, $^{13}C_3$-AAMA-sulfoxide and $^2H_3$-AAMA-sulfoxide

AAMA-sulfoxide, $^{13}C_3$-AAMA-sulfoxide and $^2H_3$-AAMA-sulfoxide were prepared by oxidation of AAMA, $^{13}C_3$-AAMA and $^2H_3$-AAMA with hydrogen peroxide (H_2O_2) as described by Werner et al. (*227*) (**Figure 25**). Care was taken to add an exact 10% excess of H_2O_2 (30%-solution) to solutions of AAMA, $^{13}C_3$-AAMA and $^2H_3$-AAMA in glacial acetic acid. A smaller amount of H_2O_2 results in incomplete reaction, whereas too much H_2O_2 produces sulfones. Yields were 85%, 83% and 87% for AAMA, $^{13}C_3$-AAMA and $^2H_3$-AAMA, respectively.
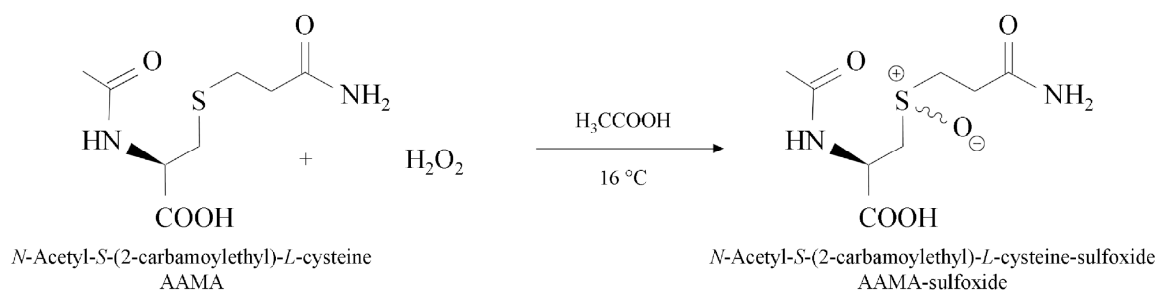
Figure 25   Sulfoxidation of AAMA with hydrogen peroxide.

4.3.4   Synthesis of $^{13}C_3$-Glycidamide

$^{13}C_3$-GA was obtained by oxidation of $^{13}C_3$-AA with dimethyldioxirane in acetone. First, dimethyldioxirane was prepared by conversion with Oxone® according to Adam et al. (*228*) (**Figure 26**).
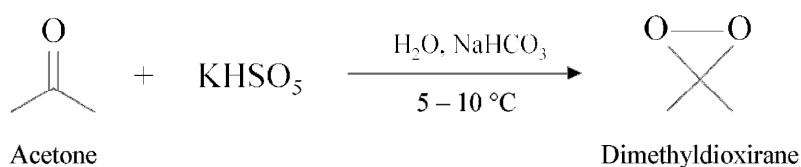
Figure 26   Synthesis of dimethyldioxirane.

AA was epoxidized to GA by reaction with dimethyldioxirane at room temperature (**Figure 27**). As dimethyldioxirane is relatively unstable under these conditions, the synthesis was carried out in two steps. The progress of the reaction was verified after the first addition of dimethyldioxirane as well as after the second addition by direct infusion of the reaction solution into the mass spectrometer (Q-TRAP 2000). The monitored mass transitions (positive ionization) were m/z 72 → 55 (i.e. loss of NH_3) and m/z 88 → 44 (i.e. loss of $CONH_2$) for AA and GA, respectively. The reaction was stopped, when AA could not be detected in the mass spectrum anymore. To remove polymerized AA from the reaction batch, the solvent was evaporated under vacuum (100 mbar) and the polymer was precipitated by addition of acetone. Drying and storage of GA was performed under nitrogen at -20 °C, as GA is very hygroscopic. Yield was 80% calculated from the employed amount of AA.
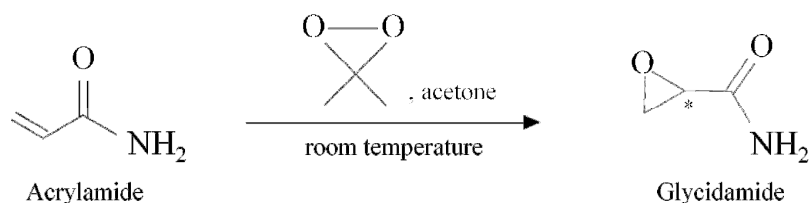
Figure 27   Epoxidation of acrylamide to glycidamide.

4.3.5   Synthesis of GAMA, $^{13}C_3$-GAMA and $^{2}H_3$-GAMA

Analogous to synthesis of AAMA, $^{13}C_3$-AAMA and $^{2}H_3$-AAMA, the mercapturic acids of GA and $^{13}C_3$-GA were synthesized in two steps. First, the *L*-cysteine-*S*-conjugates were prepared by reaction of GA and $^{13}C_3$-GA with *L*-cysteine according to Calleman et al. (*53*) (**Figure 28**). Yield was 94% and 97% for GA and $^{13}C_3$-GA, respectively. Because the cysteine-*S*-conjugates were too hydrophilic for preparative purification and separation via HPLC, the regioisomers GA-Cys and iso-GA-Cys as well as $^{13}C_3$-GA-Cys and $^{13}C_3$-iso-GA-Cys were employed directly in the following synthesis step.
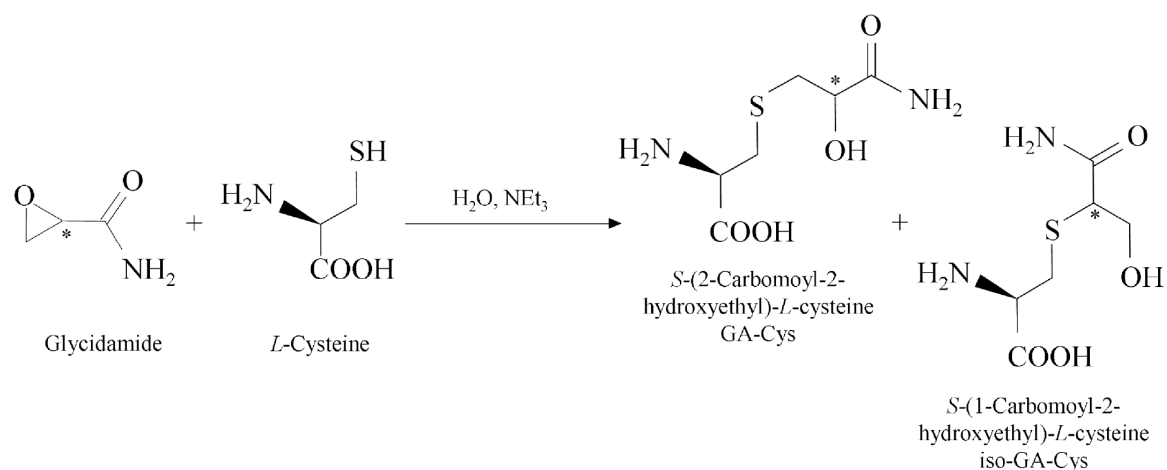
Figure 28   Synthesis of the regioisomeric cysteine-*S*-conjugates of glycidamide.

GA-Cys (both regioisomers) and $^{13}C_3$-GA (both regioisomers) were acetylated using acetic anhydride or $^{2}H_6$-acetic anhydride as described by Kellert et al. (*149*) (**Figure 29**). Acetic acid ($^{2}H_3$-acetic acid) was used as solvent instead of water to prevent acetic anhydride from hydrolysis. Thus, yields of 93%, 90% and 98% were obtained for GAMA, $^{13}C_3$-GAMA and $^{2}H_3$-GAMA, respectively.
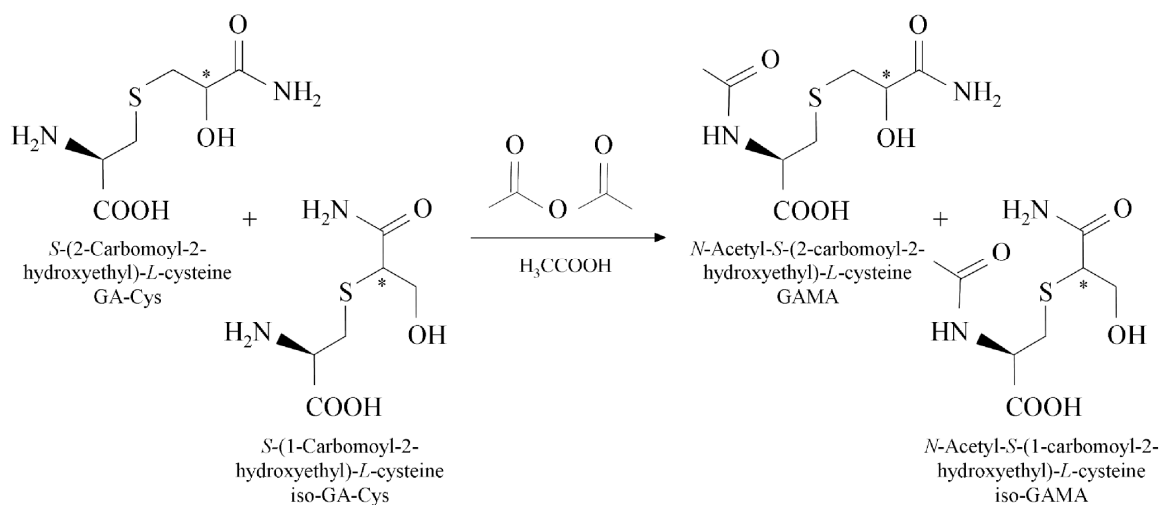
Figure 29 *N*-Acetylation of GA-Cys and iso-GA-Cys to GAMA and iso-GAMA.

4.3.6   Column Switching HILIC-MS/MS Method

LC-MS/MS Analysis of Glyceramide in Human Urine. So far, there is no LC-MS/MS method available for the quantification of glyceramide, the hydrolysis product of GA (*147*). This compound, eliminated in urine following metabolism downstream of GA, plays a crucial role for the evaluation of potential risk from GA. Whereas AAMA and AAMA-sulfoxide are urinary metabolites considered as biomarkers for detoxification, glyceramide and GAMA are metabolites derived from the mutagenic epoxide GA (*39*).

Presumably due to the lack of an easily ionizable moiety (e.g. carboxylic acid), glyceramide gave only weak response in the mass spectra recorded following negative as well as positive ionization. Several LC techniques were investigated concerning their applicability for the analysis of urinary glyceramide. However, neither HILIC-chromatography (columns tested: Zic-HILIC and Stability BS-C17) nor RP-chromatography with or without structural modifications (columns tested: ReproSil C8, ReproSil C18, ReproSil-Pur C18-AQ (all from Dr. Maisch GmbH, Ammerbuch, Germany) and Shodex ODP2 HP (Showa Denko Europe GmbH, Munich, Germany) were suitable for

efficiently retaining glyceramide. Whereas this outcome was anticipated for the RP columns, the poor retention of glyceramide on HILIC material was rather surprising. As both Zic-HILIC and BS-C17 retention is mediated by zwitterionic, resp. cationic interactions (*222, 230*), the lack of a charged moiety in glyceramide may be accountable for this result.

HILIC-MS/MS Analysis of AAMA, AAMA-sulfoxide and GAMA in Human Urine. Due to poor retention on traditional RP phases for HPLC and ion suppression by coeluting matrix components, quantification of hydrophilic compounds such as the urinary metabolites of AA by LC-MS/MS is very difficult. To minimize the influence of the urinary matrix and to increase the on-column concentration of the analytes, a simple on-line clean-up procedure was developed. By trapping the analytes on a Stability BS-C17 trap column and reversing the solvent flow, most of the interfering matrix components were removed. By applying this trap column in combination with a Zic-HILIC analytical column and MS/MS, a rapid, reliable, sensitive and specific analytical method for the simultaneous quantification of the most relevant urinary metabolites of AA was possible. AAMA, AAMA-sulfoxide and GAMA showed excellent retention on the Zic-HILIC column (**Figure 30**) and were well separated, including the regioisomers GAMA and iso-GAMA (**Figure 31**) and the two diastereomers of AAMA-sulfoxide (**Figure 32**).
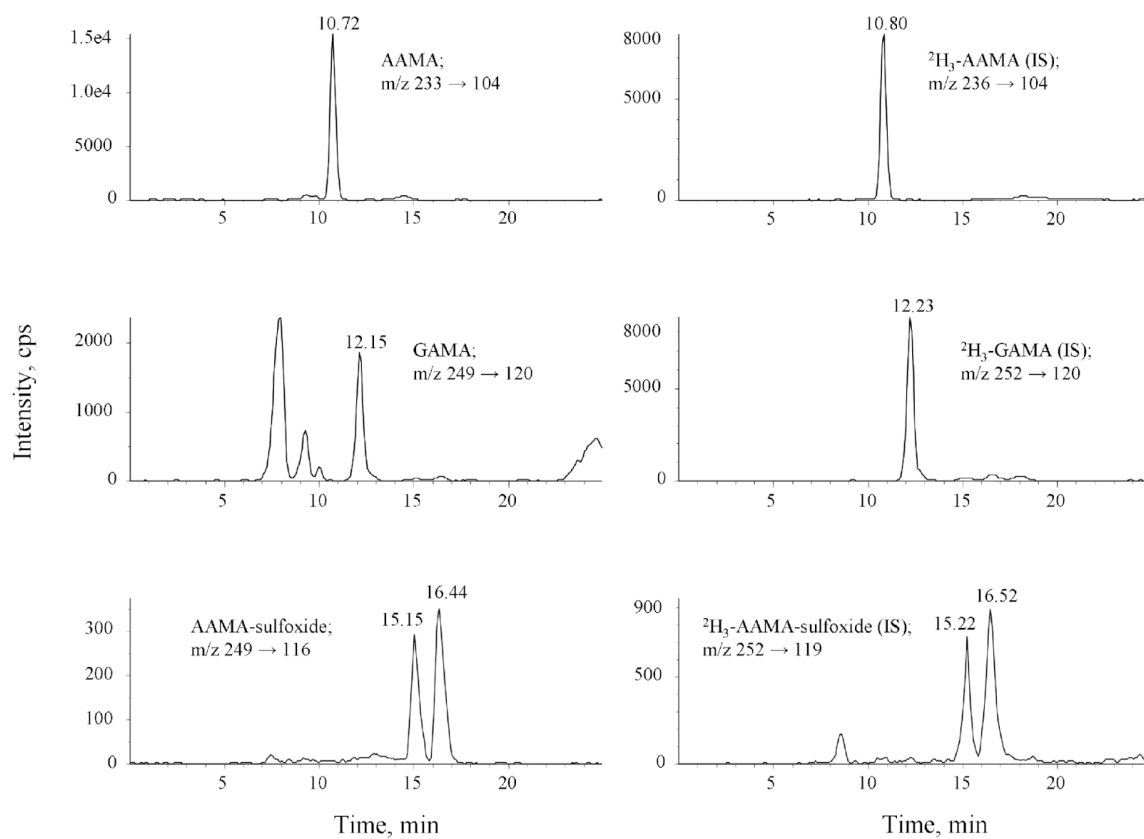
Figure 30   Chromatogram showing the mass traces for AAMA, GAMA and AAMA-sulfoxide (left-hand side) as well as of $^2H_3$-AAMA, $^2H_3$-GAMA and $^2H_3$-AAMA-sulfoxide (internal standards; right-hand side) determined in the urine of an unintentionally exposed human subject
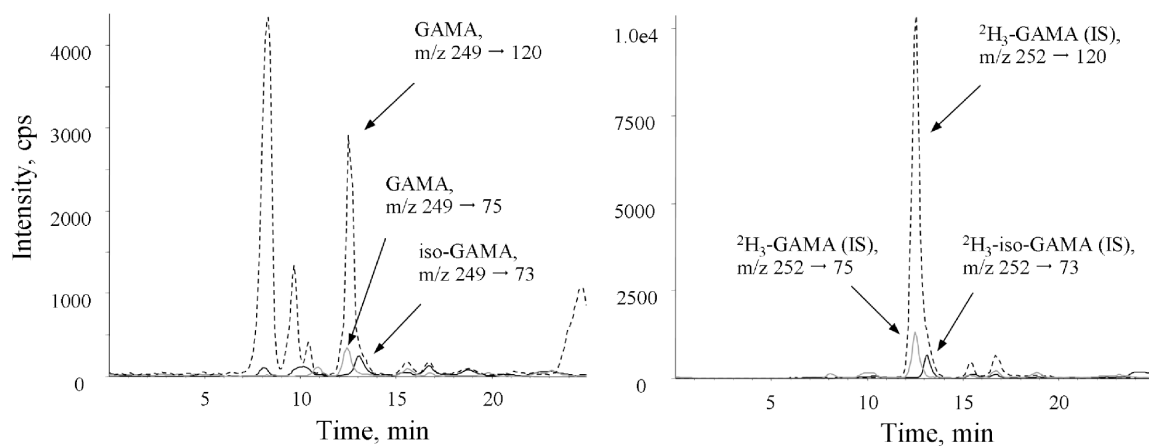
Figure 31   Chromatogram showing the mass traces for the regioisomers GAMA (grey line) and iso-GAMA (black line) as well as the mass trace accounting for both metabolites (dotted line) in the urine of a non-intentionally exposed human subject. By monitoring the common mass transition $m/z\ 249 \rightarrow 120$, both regioisomers could be conjointly quantitated. The mass traces for the corresponding internal standards are shown on the right-hand side.
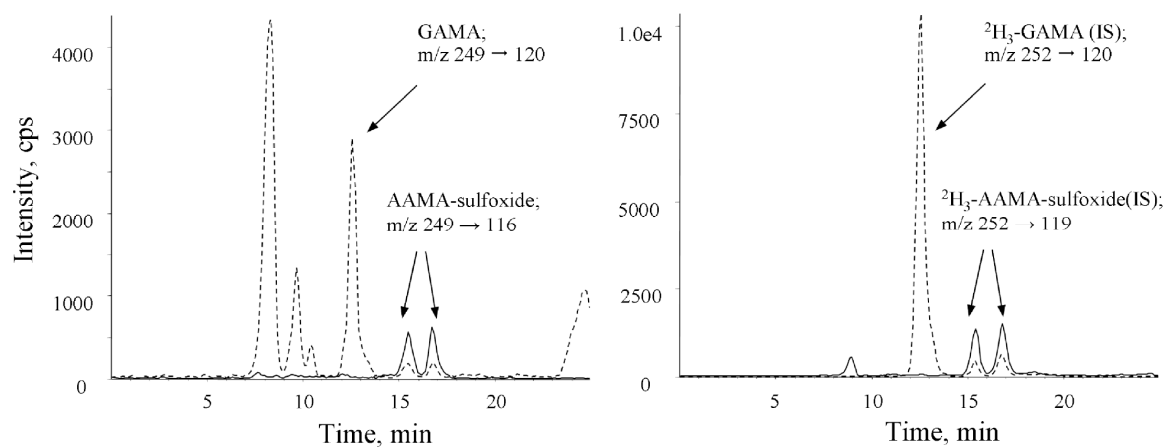
Figure 32   Chromatographic baseline separation of the isobaric urinary metabolites GAMA (dotted line) and AAMA-sulfoxide (black line). The mass traces for the corresponding internal standards are shown on the right-hand side.

GAMA and iso-GAMA were not entirely resolved chromatographically. However, both metabolites could be observed separately in the chromatogram, due to the mass transition *m/z* 249 → 73 unique to iso-GAMA (*149*) (**Figure 33**).
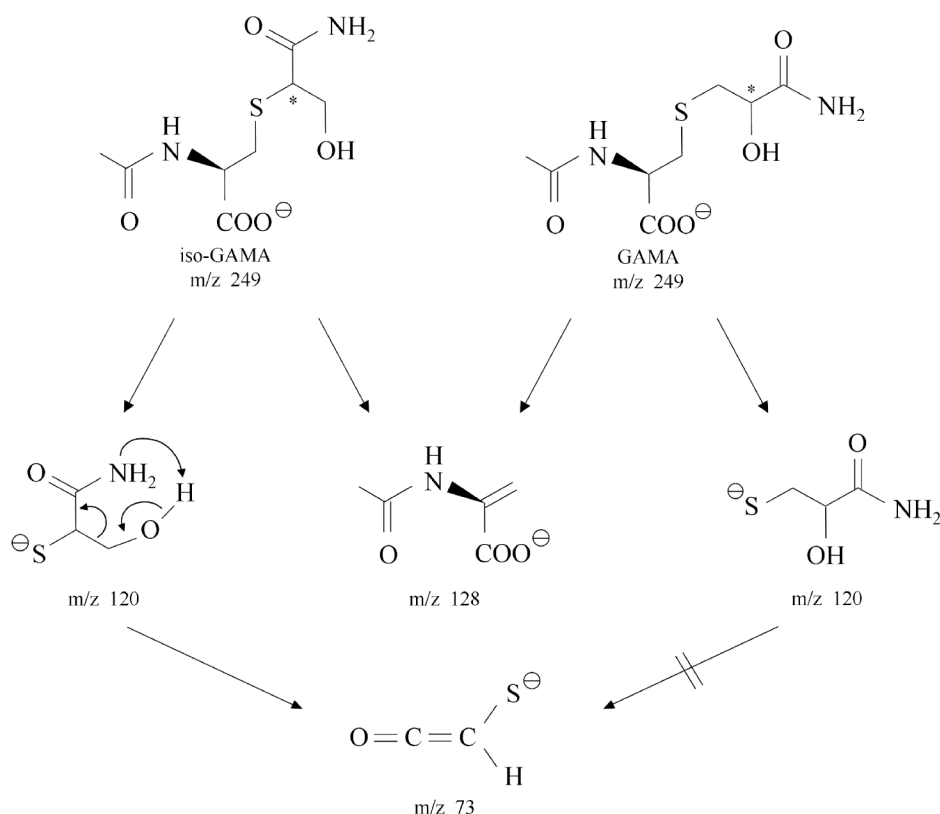
Figure 33 Fragmentation of GAMA and iso-GAMA following negative electrospray ionization and collision with nitrogen. Both mercapturic acids show a neutral loss of 129 amu (resp. *m/z* 128), resulting in isobaric fragments of *m/z* 120. The mass transition *m/z* 249 → 73 is unique to iso-GAMA due to elimination of ammonia and carbon monoxide via a specific transition state of a six-membered ring, which is not possible for GAMA. (adapted from Kellert et al., **2006** (*149*))

Due to the baseline separation of the isobaric AAMA-sulfoxide and GAMA, which share a fragmentation of *m/z* 249.2 to *m/z* 120.0 (neutral loss of 129 amu), interferences between these metabolites could be avoided. Peaks representing AAMA-sulfoxide may easily be

misinterpreted as GAMA if the peaks are not separated clearly. An inefficient separation of GAMA and AAMA-sulfoxide may explain some of the high GAMA-concentrations in human urine samples reported previously (*148, 231*). GA, the precursor of GAMA, is the DNA-reactive AA-metabolite supposedly responsible for tumor induction after AA-administration in rodents (*18, 199, 232*). Therefore, an overestimation of GAMA excretion due to interference with AAMA-sulfoxide in human urine may result in to an overestimation of the potential risk of health effects due to AA-exposures for humans.

4.3.7   Method Validation

Retention-times in HILIC-measurements vary strongly depending on the matrix and retention time shifts of up to several minutes were observed when analyzing standards of AA-metabolites using pure water or human urine samples as matrix. Therefore, the column switching method was not applicable to generate calibration curves for the AA-metabolites in water, and LODs and LOQs needed to be determined in matrix (human urine). Using the column switching method, retention time shifts between different human urine samples were negligible. Since all human urine samples contain AA-metabolites in varying concentrations, calibration curves were generated using $^{13}C_3$-labeled analytes thus avoiding extrapolation from background levels or complicated standard addition procedures (*229*). The obtained linear regression coefficients were used for calculation of metabolite concentrations, since identical concentrations of $^{13}C_3$-labeled and unlabeled standards gave almost identical peak areas (**Figure 34** and **Table 8**).
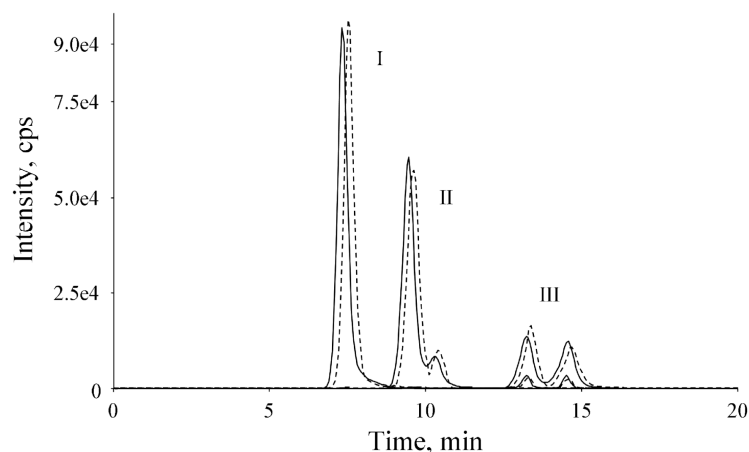
Figure 34   Chromatogram showing simultaneous analysis of unlabeled (black) and $^{13}C_3$-labeled (dotted) standards of AAMA (**I**), GAMA (**II**) and AAMA-sulfoxide (**III**) at a concentration of 500 µg/L each, using acetonitrile as solvent.

Table 8
Response factors (Area$_{^{13}C_3}$/Area$_{unlabeled}$) determined at different concentrations.

Concentration (µg/L)	AAMA			GAMA			AAMA-sulfoxide		
	Mean (n = 3)	S.D.	%CV	Mean (n = 3)	S.D.	%CV	Mean (n = 3)	S.D.	%CV
5	1.011	0.036	3.54	1.004	0.058	5.77	0.995	0.078	7.83
50	1.014	0.069	6.77	0.983	0.023	2.37	0.980	0.053	5.38
500	1.058	0.052	4.94	0.980	0.051	5.188	1.017	0.035	3.45
Pooled Mean	1.028			0.989			0.997		
Pooled S.D	0.052			0.042			0.053		
Pooled %CV	5.07			4.22			5.29		

Mean and standard deviation (S.D.) and precision (coefficient of variation, %CV).

The slopes of the calibration curves were 0.022 ($^{13}C_3$-AAMA), 0.0135 ($^{13}C_3$-GAMA) and 0.00582 ($^{13}C_3$-AAMA-sulfoxide). Calibration curves for $^{13}C_3$-AAMA, $^{13}C_3$-GAMA and $^{13}C_3$-AAMA-sulfoxide were linear up to concentrations of 1 000 µg/L with correlation coefficients r^2 = 0.9998, 0.9998 and 0.9995, respectively. LODs were 0.1 µg/L ($^{13}C_3$-AAMA), 0.5 µg/L ($^{13}C_3$-GAMA), and 1 µg/L ($^{13}C_3$-AAMA-sulfoxide), and LOQs were 0.5 µg/l ($^{13}C_3$-AAMA), 1 µg/l ($^{13}C_3$)-GAMA, and 2.0 µg/L $^{13}C_3$-AAMA-sulfoxide. The method also showed high interday and intraday precision, accuracy and reproducibility (**Table 9** and **Table 10**).

Table 9
Precision data for the determination of AAMA, GAMA and AAMA-sulfoxide in 50 individually prepared quality control samples of the same urine (test of robustness).

		AAMA	GAMA	AAMA-sulfoxide
Quality Control samples	Mean (µg/L)	14.4	2.56	12.4
	S.D.	0.91	0.30	1.63
(n = 50)	%CV	6.31	11.83	13.1

Mean and standard deviation (S.D.; n = 50) and precision (coefficient of variation, CV)

Table 10

Analytical performance for the determination of $^{13}C_3$-AAMA, $^{13}C_3$-GAMA and $^{13}C_3$-AAMA-sulfoxide in human urine.

Expected concentration (µg/L)	$^{13}C_3$-AAMA				$^{13}C_3$-GAMA				$^{13}C_3$-AAMA-sulfoxide			
	Mean (µg/L)	S.D.	%CV	Accy	Mean (µg/L)	S.D.	%CV	Accy	Mean (µg/L)	S.D.	%CV	Accy
interday												
500	528	24.0	4.5	106	561	8.33	1.5	112	548	53.5	9.8	110
50	50.0	2.29	4.6	99.3	52.9	3.50	6.6	106	48.5	2.69	5.5	97.0
5	4.85	0.31	6.4	97.0	4.58	0.44	9.6	91.5	4.29	0.65	15.2	85.8
intraday												
500	520	20.0	3.9	104	545	37.0	6.8	109	575	10.4	1.8	115
50	50.0	1.79	3.6	99.9	52.4	4.09	7.8	105	50.1	0.10	0.2	100
5	4.82	0.36	7.4	96.5	4.70	0.33	7.0	94.1	4.75	0.16	3.4	95.1

Mean and standard deviation (S.D.; n = 3), interday and intraday precision (coefficient of variation, %CV) and accuracy (Accy).

4.3.8   Analysis of AAMA, AAMA-sulfoxide and GAMA in Urine

The average daily dietary exposure to AA in adults ranges from approximately 0.3 to 0.6 µg/kg b.w. (**Table 3**). Another major source of AA in the general public is cigarette smoke (*27*). Approximately $1 - 2.3$ µg AA are inhaled per cigarette (*171*). Because smoking is a major contributor to the overall AA exposure in the general population and because it is a major risk factor for certain cancers (*233*), estimating the effect of smoking on the overall exposure in the general public is of great interest.

To determine the background burden of AA in the general population with respect to smoking habits, as well as to prove the applicability of the HILIC-MS/MS method for simultaneous quantification of the major AA-derived metabolites in urine, spot urine samples of 67 smokers (22 male and 45 female) and 67 nonsmokers (21 male and 46 female) were analyzed for AAMA, AAMA-sulfoxide and GAMA. Spot-urine samples were collected and one aliquot of each sample was analyzed for content of creatinine (mg/dL). Median concentrations for creatinine were 114 mg/dL (range: $7.7 - 570$ mg/dL) in smokers and 130 mg/dL (range: $19.6 - 673$ mg/dL) in nonsmokers. Concentrations of AAMA, AAMA-sulfoxide and GAMA are shown in **Table 11**.

Smokers excreted approximately 4 times more AAMA and AAMA-sulfoxide than non-smokers and 3 times more GAMA. This is in good accordance with previously reported ratios of urinary excreted metabolites (*148*). Statistical evaluation (Student´s t-Test) showed significant difference ($p < 0.001$) concerning the concentrations of the respective metabolites excreted in urine of smokers or nonsmokers. This suggests, that in human subjects smoking more than 5 cigarettes per day, excretion of AA-derived metabolites is mainly influenced by smoking, and that by reducing the amount of cigarettes smoked per day or by altogether quitting smoking, the AA burden can be reduced drastically. The metabolic ratio (GAMA : (AAMA + AAMA-sulfoxide)) was significantly lower in smokers compared to nonsmokers ($p < 0.001$), thus confirming previously reported results concerning the metabolic ratio GAMA : AAMA (*148*).

Table 11
Biomonitoring of AAMA, AAMA-sulfoxide and GAMA in urine of smokers and nonsmokers.

	AAMA (µg/L)	AAMA-sulfoxide (µg/L)	GAMA (µg/L)	AA : GA[a]
Nonsmokers (n = 67)				
Median	39 (35)[b]	30 (26)[b]	9 (7)[b]	0.11
Range	6 - 283 (11 - 78)[b]	7 - 121 (8 - 64)[b]	2 - 79 (3 - 13)[b]	0.07 - 0.26
Smokers (n = 67)				
Median	165 (132)[b]	121 (108)[b]	25 (22)[b]	0.09
Range	14 - 1018 (5 - 563)[b]	16 - 761 (13 - 556)[b]	4 - 172 (7 - 69)[b]	0.03 - 0.25
All (n = 134)				
Median	69 (61)[b]	50 (46)[b]	13 (10)[b]	0.11
Range	6 - 1018 (5 - 563)[b]	7 - 761 (8 - 556)[b]	2 - 172 (3 - 69)[b]	0.03 - 0.26

[a] Ratio GAMA : (AAMA + AAMA-sulfoxide).
[b] Concentration calculated in ng/mg creatinine.

Values obtained for urinary concentrations of AAMA and GAMA are in good agreement with those obtained previously (**Table 12**). Representing approximately 37% of the quantitated analytes, AAMA-sulfoxide could be verified as a major metabolite excreted in human urine following unintentional exposure to AA from the diet or smoking.

4.4   Conclusions

A highly sensitive and specific analytical method was established and validated for the simultaneous quantification of the hydrophilic urinary metabolites of AA. The application of an on-line sample clean-up system resulted in excellent retention and separation of the analytes, thereby avoiding time-consuming sample preparation prior to LC-MS/MS. For the first time, AAMA-sulfoxide could be determined in urine samples of the general population, thus confirming previous reports that AAMA may be *S*-oxidized in humans (*38*).

Table 12
Comparison of metabolite excretion in human urine after acrylamide exposure from the diet and/or cigarette smoke.

Exposure	AAMA[a]	AAMA-sulfoxide	GAMA	GA:AA[b]	Reference
Nonsmokers (n = 16)	29 µg/L	ND	5 µg/L[d]	0.22	(*145*)
Smokers (n = 13)	127 µg/L	ND	19 µg/L	0.15	
Overall (n = 29)	60 µg/L	ND	8 µg/L	0.16	
Nonsmokers (n = 5)	29 µg/L	ND	17 µg/L[d]	0.46	(*231*)
Smoker (n = 1)	337 µg/L	ND	111 µg/L	0.25	
Overall (n = 6)	35 µg/L	ND	19 µg/L	0.40	
Nonsmokers (n = 60)	41.6 µg/L	ND	8.7 µg/L[d]	0.18	(*148*)
Smokers (n = 60)	107.3 µg/L	ND	15.0 µg/L	0.13	
Nonsmokers (n = 13)	26 µg/L	ND	3 µg/L[d]	0.12	(*149*)
Occ. smokers (n = 12)	56 µg/L	ND	9 µg/L	0.16	
Smokers (n = 13)	283 µg/L	ND	20 µg/L	0.07	
Overall (n = 38)	58 µg/L	ND	8 µg/L	0.14	
Nonsmokers (n = 47)	32 µg/L	NQ	3 µg/L[d]	0.07	(*150*)
Smokers (n = 6)	184 µg/L	NQ	10 µg/L	0.06	
Nonsmokers (n = 67)	39 µg/L	30 µg/L	9 µg/L[f]	0.11	This study
Smokers (n = 67)	165 µg/L	121 µg/L	25 µg/L	0.09	
Overall (n = 134)	69 µg/L	50 µg/L	13 µg/L	0.11	

ND = not determined; NQ = not quantified.
[a] AAMA, AAMA-sulfoxide and GAMA calculated as median concentration (µg/L) in urine.
[b] ratios of GA-derived metabolites to AA-derived metabolites excreted in human urine.
[c] median overall excretion of metabolites in urine calculated as AA-equivalents (µg/24h).
[d] GAMA quantitated without iso-GAMA.
[e] excretion of AA-equivalents (µg/24h) calculated from mean excretion of AAMA and GAMA (µg) within 24 hours (see reference).
[f] GAMA includes both GAMA and iso-GAMA.

5 Human Biomonitoring of Acrylamide Exposure

5.1   Introduction

Apart from exposure assessments calculated from the amount ingested, the internal dose can also be derived from the actually measured *in vivo* doses. In general, biomonitoring concerning human exposure to AA is done by analysis of Hb-adducts as has already been indicated in **Chapter 2.3.1**. However, as measurements in urine represent a non-invasive method for the evaluation of the AA burden in a human subject, this approach was chosen for human biomonitoring of AA exposure.

Prior to the human biomonitoring study however, several aspects of AA biotransformation and kinetics of elimination had to be taken into consideration. Whereas measurements of Hb-adducts of AA and GA deliver insight into background exposure over an interval of up to 120 days (medium life-span of the erythrocyte), measurements of urinary AA metabolites are more suitable for the determination of short-time exposures. Due to the relatively fast excretion of the hydrophilic metabolites, high interindividual variability of

the excretion pattern can be expected, influenced by factors such as time of day, time of sampling after last food consumption or last urination and variable diets from day to day (*234*). To avoid most of these problems, and to obtain a good approximation on the actual background exposure levels, human subjects participating in this study were asked to collect all urine excreted over a period of 72 hours in intervals of 8 hours. Thus, intra-day, as well as inter-day variation concerning the excretion of AA metabolites could be retraced. Additionally, food consumption was documented in food diaries to allow retrospective correlation of fluctuations in metabolite excretion to dietary exposure to AA. Nonsmokers were chosen for this experiment, thus avoiding overlap due to mixed exposures.

5.2   Materials and Methods

5.2.1   Human Study: Biomonitoring of Dietary Acrylamide Exposure

Urine samples were obtained from healthy human subjects (three female and three male subjects, body weights between 52 and 75 kg, age between 23 and 28 years). All subjects were nonsmokers and did not drink alcoholic beverages 72 hours before and during the study. The study participants were asked to avoid known major dietary AA sources such as potato chips and French fries while otherwise keeping to their usual dietary habits. Urine samples from the subjects were collected in intervals of 8 hours over 72 hours (0 – 8, 8 – 16, 16 – 24, 24 – 32, 32 – 40, 40 – 48, 48 – 56, 56 – 64 and 64 – 72 hours). Individual urine volumes were recorded and five aliquots (2 mL) were stored at -20 °C until analysis. One aliquot of each sample was analyzed for content of creatinine at the local Laboratory for Clinical Chemistry. In accordance with the Declaration of Helsinki, the study was performed with informed consent, and the study protocol was reviewed and approved by the local Institutional Review Board.

5.2.2 Sample Preparation

Frozen human urine samples were thawed, vortexed and diluted with an equal volume of acetonitrile. To remove precipitated proteins and salts, samples were centrifuged for 10 min at 4 °C and 1 400 × g followed by addition of the internal standards (IS) at a final concentration of 30 µg/L of each analyte. The IS-solution was prepared by dissolving ^{2}H$_3$-AAMA, ^{2}H$_3$-GAMA and ^{2}H$_3$-AAMA-sulfoxide in water at a concentration of 3 000 µg/L. All urine samples were analyzed for content of creatinine as described in **Chapter 4.2.15**.

5.2.3 HILIC-MS/MS Analysis of AAMA, AAMA-sulfoxide and GAMA

AAMA, AAMA-sulfoxide and GAMA excreted in human urine following unintentional exposure to AA via the diet were analyzed and quantitated according to the methods described in **Chapter 4**. Again, ^{13}C-labeled analogues were used for preparation of calibration curves to avoid interferences with urinary background metabolites of AA (*229*). LODs and LOQs for ^{13}C$_3$-AAMA, ^{13}C$_3$-GAMA and ^{13}C$_3$-AAMA-sulfoxide remained unchanged at 0.1, 0.5 and 1 µg/L and 0.5, 1 and 2 µg/L, respectively.

5.3 Results and Discussion

For biomonitoring of average AA-metabolite excretion, urine from six human subjects was collected over 72 hours in 8 hour intervals (**Figure 35**). The median values of AA-metabolites excreted with urine (µg/L and ng/mg creatinine) give a good estimate of the average exposures of the human subjects to AA (**Table 13**) since variations in urinary concentrations of AA-metabolites arising from temporal factors within a day (e.g., time of sampling after food consumption or last urination) and across days (e.g., variable diets from day to day) are averaged out by monitoring over a prolonged period. The median

values for AAMA and GAMA of the nonsmoking subjects were in good accordance with previously reported data (**Table 14**). As already observed in smokers and nonsmokers (**Chapter 4**), AAMA-sulfoxide was demonstrated to be a major metabolite of AA representing approximately 38% of the metabolites excreted in urine.

Assuming continuous ingestion of acrylamide with the diet and accordingly, constant excretion of metabolites with urine, the daily intake of AA corresponds directly to the daily excretion of urinary metabolites. The overall daily excretion with urine calculated as AA-equivalents was 33.5 µg/24 hours (range: 19.7 – 50.4 µg/24 hours) for the six subjects. Accordingly, an intake of AA of 0.5 µg/kg b.w. per day (range: 0.25 - 0.81 µg/kg b.w. per day) was calculated in agreement with the exposure estimates summarized in **Table 2**.

Since the study participants tried to avoid food known as major AA sources, metabolite concentrations in urine varied only marginally over time. The impact of foods with higher AA-contents and the suitability of the method to detect changes in AA-intake are confirmed by the excretion profiles in subject M3, who had a meal of French fries on day three. This increase in exposure to AA was rapidly reflected by an increase in AA metabolite excretion (**Figure 35**). An additional excretion of 22.3 µg AA-equivalents (AAMA, AAMA-sulfoxide and GAMA excreted in urine) was observed during day three as compared to days one and two which is in good accordance with average contents of 28.3 – 48.8 µg AA in French fries per portion (70 g) (*176*).
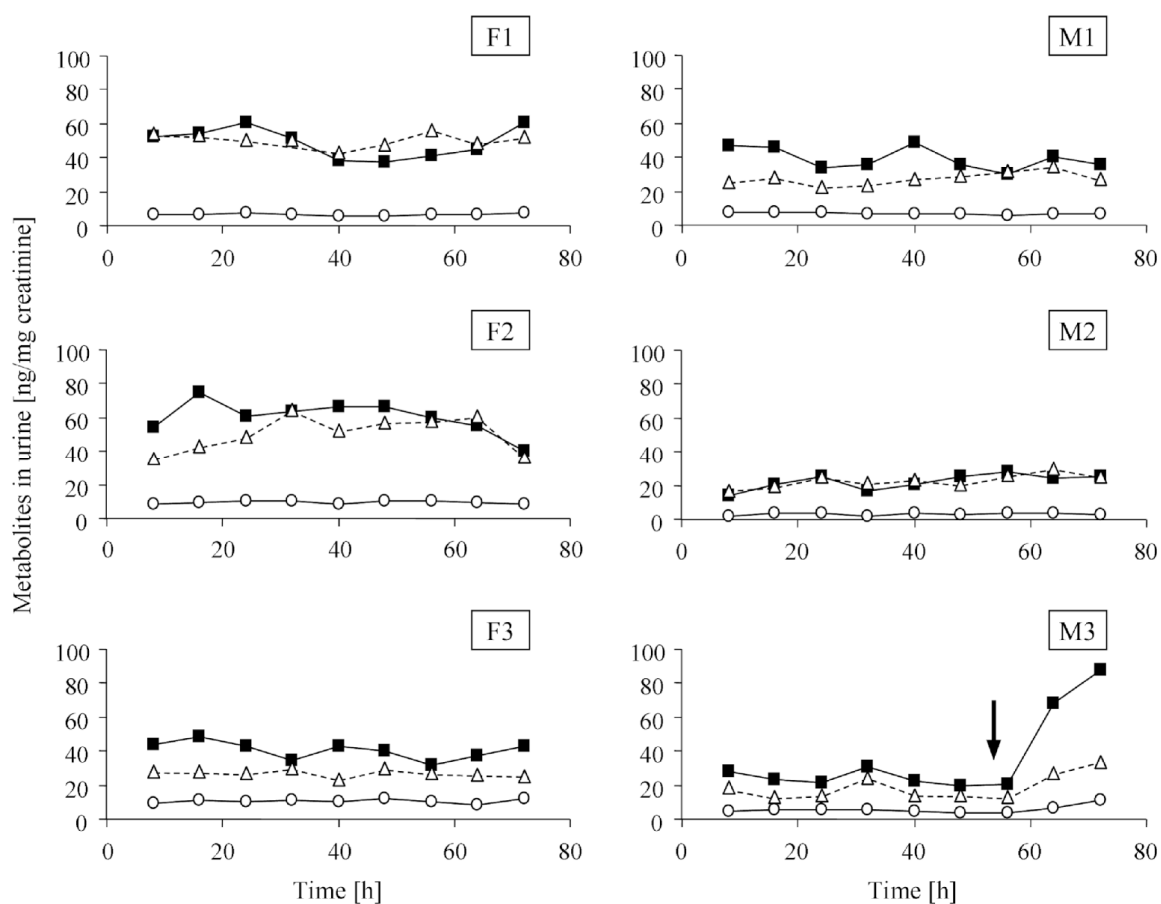
Figure 35   Urinary excretion of AAMA (■), GAMA (○) and AAMA-sulfoxide (Δ) in the urines
of six unintentionally exposed human subjects (3 female, **F1**-**F3**; 3 male, **M1**-**M3**)
determined over 72 hours in intervals of 8 hours. The arrow indicates the ingestion of
French fries by participant **M3**.

Table 13
Urinary concentrations of AAMA, AAMA-sulfoxide and GAMA.

Participant	AAMA (µg/L)	AAMA-sulfoxide (µg/L)	GAMA (µg/L)	GA : AA[a]
F1 (n = 9)				
Median	22 (52)[b]	27 (50)[b]	4 (6)[b]	0.07
Range	10 - 72 (37 - 61)[b]	11 - 70 (43 - 56)[b]	1 - 9 (6 - 8)[b]	0.06 - 0.07
F2 (n= 9)				
Median	36 (61)[b]	31 (52)[b]	7 (10)[b]	0.08
Range	11 - 64 (40 - 74)[b]	10 - 55 (35 - 64)[b]	2 - 11 (8 - 11)[b]	0.07 - 0.11
F3 (n = 9)				
Median	37 (43)[b]	23 (27)[b]	9 (10)[b]	0.15
Range	15 - 78 (31 - 48)[b]	11 - 57 (24 - 29)[b]	4 - 24 (9 - 12)[b]	0.14 - 0.18
M1 (n = 9)				
Median	25 (36)[b]	15 (28)[b]	4 (7)[b]	0.10
Range	8 - 47 (30 - 49)[b]	10 - 32 (23 - 35)[b]	2 - 11 (5 - 8)[b]	0.08 - 0.10
M2 (n = 9)				
Median	16 (25)[b]	14 (23)[b]	2 (3)[b]	0.07
Range	8 - 38 (14 - 29)[b]	8 - 37 (16 - 30)[b]	1 - 7 (2 - 4)[b]	0.05 - 0.09
M3 (n = 9)				
Median	14 (24)[b]	10 (14)[b]	3 (5)[b]	0.11
Range	11 - 80 (20 - 88)[b]	7 - 31 (13 - 34)[b]	2 - 10 (4 - 11)[b]	0.07 - 0.15
Overall (n = 54)[c]				
Median	24 (40)[b]	17 (28)[b]	4 (7)[b]	0.09
Range	8 - 80 (14 - 88)[b]	7 - 70 (13 - 64)[b]	1 - 24 (2 - 12)[b]	0.05 - 0.18

[a] Ratio GAMA:(AAMA+AAMA-sulfoxide).
[b] Urinary concentrations related to creatinine (ng/mg creatinine).
[c] Median and range calculated from all 54 samples derived from the six individuals over 9 consecutive sampling periods.

Table 14

Comparison of metabolite excretion in human urine after acrylamide exposure from the diet and/or cigarette smoke.

Exposure	AAMA[a]	AAMA-sulfoxide	GAMA	GA:AA[b]	Excretion of AA-equivalents (µg / 24 hours)[c]	Reference
Nonsmokers (n = 16)	29 µg/L	ND	5 µg/L[d]	0.22	NC	(145)
Smokers (n = 13)	127 µg/L	ND	19 µg/L	0.15	NC	
Overall (n = 29)	60 µg/L	ND	8 µg/L	0.16	NC	
Nonsmokers (n = 5)	29 µg/L	ND	17 µg/L[d]	0.46	35	(231)
Smoker (n = 1)	337 µg/L	ND	111 µg/L	0.25	305	
Overall (n = 6)	35 µg/L	ND	19 µg/L	0.40	38	
Nonsmokers (n = 60)	41.6 µg/L	ND	8.7 µg/L[d]	0.18	26.7[e]	(148)
Smokers (n = 60)	107.3 µg/L	ND	15.0 µg/L	0.13	64.1	
Nonsmokers (n = 13)	26 µg/L	ND	3 µg/L[d]	0.12	NC	(149)
Occ. smokers (n = 12)	56 µg/L	ND	9 µg/L	0.16	NC	
Smokers (n = 13)	283 µg/L	ND	20 µg/L	0.07	NC	
Overall (n = 38)	58 µg/L	ND	8 µg/L	0.14	NC	
Nonsmokers (n = 47)	32 µg/L	NQ	3 µg/L[d]	0.07	16	(150)
Smokers (n = 6)	184 µg/L	NQ	10 µg/L	0.06	74	
Nonsmokers (n = 54)[g]	24.0 µg/L	16.7 µg/L	3.8 µg/L[f]	0.09	33.5	This study

ND = not determined; NQ = not quantified; NC = not calculated.

[a] AAMA, AAMA-sulfoxide and GAMA calculated as median concentration (µg/L) in urine.
[b] ratios of GA-derived metabolites to AA-derived metabolites excreted in human urine.
[c] median overall excretion of metabolites in urine calculated as AA-equivalents (µg/24h).
[d] GAMA quantitated without iso-GAMA.
[e] excretion of AA-equivalents (µg/24h) calculated from mean excretion of AAMA and GAMA (µg) within 24 hours.
[f] GAMA includes both GAMA and iso-GAMA.
[g] median values calculated from 54 urine samples derived from the six individuals over 9 consecutive sampling intervals.

Interindividual differences in expression and activity exist for most of the enzymes involved in biotransformation of exogenous chemicals. Such variations may be caused by genetic polymorphisms, induction or inhibition of the enzyme by xenobiotics or environmental factors, and also by physiological (e.g. age or pregnancy) or pathophysiological (e.g. liver disease) conditions (*76*). Polymorphisms could influence the risk from hazardous substances. Accordingly, individuals with impaired enzyme activity could be at a higher risk if major elimination or detoxification pathways are affected and at a lower risk if the affected enzyme is responsible for bioactivation.

Individual calculation of the ratio GAMA : (AAMA + AAMA-sulfoxide) for each study participant and interindividual comparison showed significant differences as determined by Students t-Test (p-value <0.001). Whereas two participants (F1 and M2) exhibited significantly lower metabolic ratios, one subject (F3) had a significantly higher ratio compared to the others (**Table 11** and **Figure 36**). Similar results were obtained for the ratio GAMA : AAMA. Whether these results are due to genetic polymorphisms or to other factors such as temporal changes in the activity of metabolizing enzymes is not clear. A possible explanation could be the influence of body weight or body fat, roughly characterized by the body-mass-index (BMI = weight (kg) × height^{-2} (kg^{-2})). With increased BMI (range: 19.5 – 25.7), an increased metabolic ratio was observed with the most pronounced effects among female subjects. However, with only six participants, the study cohort is much too small to generate general conclusions on the occurrence and etiology of interindividual differences in AA metabolism.

In the future, a similar study design (e.g. with standardized meals) combined with genotyping and measurement of catalytic enzyme activity in a larger study cohort may help understand the underlying mechanisms.

In terms of risk assessment, it must be noted that, since both the parent AA and the metabolite GA have adverse effects, different catalytic activities of CYP 2E1 may result in different spectra of adverse effects.
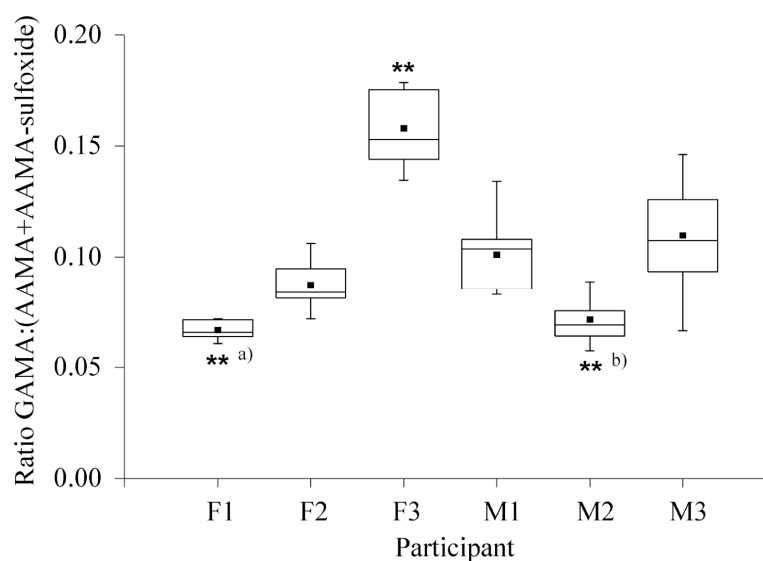
Figure 36   Interindividual differences in acrylamide biotransformation in six human subjects (3 females, **F1-F2**; 3 males, **M1-M3**) during nine consecutive 8-hour sampling periods, demonstrated by the metabolic ratio GAMA : (AAMA + AAMA-sulfoxide). Box-plots display median values, 25th and 75th percentiles (box), and mean concentrations (■) as well as minimum and maximum values (whiskers).
[a)]Ratios for **F1** were significantly different (p-value <0.001) from all other participants except **M2**.
[b)]Ratios for **M2** were significantly different (p-value <0.001) from all other participants except **F1**.

5.4   Conclusions

By monitoring the excretion of the major urinary metabolites of AA in six nonsmoking human subjects, the median daily exposure to AA from food was determined to be approximately 0.5 µg/kg b.w.. This value is in excellent agreement with estimates based on AA concentrations in food and on food consumption surveys (**Table 3**). It has also been shown that in this study cohort, the excretion of AA-derived metabolites in urine varied only marginally over time, whereas the intake of food with high content of AA (e.g. French fries) was instantly reflected in an increase in metabolite concentration. Additionally, possible inter-individual differences in AA biotransformation were evaluated. This may be an important issue for future risk assessment of AA, as variation in the extent of formation of GA possibly results in differences in risk for cancer mediated by AA.

6 Biotransformation and Toxicokinetics of Acrylamide in Rats

6.1   Introduction

Rodent metabolism of AA has been studied thoroughly over the last years. However, all of these studies were performed using doses exceeding human exposure by several orders of magnitude. Also, no effort was made to determine AAMA-sulfoxide in rat or mouse urine. In order to provide a suitable basis for inter-species comparability of biotransformation and toxicokinetics of AA, male Fischer 344 rats were exposed orally to a single dose of 20 µg/kg b.w. and of 100 µg/kg $^{13}C_3$-AA. b.w., respectively, thus representing a possible worst case AA uptake in humans from highly contaminated foodstuffs such as French fries or gingerbread (*181*).

6.2 Materials and Methods

6.2.1 Rat Study: Animals and Handling

Male Fischer 344 rats were purchased from Harlan-Winkelmann (Borchen, Germany) and acclimatized for seven days. Standard feed (ssniff® Spezialdiäten GmbH, Soest, Germany) and water were supplied *ad libitum* and animals were maintained under standards conditions (12 hour light-dark cycle, temperature $21 - 23\,°C$, humidity $45 - 55\%$). All animal experimentation was performed under permit from the appropriate authorities in an approved animal care facility of the department. Prior to exposure to $^{13}C_3$-AA, rats were transferred into plastic metabolic cages (one rat per cage) for 24 hours to collect predose urine. At the time of dosing, the animals weighed $192 - 224$ g and were 9 weeks old. Five animals were administered a single dose of $20\,\mu g/kg$ b.w. (270.27 nmol/kg b.w.) $^{13}C_3$-AA and another five animals were exposed to a single dose of $100\,\mu g/kg$ b.w. (1.351 µmol/kg b.w.) $^{13}C_3$-AA in deionized water via oral gavage. Control animals (n = 5) were administered vehicle only. $^{13}C_3$-AA was used instead of unlabeled AA to prevent interference with AA from the rat feed. Immediately after dosing, the rats were transferred back into the metabolic cages and urine was collected on ice in predetermined intervals $(0 - 6,\ 6 - 12,\ 12 - 24,\ 24 - 29,\ 29 - 34,\ 34 - 48,\ 48 - 58,\ 58 - 72,\ 72 - 82$ and $82 - 96$ hours). Urine volumes were recorded and samples were aliquoted (500 µL) and stored at -20 °C until analysis by HILIC-MS/MS.

6.2.2 Sample Preparation

Frozen rat urine samples were thawed, vortexed and diluted with one part water and two parts acetonitrile. To remove precipitated proteins and salts, samples were then centrifuged for 10 min at $4\,°C$ and $1\,400 \times g$ followed by addition of the internal standards (IS) at a final concentration of $30\,\mu g/L$ of each standard. The IS-solution was prepared by

dissolving ^{2}H$_3$-AAMA, ^{2}H$_3$-AAMA-sulfoxide and ^{2}H$_3$-GAMA in water at a concentration of 3 000 µg/L.

6.2.3   HILIC-MS/MS Analysis of ^{13}C$_3$-AAMA and ^{13}C$_3$-GAMA in Rat Urine

Rat urine samples obtained following single oral administration of ^{13}C$_3$-AA were analyzed for ^{13}C$_3$-AAMA and ^{13}C$_3$-GAMA using the methods described in **Chapter 4**. HILIC-MS/MS analysis of ^{13}C$_3$-AAMA and ^{13}C$_3$-GAMA in rat urine was possible without altering the liquid chromatography method (**Figure 37**).
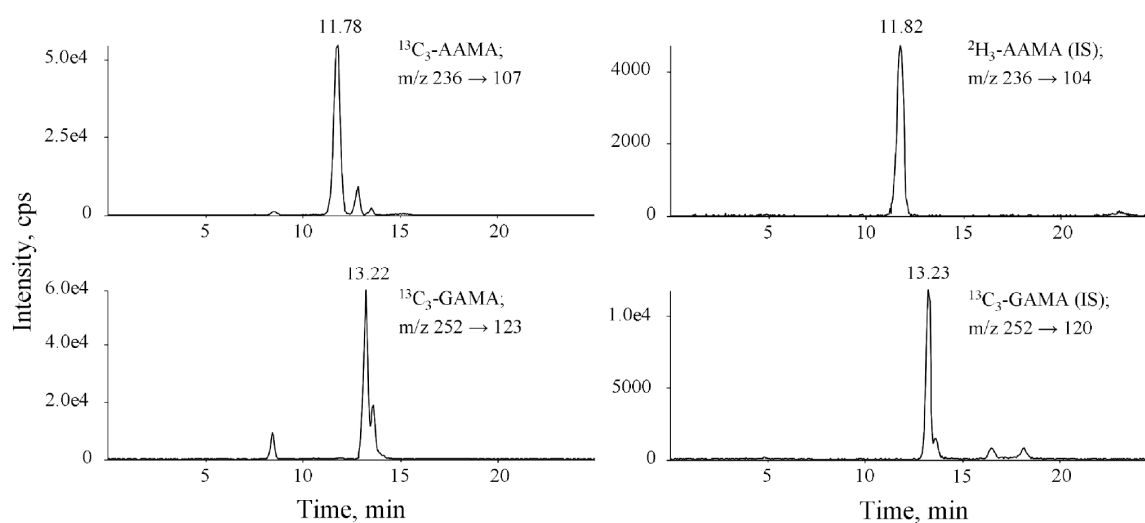


Figure 37   Chromatogram showing the mass traces for ^{13}C$_3$-AAMA and ^{13}C$_3$-GAMA (left hand side) as well as for ^{2}H$_3$-AAMA and ^{2}H$_3$-GAMA (internal standards, IS; right hand side) determined in the urine of a male Fischer 344 rat 12 hours following administration of 100 µg/kg b.w. ^{13}C$_3$-acrylamide. ^{13}C$_3$-AAMA-sulfoxide could not be detected in rat urine.

Calibration and Quantitation. For analysis of $^{13}C_3$-AAMA, $^{13}C_3$-GAMA and $^{13}C_3$-AAMA-sulfoxide in rat urine following administration of $^{13}C_3$-AA, calibration samples were prepared in rat urine with concentrations of $^{13}C_3$-AAMA, $^{13}C_3$-GAMA and $^{13}C_3$-AAMA-sulfoxide ranging from 5.0 to 10 000 µg/L. Samples were prepared and analyzed in duplicate according to the methods described above. Calibration curves were calculated by linear regression and weighted 1/x. Quantitation was carried out using the Analyst 1.4.2 software (Applied Biosystems). Limits of detection (LOD, defined by a signal-to-noise ratio S/N ≥3) for analysis in rat urine were 5, 10 and 50 µg/L for $^{13}C_3$-AAMA, $^{13}C_3$-GAMA and $^{13}C_3$-AAMA-sulfoxide and limits of quantification (LOQ, S/N ≥10) were 10, 20 and 100 µg/L. The increased LODs and LOQs in rat urine as compared to human urine (**Chapter 4.3.7**) may be due to the higher degree of dilution of the samples (1 : 4 compared to 1 : 2) and to a higher amount of interfering salts and other components in rat urine causing ion suppression. Calibration curves in rat urine were linear for $^{13}C_3$-AAMA from 10 µg/L to 10 000 µg/L with a correlation coefficient of $r^2 = 0.9987$, for $^{13}C_3$-GAMA from 20 µg/L to 10 000 µg/L with $r^2 = 0.9999$ and for $^{13}C_3$-AAMA-sulfoxide from 100 µg/L to 10 000 µg/L with $r^2 = 0.9995$.

6.2.4   Toxicokinetic Analysis

Toxicokinetic parameters for $^{13}C_3$-AAMA and $^{13}C_3$-GAMA in rat urine after single oral administration of $^{13}C_3$-AA were determined from the results of the quantitative HILIC-MS/MS measurements. Molar excretion over time was displayed in a graph (**Figure 38**). By polynomial regression (Excel, Microsoft-Office 2007) and subsequent integration using Functions$^{®}$ (www.numericalmathematics.com) the $AUC_{0-∞}$ (area under the time-concentration curve) could be calculated. The values for t_{max} (time of maximum concentration in urine) and c_{max} (maximum concentration in urine) for each metabolite were also evaluated using Functions$^{®}$. First order elimination rate constants (k_e) were determined from the slope of the terminal phase of the ln-linear concentration-time curves. Half lives ($t_{1/2}$) were determined from elimination rate constants using the relationship $t_{1/2} = ln2 / k_e$.

6.3   Results and Discussion

6.3.1   Urinary Excretion of $^{13}C_3$-AAMA and $^{13}C_3$-GAMA following single oral administration of $^{13}C_3$-Acrylamide to Rats

Following oral gavage administration of 20 µg/kg b.w. $^{13}C_3$-AA to male Fischer 344 rats (n = 5) the total recovery in % of dose (0 – 96 hours) was 66.3 ± 11.4%. Following administration of 100 µg/kg b.w. $^{13}C_3$-AA (n = 5), 70.5 ± 10.5% of dose were recovered in urine. No $^{13}C_3$-AAMA-sulfoxide could be detected in any of the rat urine samples. $^{13}C_3$-AAMA and $^{13}C_3$-GAMA were quantified in all urine samples collected up to 96 hours after administration. **Table 15** summarizes the values for molar recoveries and % of dose as well as % of all metabolites determined (i.e. $^{13}C_3$-AAMA and $^{13}C_3$-GAMA)**.**

Table 15
Urinary metabolites (nmol) and recovery following gavage administration of $^{13}C_3$-acrylamide to male Fischer 344 rats (0 – 96 h).

	$^{13}C_3$-AAMA	$^{13}C_3$-GAMA
Low Dose Group (20 µg/kg b.w.)		
Sum	19.0 ± 3.1	18.5 ± 3.8
% of Total*	50.8 ± 3.4	49.2 ± 3.4
% of Dose	33.6 ± 5.0	32.7 ± 7.0
High Dose Group (100 µg/kg b.w.)		
Sum	112 ± 25	90.8 ± 14.1
% of Total*	54.9 ± 4.2	45.1 ± 4.2
% of Dose	38.8 ± 7.3	31.7 ± 4.8

Mean values ± standard deviation (n = 5).
* % of all metabolites determined in urine.

In the low dose study, 51% of all determined metabolites were excreted as $^{13}C_3$-AAMA and 49% as $^{13}C_3$-GAMA. In the high dose study, 55% were excreted as $^{13}C_3$-AAMA and 45% as $^{13}C_3$-GAMA. The molar ratios GAMA : AAMA were 0.974 ± 0.132 in the low dose study and 0.830 ± 0.138 in the high dose study. Accordingly, the fraction of metabolites excreted as $^{13}C_3$-GAMA was slightly smaller in the high dose study than in the low dose study, possibly indicating saturation of CYP 2E1. Statistical calculations however, did not yield a significant result, thus indicating, that at doses below 100 µg/kg b.w., AA-biotransformation in rats is not substantially influenced by interactions with metabolizing enzymes.

6.3.2   Kinetics of Urinary Excretion of $^{13}C_3$-AAMA and $^{13}C_3$-GAMA in Rats

Urinary excretion of $^{13}C_3$-AAMA and $^{13}C_3$-GAMA following administration of 20 µg/kg b.w. $^{13}C_3$-AA to male Fischer 344 rats (n = 5) is displayed in **Figure 38A**. **Figure 38B** shows the molar urinary excretion over time following administration of 100 µg/kg b.w. $^{13}C_3$-AA. $^{13}C_3$-AAMA is the most rapidly responding metabolite, whereas concentrations of $^{13}C_3$-GAMA in urine increase comparatively slower due to the time required for biotransformation by CYP 2E1.

As already indicated in earlier studies with ^{14}C-labeled AA (*43*), excretion of both metabolites is biphasic with a fast initial excretion phase up to approximately 34 hours following administration and a prolonged wash out phase over several days. Toxicokinetic parameters calculated from the urinary excretion of $^{13}C_3$-AAMA and $^{13}C_3$-GAMA following single oral administration of 20 µg/kg b.w. and 100 µg/kg b.w. $^{13}C_3$-AA to male Fischer 344 rats (n = 5) are summarized in **Table 16**. In agreement with the biphasic excretion of AA-derived metabolites in rat urine, values characterizing excretion behavior, i.e. coefficients of elimination (k_e) and half lives ($t_{1/2}$), were calculated for the corresponding elimination intervals. For the initial fast excretion phase, k_e (I) and $t_{1/2}$ (I) were calculated from the ln-linear interval up to 34 hours following exposure. The wash out phase (34 hours - ∞) is characterized by k_e (II) and $t_{1/2}$ (II). Values for $t_{1/2}$ (I) ranged

from 3.59 to 5.37 hours for $^{13}C_3$-AAMA and from 2.30 to 5.64 hours for $^{13}C_3$-GAMA and values for $t_{1/2}$ (II) ranged from 41 hours to 6 days for $^{13}C_3$-AAMA and from 27 hours to 3 days for $^{13}C_3$-GAMA. These results are in good accordance with previous studies, where half-lives of 5 hours ($t_{1/2}$ (I)) and 8 days ($t_{1/2}$ (II)) were determined for urinary excretion of total ^{14}C (*43*). To simplify comparison with excretion data derived from the human studies (**Chapter 7**), excretion parameters were also calculated over the complete period of excretion (k_e (I + II) and $t_{1/2}$ (I + II)). These values however, are only approximations based on noncompartmental first-order kinetics.
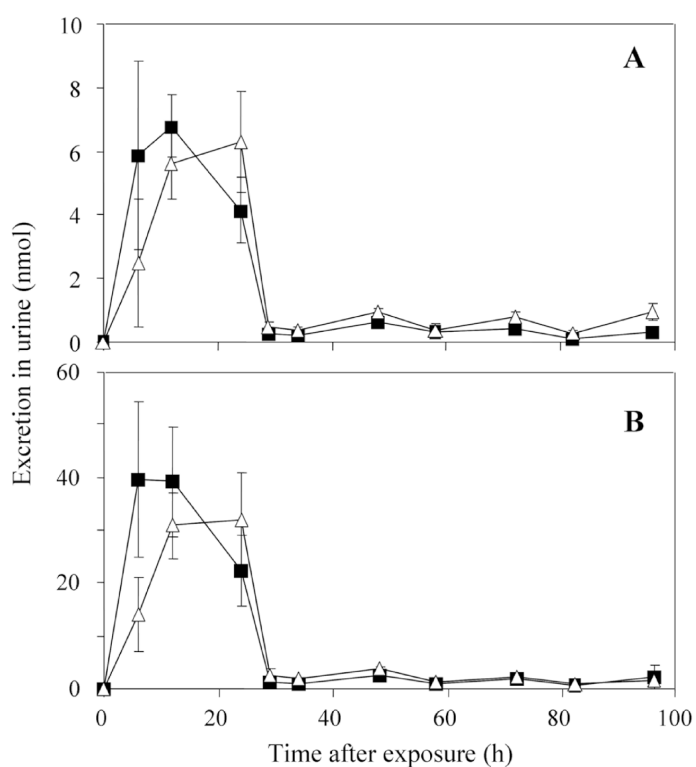
Figure 38 Urinary excretion of $^{13}C_3$-AAMA and $^{13}C_3$-GAMA in rat urine (n = 5/dose group) following administration of 20 µg/kg b.w. (**A**) and 100 µg/kg b.w. $^{13}C_3$-acrylamide (**B**), respectively.

Results of the rat studies are in good accordance with those obtained by other work-groups after administration of 3 mg/kg b.w. and 0.1 mg/kg b.w. AA, respectively (**Table 17**). The comparatively lower concentration values for GAMA obtained following administration of 50 mg/kg b.w. AA to rats (*39*) can be explained by an inverse dose dependency. As the amount of AA administered is decreased, the amount metabolized to GA increases in mice and rats (*54, 235*).

6.4   Conclusions

Biotransformation and toxicokinetics of AA have been determined in Fischer 344 rats at doses similar to the daily dietary intake in humans. Almost 50% of the metabolites in rat urine could be assigned to GAMA, the mercapturic acid metabolite of the mutagenic epoxide GA. As expected, no AAMA-sulfoxide could be determined in rat urine following administration of AA. For the first time, rats were administered the same dose as humans, thus allowing for direct comparability.

Table 16

Toxicokinetic analysis of urinary elimination of metabolites following single oral administration of $^{13}C_3$-acrylamide to male Fischer 344 rats (n = 5/dose group).

	Low Dose Group (20 μg/kg b.w.)		High Dose Group (100 μg/kg b.w.)	
	$^{13}C_3$-AAMA	$^{13}C_3$-GAMA	$^{13}C_3$-AAMA	$^{13}C_3$-GAMA
$AUC_{0-\infty}$ nmol × h	160 ± 21	176 ± 26	905 ± 225	872 ± 150
t_{max} h	11.7 ± 2.2	17.9 ± 2.0	10.9 ± 2.7	17.7 ± 1.7
c_{max} nmol	7.27 ± 1.49	8.58 ± 0.51	45.2 ± 9.7	44.4 ± 6.8
k_e (I) h^{-1}	0.157 ± 0.021	0.131 ± 0.007	0.158 ± 0.023	0.171 ± 0.073
$t_{1/2}$ (I) h	4.5 ± 0.6	5.3 ± 0.3	4.5 ± 0.6	4.5 ± 1.2
k_e (II) h^{-1}	0.012 ± 0.004	0.017 ± 0.005	0.007 ± 0.003	0.013 ± 0.006
$t_{1/2}$ (II) h	60.0 ± 19.0	42.4 ± 9.9	104 ± 31	58.0 ± 18.3
k_e (I+II) h^{-1}	0.032 ± 0.006	0.020 ± 0.004	0.035 ± 0.004	0.032 ± 0.006
$t_{1/2}$ (I+II) h	22.8 ± 5.3	35.0 ± 6.3	19.8 ± 2.3	22.8 ± 5.7

Mean values ± standard deviations for area under the curve (AUC), time of maximum concentration in urine (t_{max}), maximum concentration in urine (c_{max}), coefficients of elimination (k_e) and elimination half lives ($t_{1/2}$).

According to the biphasic elimination of AA-derived metabolites in rat urine, k_e and $t_{1/2}$ were calculated for the 0-34 hour elimination interval (I) and the 34 hour - ∞ elimination interval (II), respectively. Additionally, k_e and $t_{1/2}$ were calculated over the whole excretion period (0-∞; I+II) for reasons of comparability to human data.

Table 17
Comparison of molar percentages of dose excreted in urine of mice and rats after oral administration of acrylamide.
All information given is referenced to collection periods of 24 h after administration.

Species - dose	AA	AAMA	AAMA-sulfoxide	GA	GAMA	Glyceramide	$\sum GA^a : \sum AA^b$	Total of dose[c]
M - 50 mg/kg[d]	NQ	21.0 ± 1.10	ND	8.6 ± 1.1	17 ± 0.60	2.70 ± 0.60	1.3	50.4
M - 0.1 mg/kg[e]	0.6 - 0.7	5 - 9	ND	16 - 18	9 - 22	ND	4.2	33 - 48
R - 50 mg/kg[d]	NQ	34.0 ± 1.80	ND	2.8 ± 0.50	12 ± 0.60	1.20 ± 0.40	0.47	50.7
R - 50 mg/kg[f]	NQ	38	ND	3.9	10.5	0.6	0.39	53
R - 3 mg/kg[g]	NQ	29.0 ± 4.50	ND	ND	21 ± 2.42	ND	0.72	50.0 ± 8.60
R - 0.1 mg/kg[e]	2	31	ND	6	27 - 29	ND	1 - 1.1	64 - 66
R - 20 µg/kg[h]	ND	29.7 ± 5.13	ND	ND	25.4 ± 6.20	ND	0.86	55.1 ± 11.8
R - 0.1 mg/kg[h]	ND	34.9 ± 7.40	ND	ND	26.7 ± 4.64	ND	0.77	61.7 ± 10.5

NQ = not quantified, ND = not determined
[a] This sum represents GA + GAMA + Glyceramide.
[b] This sum represents AA + AAMA + AAMA-sulfoxide.
[c] Total amount excreted within 24 hours after exposure calculated as % of dose.
[d] Sumner et al., **1992**. Gavage male rats; gavage male mice.
[e] Doerge et al., **2007**. Gavage male mice; gavage male rats.
[f] Sumner et al., **2003**. Gavage male rats.
[g] Fennell et al., **2005**. Gavage male rats.
[h] This study. Gavage male rats.

7 Biotransformation and Toxicokinetics of Acrylamide in Humans

7.1   Introduction

To investigate biotransformation and toxicokinetics of AA in humans at doses resembling the dietary uptake, a human study was conducted with single oral administration of $^{13}C_3$-AA. ^{13}C-labeled AA was used to prevent interference with AA from the diet. As has been determined previously by human biomonitoring (**Chapter 5.3**), the mean daily exposure from the diet is approximately 0.5 µg/kg b.w. AA. Accordingly, this dose was chosen for the low dose experiment in the present study. A second dose of 20 µg/kg b.w. $^{13}C_3$-AA[1] was selected to provide direct comparability with the low dose experiment in rats (**Chapter 6**).

---

[1] Although the dose of 20 µg/kg b.w. exceeds the mean daily AA exposure by a factor of 40, it nevertheless represents a possible (worst case) uptake easily achieved by ingestion of, e.g. 300 g or 180 g of highly contaminated French fries (3770 µg AA/kg) and gingerbread (7834 µg AA/kg), respectively (*180*).

7.2   Materials and Methods

7.2.1   Human Subjects and Study Design

Six subjects (3 female, 3 male) volunteered to participate in the study. They weighed between 52 and 75 kg and were between 23 and 28 years old. All subjects were nonsmokers and did not drink any alcoholic beverages 72 hours before and during the study. They also refrained from eating foodstuffs prepared with garlic to eliminate possible interactions of the cytochrome P450 enzyme CYP 2E1 with diallyl sulfide and related compounds (*63*). Dietary protocols were maintained 72 hours before and during the study and the study participants were asked to avoid major AA sources like potato chips and French fries.

Prior to the study, all volunteers underwent physical and medical examination. Blood samples of each volunteer were analyzed at the local Laboratory for Clinical Chemistry for parameters indicative of kidney or liver damage and thyroid function. Only apparently healthy subjects participated in this study. In accordance with the Declaration of Helsinki, the study was performed with informed consent and the study protocol was reviewed and approved by the local institutional review board.

The same individuals participated in the low and high dose experiments with an interval of two weeks in between to allow for the excretion of all metabolites from the first $^{13}C_3$-AA exposure. Study design for both parts was identical.

Predose spot urine and blood samples (9 mL) were taken from each volunteer. In the first part (low dose study) the volunteers were exposed orally to 0.5 µg/kg b.w. (6.76 nmol/kg b.w.) $^{13}C_3$-AA in 100 mL drinking water before breakfast. In the second part (high dose study) the oral dose was 20 µg/kg b.w. (270.27 nmol/kg b.w.) $^{13}C_3$-AA. Urine was collected in predetermined intervals (0 – 4, 4 – 9, 9 – 14, 14 – 22, 22 – 30, 30 – 38, 38 – 46, 46 – 54, 54 – 62, 62 – 70, 70 – 78, 78 – 86 and 86 – 94 hours). Five aliquots (2 mL) of each sample were stored at -20 °C until analysis by HILIC-MS/MS.

Blood samples (9 mL) were taken by venopuncture 0.5, 1, 1.5, 2, 3, 4, 6, 8, 12 and 24 hours following administration of $^{13}C_3$-AA. Samples were allowed to clot at room temperature for approximately 20 to 30 min. Then, samples were centrifuged to obtain serum and five aliquots (500 µL) of each sample were stored at -20 °C until analysis by LC-MS/MS.

7.2.2   Sample Preparation

Urine Samples. Frozen human urine samples were thawed, vortexed and diluted with an equal volume of acetonitrile. To remove precipitated proteins and salts, samples were centrifuged for 10 min at 4 °C and 1 400 × g followed by addition of the internal standards (IS) at a final concentration of 30 µg/L of each standard. The IS-solution was prepared by dissolving $^2H_3$-AAMA, $^2H_3$-GAMA and $^2H_3$-AAMA-sulfoxide in water at a concentration of 3 000 µg/L.

Serum Samples. Prior to LC-MS/MS analysis for $^{13}C_3$-AA, human serum samples were purified by solid phase extraction (*236*). Briefly, 100 µL serum were diluted with 100 µL water containing 50 ng GA as internal standard. 50 mg Isolute ENV+ SPE cartridges (Biotage Sweden AB, Uppsala, Sweden) were preconditioned by sequential application of 1 mL methanol and 2 × 1 mL water. Samples were transferred onto the SPE cartridges and washed with 2 × 100 µL water and 200 µL of 2% methanol in water (v/v). Subsequently, samples were eluted with 4 × 100 µL 10% acetonitrile in water (v/v) into 1.5 mL collection vials. Samples were concentrated to approximately 50 – 80 µL under a stream of nitrogen in a heat block at approximately 55 °C. Care was taken to avoid reducing samples to dryness. After reconstituting each sample to a volume of 100 µL by addition of water, aliquots of 10 µL were analyzed via LC-MS/MS.

7.2.3   HILIC-MS/MS Analysis of $^{13}C_3$-AAMA, $^{13}C_3$-AAMA-sulfoxide and $^{13}C_3$-GAMA in Human Urine

For measurements of $^{13}C_3$-AAMA, $^{13}C_3$-GAMA and $^{13}C_3$-AAMA-sulfoxide in human urine following administration of $^{13}C_3$-AA, calibration samples were prepared in blank human urine with concentrations of $^{13}C_3$-AAMA, $^{13}C_3$-GAMA and $^{13}C_3$-AAMA-sulfoxide ranging from 0.5 to 3 000 µg/L. $^{2}H_3$-AAMA, $^{2}H_3$-GAMA and $^{2}H_3$-AAMA-sulfoxide were used as internal standards. HILIC-MS/MS Analysis was performed according to the methods described in **Chapter 4**. No deterioration concerning retention during HPLC or sensitivity (LOD and LOQ) of the mass spectrometric analysis and quantification could be observed following adjustment of the mass transitions to the respective ^{13}C-labeled analogues (**Figure 39**).

7.2.4   HPLC-MS/MS Analysis of $^{13}C_3$-Acrylamide in Human Serum Samples

After purification via solid phase extraction, human serum samples were analyzed for $^{13}C_3$-AA. The LC-MS/MS system consisted of an Agilent Series 1100 binary pump, degasser and autosampler (Agilent, Waldbronn, Germany) and a triple-stage quadrupole mass spectrometer (API 3000, Applied Biosystems, Darmstadt, Germany) equipped with an electrospray ionization source. The column used was a Reprosil-Pur C18-Aq column (3 µm, 150 × 2 mm, Dr. Maisch, Ammerbuch, Germany). A guard column (Reprosil-Pur C18-Aq, 5 µm, 10 × 2 mm, Dr. Maisch) was applied. Injection volume was 10 µL. Elution was isocratic at a flow rate of 200 µL/min with 98% solvent A (5% methanol in 0.1% formic acid, v/v) and 2% solvent B (100% acetonitrile). Run-time was 10 min.
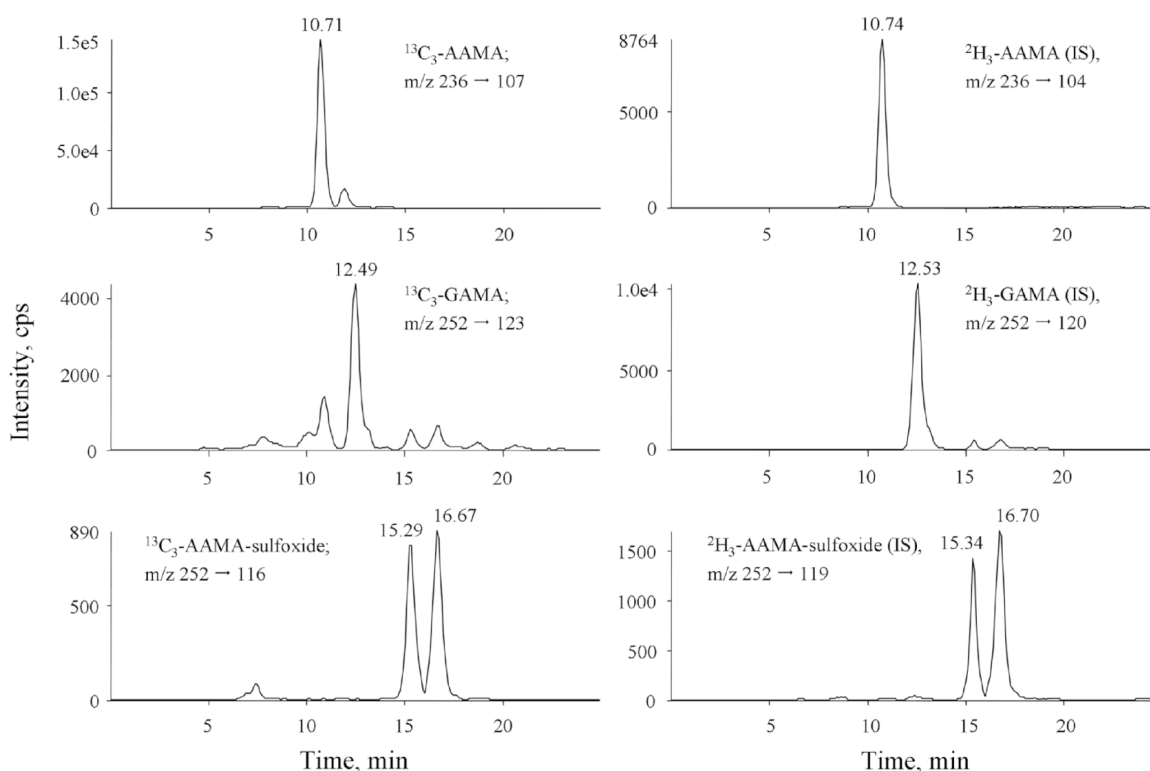
Figure 39 Chromatogram showing the mass traces for $^{13}C_3$-AAMA, $^{13}C_3$-GAMA and $^{13}C_3$-AAMA-sulfoxide (left hand side) as well as for $^2H_3$-AAMA, $^2H_3$-GAMA and $^2H_3$-AAMA-sulfoxide (internal standards; right hand side) determined in the urine of a female human subject 9 hours following single oral administration of 20 µg/kg b.w. $^{13}C_3$-acrylamide.

Positive ions were analyzed by multiple reaction monitoring (MRM) with a dwell time of 200 msec for each transition. Ion spray voltage was 4 000 V with a source temperature of 400 °C using nitrogen as curtain and collision gas. Focusing potential was set to 120 V and entrance potential to 10 V. Analyte specific acquisition parameters were obtained by infusion of standards using the quantitative optimization function of the Analyst 1.4.1 software (Applied Biosystems). $^{13}C_3$-AA was determined by monitoring the mass transition m/z 75 → 58 (i.e. loss of NH_3). Collision energy was set to 17 V and cell exit potential to 8 V. The mass transition for the internal standard GA was m/z 88 → 44 (i.e. loss of $CONH_2$) with collision energy set to 25 V and cell exit potential to 6 V. Declustering potential for both transitions was 21 V. GA could be used as an internal

standard, since no background GA was detected in any of the serum samples from this study (<LOD). A chromatogram showing the mass traces of $^{13}C_3$-AA and GA in human serum is presented in **Figure 40**.
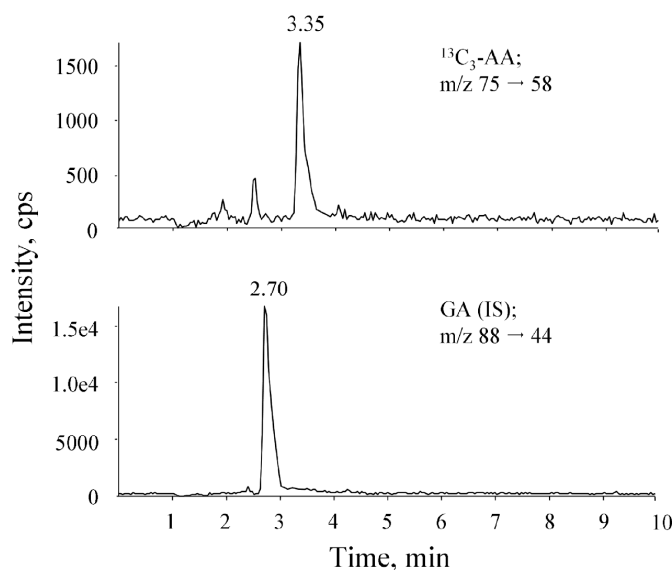
Figure 40   Chromatogram showing the mass traces for $^{13}C_3$-AA and GA (internal standard) determined in a serum sample obtained from a female human subject (**F3**) 1.5 hours following single oral administration of 20 µg/kg b.w. $^{13}C_3$-acrylamide.

Calibration and Quantification. For the calibration curve, blank serum samples were spiked with $^{13}C_3$-AA at concentrations ranging from 1.0 to 200 µg/L. Samples were then prepared and analyzed in duplicate according to the methods described above. The calibration curve was calculated by linear regression and weighted 1/x. Quantitation was carried out using the Analyst 1.4.2 software (Applied Biosystems). Limit of detection (LOD, defined by a signal-to-noise ratio S/N $\geq$3) and limit of quantification (LOQ, S/N $\geq$10) for $^{13}C_3$-AA in human serum were determined to be 0.5 and 1.0 µg/L, respectively. The calibration curve was linear over the whole range with a correlation coefficient of $r^2 = 0.9999$. Recovery of the SPE method and stability of the LC-MS/MS method were

determined by addition of $^{13}C_3$-AA to blank serum samples at three different concentrations (2 µg/L, 5 µg/L and 10 µg/L) before and after solid phase extraction. Each sample was prepared and analyzed in triplicate according to the methods described above. Mean recovery was calculated as 80.2 ± 6.1%.

7.2.5   Toxicokinetic Analysis

Toxicokinetic parameters for $^{13}C_3$-AAMA, $^{13}C_3$-GAMA and $^{13}C_3$-AAMA-sulfoxide in human urine after single oral administration of $^{13}C_3$-AA were determined from the results of the quantitative HILIC-MS/MS measurements. Molar excretion over time was displayed in a graph (**Figure 41**). By polynomial regression (Excel, Microsoft-Office 2007) and subsequent integration using Functions$^{®}$ (www.numericalmathematics.com) the $AUC_{0-\infty}$ (area under the time-concentration curve) could be calculated. The values for t_{max} (time of maximum concentration in urine) and c_{max} (maximum concentration in urine) for each metabolite were also evaluated using Functions$^{®}$. First order elimination rate constants (k_e) were determined from the slope of the terminal phase of the ln-linear concentration-time curves. Half lives ($t_{1/2}$) were determined from elimination rate constants using the relationship $t_{1/2} = \ln 2/k_e$.

Human serum toxicokinetics of $^{13}C_3$-AA ($AUC_{0-\infty}$, t_{max}, c_{max}, k_e and $t_{1/2}$) were determined accordingly. As concentrations in serum samples collected at 3 hours following administration of $^{13}C_3$-AA were between LOD and LOQ, these samples were given a value of LOQ divided by the square root of 2 to facilitate calculations.

7.3   Results

7.3.1   Urinary Excretion of $^{13}C_3$-AAMA, $^{13}C_3$-AAMA-sulfoxide and $^{13}C_3$-GAMA in Humans following Single Oral Administration of $^{13}C_3$-Acrylamide

Six human subjects (3 female, 3 male) were exposed orally to 0.5 µg/kg b.w. and 20 µg/kg b.w. $^{13}C_3$-AA in 100 mL drinking water in two separate studies. In each experiment, urine samples were collected for 94 hours in intervals. Subsequently, aliquots were analyzed for content of $^{13}C_3$-AAMA, $^{13}C_3$-AAMA-sulfoxide and $^{13}C_3$-GAMA.

In the high dose study, metabolite levels in urine were well above the LOQ up to 94 hours following exposure. In the low dose study, $^{13}C_3$-AAMA-sulfoxide and $^{13}C_3$-GAMA were only detectable up to 46 hours after the administration of $^{13}C_3$-AA. The total amount excreted after administration of 0.5 µg/kg b.w. (0 – 46 hours) was 71.3 ± 5.1% of the administered dose. After administration of 20 µg/kg b.w., 70.0 ± 3.1% of dose could be recovered in urine (0 – 94 hours).

The individual recoveries for all quantitated metabolites are shown in **Table 18**. Molar percentages of the individual analytes relative to the total dose of $^{13}C_3$-AA administered were calculated using the individual urine volumes. After single oral administration to humans, the main metabolite of $^{13}C_3$-AA was $^{13}C_3$-AAMA accounting for approximately 71% of all relevant metabolites excreted with urine. 20% were excreted as $^{13}C_3$-AAMA-sulfoxide. Compared to urinary excretion in rats, $^{13}C_3$-GAMA (including $^{13}C_3$-iso-GAMA) was a minor metabolite in humans: only about 9% could be assigned to the mercapturic acid(s) of the mutagenic epoxide GA. The median molar ratios GAMA : (AAMA + AAMA-SO) were 0.100 ± 0.018 in the low dose study and 0.101 ± 0.023 in the high dose study. No significant differences were observed concerning urinary recovery in the low dose and in the high dose experiment as well as between female and male human subjects (Student´s t-Test).

Table 18

Urinary metabolites (nmol) and recovery following single oral administration of 0.5 µg/kg b.w. and 20 µg/kg b.w. $^{13}C_3$-acrylamide to female (n = 3) and male (n = 3) human subjects.

	$^{13}C_3$-AAMA	$^{13}C_3$-AAMA-sulfoxide	$^{13}C_3$-GAMA
	Low Dose Group (0.5 µg/kg b.w.)		
Female (n = 3)			
Sum (0 – 46 h)	211 ± 53	48.2 ± 7.9	29.0 ± 9.7
% of Total*	72.9 ± 2.3	17.1 ± 3.5	10 ± 2
% of Dose	49.4 ± 4.1	11.5 ± 2.4	6.7 ± 1.1
Male (n =3)			
Sum (0 – 46 h)	261 ± 37	62.5 ± 3.3	28.5 ± 1.5
% of Total*	73.9 ± 3.2	19.8 ± 3.9	8.1 ± 0.6
% of Dose	54.1 ± 1.3	14.9 ± 3.3	6.0 ± 0.6
All (n = 6)			
Sum (0 – 46 h)	236 ± 49	55.3 ± 9.5	28.8 ± 6.2
% of Total*	73.4 ± 2.6	18.4 ± 3.6	9.1 ± 1.5
% of Dose	51.7 ± 3.8	13.2 ± 3.2	6.3 ± 0.9
	High Dose Group (20 µg/kg b.w.)		
Female (n = 3)			
Sum (0 – 94 h)	$8.07 \times 10^3 \pm 1.55 \times 10^3$	$2.40 \times 10^3 \pm 0.44 \times 10^3$	$1.11 \times 10^3 \pm 0.51 \times 10^3$
% of Total*	69.6 ± 2.7	21.1 ± 5.0	9.3 ± 2.9
% of Dose	47.4 ± 1.3	14.5 ± 3.9	6.3 ± 1.9
Male (n =3)			
Sum (0 – 94 h)	$9.85 \times 10^3 \pm 1.75 \times 10^3$	$2.73 \times 10^3 \pm 1.78 \times 10^3$	$1.25 \times 10^3 \pm 0.12 \times 10^3$
% of Total*	70.9 ± 4.0	20.1 ± 3.8	9.1 ± 0.5
% of Dose	50.9 ± 3.0	14.4 ± 2.9	6.5 ± 0.2
All (n = 6)			
Sum (0 – 94 h)	$8.96 \times 10^3 \pm 1.77 \times 10^3$	$2.56 \times 10^3 \pm 0.35 \times 10^3$	$1.18 \times 10^3 \pm 0.34 \times 10^3$
% of Total*	70.2 ± 3.1	20.6 ± 4.0	9.2 ± 1.9
% of Dose	49.2 ± 2.8	14.5 ± 3.1	6.4 ± 1.2

Mean values ± standard deviation.
* % of total of all metabolites determined in urine.

7.3.2   Kinetics of Urinary Excretion of $^{13}C_3$-AAMA, $^{13}C_3$-AAMA-sulfoxide and $^{13}C_3$-GAMA in Humans

Molar excretion of $^{13}C_3$-AAMA, $^{13}C_3$-AAMA-sulfoxide and $^{13}C_3$-GAMA in urine of female (n = 3) and male (n = 3) human subjects is displayed in **Figure 41**. Following administration of 0.5 µg/kg b.w., excretion was monitored over 46 hours (**Figure 41 AI-AIII**). Following administration of 20 µg/kg b.w., the observation period was 94 hours (**Figure 41 BI-BIII**). $^{13}C_3$-AAMA is the most rapidly responding metabolite, whereas urinary concentrations of $^{13}C_3$-AAMA-sulfoxide and $^{13}C_3$-GAMA increase comparatively slower due to the time required for biotransformation via CYP 2E1 and FMO/Cytochrome P450, respectively.
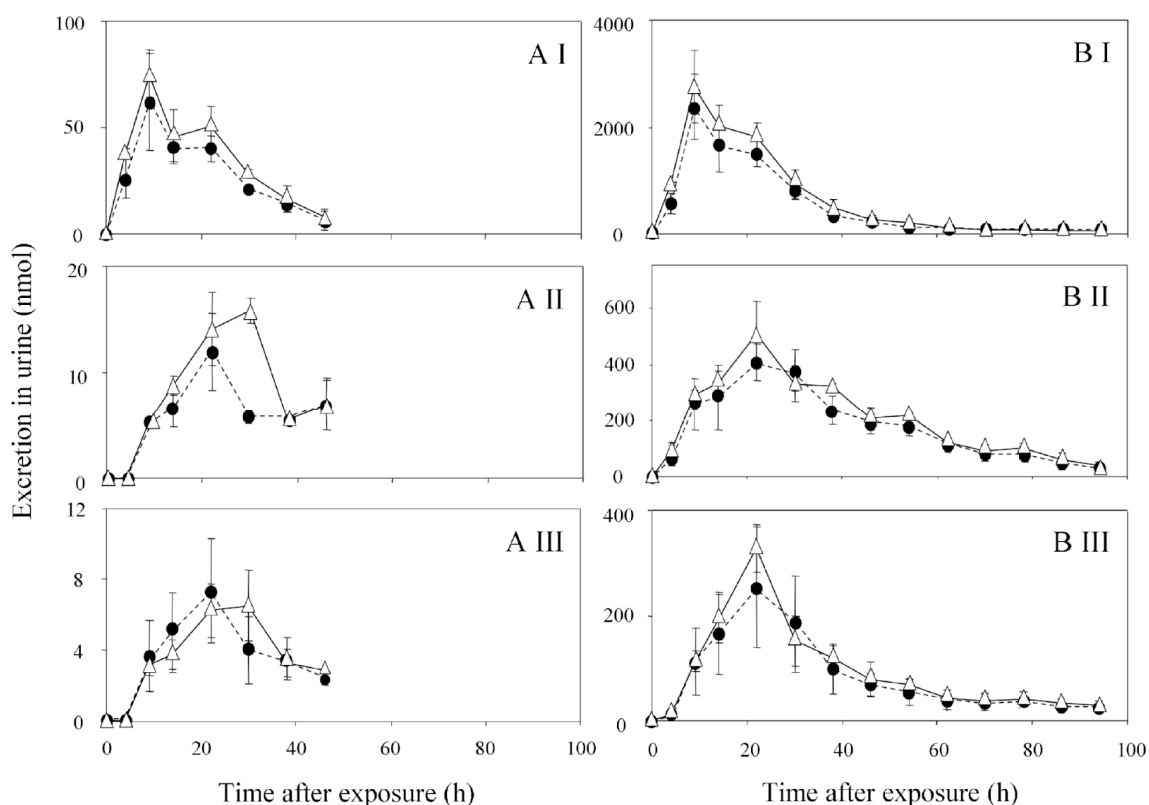
Figure 41   Excretion of $^{13}C_3$-AAMA (**I**), $^{13}C_3$-AAMA-sulfoxide (**II**) and $^{13}C_3$-GAMA (**III**) in urine of female (●; n = 3) and male (Δ; n = 3) human subjects following single oral administration of 0.5 µg/kg b.w. (**A**) and 20 µg/kg b.w. $^{13}C_3$-acrylamide (**B**), respectively.

Table 19

Toxicokinetic analysis of urinary elimination of metabolites following single oral administration of 20 μg/kg b.w. $^{13}C_3$-acrylamide to human subjects (n = 6; 3 male, 3 female).

	$^{13}C_3$-AAMA	$^{13}C_3$-AAMA-sulfoxide	$^{13}C_3$-GAMA	
Females (n = 3)				
$AUC_{0-\infty}$	$56.3 \times 10^3 \pm 11.3 \times 10^3$	$18.0 \times 10^3 \pm 3.0 \times 10^3$	$8.42 \times 10^3 \pm 3.87 \times 10^3$	nmol × h
t_{max}	10.2 ± 0.1	24.5 ± 1.5	23.1 ± 0.3	h
c_{max}	$2.48 \times 10^3 \pm 0.64 \times 10^3$	$0.41 \times 10^3 \pm 0.07 \times 10^3$	$0.26 \times 10^3 \pm 0.12 \times 10^3$	nmol
k_e	0.048 ± 0.005	0.035 ± 0.010	0.028 ± 0.003	h^{-1}
$t_{1/2}$	14.5 ± 1.6	21.3 ± 7.0	25.2 ± 2.2	h
Males (n = 3)				
$AUC_{0-\infty}$	$69.3 \times 10^3 \pm 18.5 \times 10^3$	$20.2 \times 10^3 \pm 1.3 \times 10^3$	$9.54 \times 10^3 \pm 0.94 \times 10^3$	nmol × h
t_{max}	10.1 ± 0.1	21.5 ± 1.4	22.3 ± 0.8	h
c_{max}	$2.85 \times 10^3 \pm 0.72 \times 10^3$	$0.49 \times 10^3 \pm 0.11 \times 10^3$	$0.32 \times 10^3 \pm 0.03 \times 10^3$	nmol
k_e	0.050 ± 0.002	0.032 ± 0.003	0.025 ± 0.002	h^{-1}
$t_{1/2}$	13.8 ± 0.6	21.6 ± 2.2	27.39 ± 2.4	h
All (n = 6)				
$AUC_{0-\infty}$	$62.8 \times 10^3 \pm 15.4 \times 10^3$	$19.1 \times 10^3 \pm 2.4 \times 10^3$	$8.98 \times 10^3 \pm 2.60 \times 10^3$	nmol × h
t_{max}	10.2 ± 0.1	23.0 ± 2.1	22.7 ± 0.7	h
c_{max}	$2.66 \times 10^3 \pm 0.64 \times 10^3$	$0.45 \times 10^3 \pm 0.09 \times 10^3$	$0.29 \times 10^3 \pm 0.08 \times 10^3$	nmol
k_e	0.049 ± 0.003	0.034 ± 0.007	0.027 ± 0.002	h^{-1}
$t_{1/2}$	14.2 ± 1.1	21.5 ± 4.6	26.3 ± 2.4	h

Mean values ± standard deviations for area under the curve (AUC), time of maximum concentration in urine (t_{max}), maximum concentration in urine (c_{max}), coefficients of elimination (k_e) and elimination half lives ($t_{1/2}$).

Toxicokinetic parameters for the individual metabolites calculated from data derived from the high dose study are displayed in **Table 19**. $^{13}C_3$-AAMA reached its maximum concentration in urine approximately 10 hours following administration, whereas concentrations for $^{13}C_3$-GAMA and $^{13}C_3$-AAMA-sulfoxide increased comparatively slower and maximum concentrations could be observed approximately 23 hours after dosing. $^{13}C_3$-AAMA was also excreted more rapidly compared to $^{13}C_3$-GAMA and $^{13}C_3$-AAMA-sulfoxide. Values for $t_{1/2}$ were 14, 26 and 22 hours for $^{13}C_3$-AAMA, $^{13}C_3$-GAMA and $^{13}C_3$-AAMA-sulfoxide, respectively. No significant differences were observed concerning toxicokinetics and biotransformation of $^{13}C_3$-AA in the low dose and in the high dose experiment as well as between female and male human subjects (Student´s t-Test).

7.3.3   Human Serum Toxicokinetics of $^{13}C_3$-Acrylamide

Blood samples were taken from the six human subjects (3 female, 3 male) before dosing and 0.5, 1, 1.5, 2, 3, 4, 6, 8, 12 and 24 hours following administration of 20 µg/kg b.w. $^{13}C_3$-AA. The obtained serum samples were analyzed for $^{13}C_3$-AA via LC-MS/MS. $^{13}C_3$-AA could only be quantified in the samples collected up to 2 hours following exposure (**Figure 42**). Concentrations at 3 hours after administration of $^{13}C_3$-AA were between LOD and LOQ in all samples.
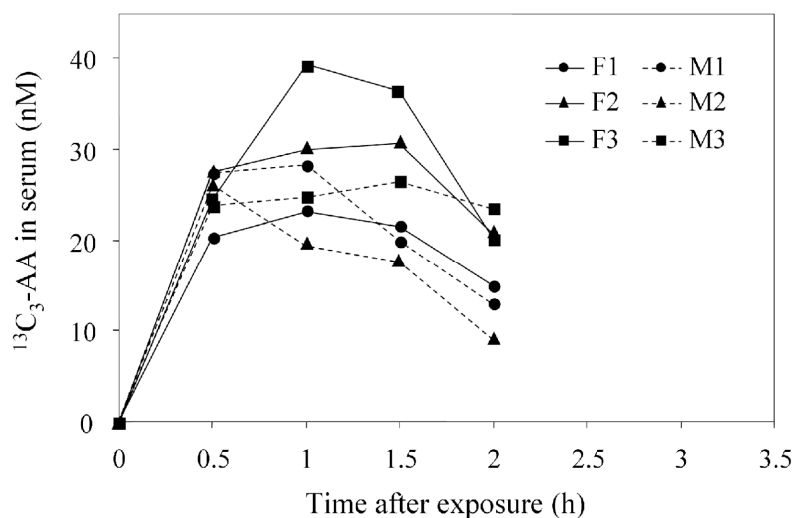
Figure 42 Concentrations of $^{13}C_3$-AA in serum of female (n = 3, F1-F3) and male (n = 3, **M1-M3**) human subjects following single oral administration of 20 µg/kg b.w. $^{13}C_3$-acrylamide.

Toxicokinetic parameters are shown in **Table 20**. As no significant gender-differences could be observed concerning the serum toxicokinetics of AA in humans, values are given as mean irrespective of gender.

Table 20
Serum toxicokinetics following oral administration of 20 µg/kg b.w. $^{13}C_3$-acrylamide to human subjects (n = 6; 3/gender).

	$^{13}C_3$-AA	
$AUC_{0-\infty}$	56.6 ± 9.0	nM × h
t_{max}	0.94 ± 0.21	h
c_{max}	29.2 ± 4.5	nM
k_e	0.964 ± 0.277	h^{-1}
$t_{1/2}$	0.79 ± 0.30	h

Mean values ± standard deviations (n=6; 3male, 3 female) for area under the curve (AUC), time of maximum concentration in serum (t_{max}), maximum serum concentration (c_{max}), coefficient of elimination (k_e) and elimination half life ($t_{1/2}$).

7.4   Discussion

In order to help understand the biotransformation pathways and toxicokinetic properties of AA in humans after uptake of low doses, two studies with single oral administration of $^{13}C_3$-AA at doses covering the range of human dietary exposure (from mean exposure to worst case exposure) were conducted. Urine samples were collected in intervals over 46 and 94 hours, monitoring the major part of the excretion phase. All samples were analyzed for the three major metabolites excreted in human urine: $^{13}C_3$-AAMA, $^{13}C_3$-GAMA and $^{13}C_3$-AAMA-sulfoxide.

Comparison with other Studies in Humans. Most workgroups only determine metabolites excreted during the first 24 hours following administration (*38-41, 147*). A considerable part of AAMA-sulfoxide and GAMA is actually excreted afterwards (**Figure 41**). To improve comparability of results, molar percentages of dose excreted in urine during the first 24 hours (22 hours) following exposure were calculated (**Table 21**). Results concerning measurements of $^{13}C_3$-AAMA and $^{13}C_3$-GAMA are consistent with previous studies in the low dose range. After ingestion of potato chips containing 0.94 mg AA, unchanged AA, AAMA and GAMA had been quantified in the urines of humans subjects (n = 6) over a period of 72 hours (*153*). The total recovery was 60.3 ± 11.2% of the administered dose, with 4.4 ± 1.5%, 50.0 ± 9.4% and 5.9 ± 1.2% of dose accounting for unchanged AA, AAMA and GAMA, respectively. Similar values for $t_{1/2}$ were obtained for AAMA and GAMA compared to our results for $^{13}C3$-AAMA and $^{13}C_3$-GAMA. In another study, urinary metabolites levels for $^2H_3$-AAMA and $^2H_3$-GAMA have been monitored over 46 hours after administration of 0.99 mg $^2H_3$-AA to a male volunteer (*154*). The overall excretion was 56.2% of dose with 52.7% of dose recovered as $^2H_3$-AAMA and 4.6% as $^2H_3$-GAMA. These values are in good accordance with our results from the human low dose and high dose study recoveries after 94 and 46 hours, respectively (**Table 18**). Both workgroups however did not quantify AAMA-sulfoxide. Following administration of 0.5, 1.0 and 3.0 mg/kg b.w. $^{13}C_3$-AA to human subjects, Fennell et al. (*147*) recovered

approximately 8% of dose as AAMA-sulfoxide (0 – 24 hours), which is in good accordance with our results (**Table 21**). The values obtained for GAMA however, are distinctly lower, maybe indicating a saturation of CYP 2E1 in humans at doses 1 000 – 6 000 times the median daily dietary exposure.

Acrylamide Serum Toxicokinetics. AA is eliminated very quickly from the blood compartment. Half lives calculated from $^{13}C_3$-AA serum concentrations following administration of 20 µg/kg b.w. $^{13}C_3$-AA were approximately 0.79 hours. This is in good accordance with a value of 0.73 hours determined in mice after administration of 50 mg/kg b.w. $^{13}C_3$-AA (*236*). Additionally, concentrations of free AA in serum were extremely low (<0.5% of dose), indicating a high affinity of AA to hemoglobin and other proteins present in the blood specimens (*43*).

7.5   Conclusions

For the first time, excretion of $^{13}C_3$-AAMA, $^{13}C_3$-GAMA and $^{13}C_3$-AAMA-sulfoxide has been monitored in human urine following single exposure to $^{13}C_3$-AA at doses similar to daily exposure from food. Approximately 70% of the measured metabolites could be assigned to $^{13}C_3$-AAMA, 20% were identified as $^{13}C_3$-AAMA-sulfoxide, and $^{13}C_3$-GAMA accounted for approximately 9%. The obtained biotransformation and toxicokinetics data may help to improve the basis for human risk assessment of dietary AA.

Table 21
Comparison of molar percentages of dose excreted human urine after oral administration of acrylamide.
All information given is referenced to collection periods of 24 h after administration.

Dose	AA	AAMA	AAMA-sulfoxide	GA	GAMA	Glyceramide	$\sum GA^a : \sum AA^b$	Total of dose[c]
3.0 mg/kg[d]	NQ	22.0 ± 5.30	4.20 ± 1.10	0.79 ± 0.24	ND	3.30 ± 1.10	0.16	34.0 ± 5.70
13 µg/kg[e]	ND	45.1	ND	ND	2.8	ND	0.06	47.7
0.5 mg/kg[f]	4.67 ± 1.34	31.2 ± 6.55	8.26 ± 2.39	0.43 ± 0.20	0.82 ± 0.16	ND	0.03	45.6 ± 8.50
1.0 mg/kg[f]	5.02 ± 1.65	34.4 ± 5.21	8.68 ± 1.21	0.63 ± 0.33	0.82 ± 0.11	ND	0.03	49.9 ± 6.30
3.0 mg/kg[f]	3.23 ± 0.49	27.8 ± 7.99	7.25 ± 2.40	0.65 ± 0.21	0.70 ± 0.22	ND	0.03	39.9 ± 9.90
0.5 µg/kg[g]	ND	41.4 ± 3.47	7.19 ± 1.40	ND	3.83 ± 0.78	ND	0.08	52.4 ± 3.59
20 µg/kg[g]	ND	37.4 ± 2.92	6.33 ± 1.77	ND	3.23 ± 0.69	ND	0.07	46.9 ± 3.70

NQ = not quantified, ND = not determined
[a] This sum represents GA + GAMA + Glyceramide.
[b] This sum represents AA + AAMA + AAMA-sulfoxide.
[c] Total amount excreted within 24 hours after exposure calculated as % of dose.
[d] Fennell et al., **2005**. Oral administration male humans.
[e] Boettcher et al., **2006**. Oral administration male human. Excretion within 22 hours following exposure.
[f] Fennell et al., **2006**. Oral administration male humans.
[g] This study. Oral administration male and female humans. Excretion within 22 hours following exposure.

8 Inter-Species Differences: Implications for Risk Assessment

Human risk assessment for genotoxic substances is generally based on data derived from animal studies. However, linear extrapolation of a response in experimental animals down to human exposure may for a number of reasons be inappropriate leading to over- or underestimation of the human risk (*35*). Both in rodents and in humans, AA is metabolized to the DNA-reactive epoxide GA (*39, 142*), which is thought to be responsible for the initiation of cancer in rodents (*199*). Therefore, the extent of bioactivation to GA is an important factor for risk assessment regarding carcinogenicity of AA in humans.

From the experimental data obtained during the toxicokinetics studies in rats and humans, major differences in the pattern of urinary excreted metabolites could be observed. Most interestingly, no AAMA-sulfoxide was found in any of the rat urines. More importantly in terms of risk assessment however, humans excrete much less GAMA than rats. Only 9% of the measured metabolites could be assigned to the genotoxic metabolite in human urine, compared to approximately 49% in rat urine (**Table 22**). Assuming that the major part of GA is conjugated with GSH and excreted as GAMA, it must be concluded that in humans

AA is transformed to GA to a much lower extent. The obtained data confirm previous results (*38, 147, 153*) which indicate that biotransformation via the oxidative pathway seems to be less important in humans than in rodents.

Table 22
Comparison of urinary recovery of acrylamide-derived metabolites following single oral administration of 20 µg/kg b.w. $^{13}C_3$-acrylamie to male Fischer 344 rats and male (n = 3) and female (n = 3) human subjects.

	$^{13}C_3$-AAMA	$^{13}C_3$-AAMA-sulfoxide	$^{13}C_3$-GAMA
Rats (n = 5)			
Sum (0 – 96 h)	19.0 ± 3.1	–	18.5 ± 3.8
% of Total*	50.8 ± 3.4	–	49.2 ± 3.4
% of Dose	33.6 ± 5.0	–	32.7 ± 7.0
Humans (n = 6)			
Sum (0 – 94 h)	$8.96 \times 10^3 \pm 1.77 \times 10^3$	$2.56 \times 10^3 \pm 0.35 \times 10^3$	$1.18 \times 10^3 \pm 0.34 \times 10^3$
% of Total*	70.2 ± 3.1	20.6 ± 4.0	9.2 ± 1.9
% of Dose	49.2 ± 2.8	14.5 ± 3.1	6.4 ± 1.2

Mean values ± standard deviation (n = 5).
* % of all metabolites determined in urine.

A possible explanation for the observed species differences in AA biotransformation may be inter-species variability concerning the activity of the enzymes involved in metabolic conversion. It has been suggested that FMOs are poorly expressed in rats, whereas humans exhibit comparatively high activity of these enzymes (*237*). As FMOs may be involved in *S*-oxygenation of AAMA, this possibly explains the exclusive formation of AAMA-sulfoxide in humans. Species differences have also been reported for CYP 2E1. There is evidence that in mice, the CYP 2E1 mediated epoxidation of AA to GA occurs more efficiently compared to rats (*39*). Following oral administration of 50 mg/kg b.w. AA to rats and mice, only 30% of the excreted metabolites could be assigned to GA and GA-derived biotransformation products in rats, whereas in mice approximately 60% of

metabolites were recovered as GA, GAMA or glyceramide. In this context, a lower sensitivity to the carcinogenic action of AA has been suggested for rats compared to mice, as demonstrated by *in vivo* measurement of micronucleus frequency following i.p. administration of AA (*200*). Lower expression of CYP 2E1 in humans may therefore also be the reason for the decreased amounts of GAMA excreted in human urine compared to rat urine. As a consequence, humans may have a comparatively lower risk for cancer from AA.

The fact that AA is epoxidized to GA to a much lower extent compared to rodents must be incorporated in future risk assessments. A possible approach would be the use of conversion factors in species extrapolation correcting for differences in metabolic rate. An option to avoid species extrapolation in risk assessment is the use of physiologically based toxicokinetic (PBTK) modeling. The biotransformation and toxicokinetics data obtained from our human study may be used for this approach in order to get a better understanding of the actual human risk.

A completely new issue for toxicological concern may arise from the human-only formation of AAMA-sulfoxide. Hitherto unknown toxic effects may be generated by this potentially pro-reactive metabolite which cannot be observed in the rodent model. There have been reports of structurally related compounds (e.g. the sulfoxide of the acrolein mercapturic acid) causing predominantly kidney or bladder toxicity (*238-241*). The mechanism of sulfoxide toxicity is discussed as a nonenzymatic *β*-elimination, resulting in release of the parent compound as a reactive electrophile, which may readily react with proteins in the kidney or bladder. Recently, a small increase in renal cell cancer has been observed in an epidemiological study, suggesting an association between dietary AA and renal cell cancer in humans (*118*). Experimental data on the toxicity of AAMA-sulfoxide is still lacking, but should be included in future risk considerations concerning AA toxicity in humans.

In conclusion, major species differences have been observed concerning biotransformation of AA in rats and humans. Rats excrete about 5 times more GAMA than humans. However, the consequences arising from formation of small amounts of GA in humans are still unclear. Although the general risk for cancer from AA may be smaller in humans compared to rats, no safe level of exposure can be determined for human exposure to AA due to the underlying non-threshold mechanism suggested for DNA-reactive genotoxic substances such as GA. Therefore, taking into consideration all remaining gaps and uncertainties concerning human risk assessment of dietary AA, application of the ALARA principle seems to be the most reasonable approach in dealing with AA at the present.

9 Summary

The widely used chemical acrylamide (AA) has been classified as a probable human carcinogen (*23, 24*). This classification was based on positive results in rodent carcinogenicity studies (*21, 22*) as well as on a number of *in vitro* mutagenicity assays (*16, 127, 242*). In 2002, AA was discovered to be formed during the preparation of starch-containing foods (*28, 29*). According to the latest FDA exposure assessment (2006), the average daily intake has been estimated from AA levels in foodstuffs and from nutritional habits to be around 0.4 µg/kg b.w. with a 90th percentile of 0.95 µg/kg b.w. (*176*). In children and adolescents however, the daily AA intake is about 1.5 times higher, due to lower body weight and differing consumption patterns (*175*). Apart from the diet, humans may be exposed to AA during the production or handling of monomeric AA, from AA residues in polyacrylamides, and from cigarette smoke (*1, 171*).

After oral administration, AA is readily absorbed and distributed throughout the organism (*42, 43*). AA is metabolized to the reactive epoxide glycidamide (GA) via the CYP 450 isoenzyme CYP 2E1. Both, AA and GA are conjugated with glutathione. After enzymatic

processing, the mercapturic acids *N*-Acetyl-*S*-(2-carbamoylethyl)-*L*-cysteine (AAMA) as well as the regioisomers *N*-Acetyl-*S*-(2-carbamoyl-2-hydroxyethyl)-*L*-cysteine (GAMA) and *N*-Acetyl-*S*-(1-carbamoyl-2-hydroxy-ethyl)-*L*-cysteine (iso-GAMA) are excreted with urine (*39*). An additional pathway for the metabolic conversion of GA is the epoxide hydrolase mediated hydrolysis to the diol compound glyceramide (*38, 39*). Following administration of AA at doses exceeding the daily dietary intake by a factor of 1000 - 6000 to human subjects, a new urinary metabolite was found, which could be identified as the *S*-oxide of AAMA (AAMA-sulfoxide) (*38*).

In general, data from animal studies are used for risk assessment of (potential) human carcinogens. However, inter-species differences in toxicodynamics or toxicokinetics, e.g. in biotransformation may lead to under- or overestimation of human risk (*35*). The objective of this work was to establish a highly specific and sensitive analytical method to quantify the major urinary metabolites of AA. Other aims apart from measurements concerning the human background exposure were the evaluation of biotransformation and toxicokinetics of AA in humans and rats after oral administration of $^{13}C_3$-AA. The obtained data was intended to help avoid linear extrapolation from animal models for future risk assessments of AA carcinogenicity.

A hydrophilic interaction liquid chromatography tandem mass spectrometry method (HILIC-MS/MS) using a zwitterionic stationary phase (Zic-HILIC) was developed and validated to quantitate the mercapturic acids of AA and GA as well as AAMA-sulfoxide in human urine. In contrast to reversed phases, the application of Zic-HILIC resulted in efficient retention and separation of these highly polar compounds. Off-line sample work-up was avoided by application of column switching with a Stability BS-C17 trap column prior to the analytical column, thus minimizing interferences with the urinary matrix.

As a proof of concept, spot urine samples of 67 smokers (22 male and 45 female) and 67 nonsmokers (21 male and 46 female) were analyzed for background levels of AAMA, GAMA and AAMA-sulfoxide. Concentrations were above LOQ in all samples. Median concentrations for AAMA, GAMA and AAMA-sulfoxide were 165 µg/L (14 –

1018 µg/L), 25 µg/L (4 – 172 µg/L) and 121 µg/L (16 – 761 µg/L) in smokers and 39 µg/L (6 – 283 µg/L), 9 µg/L (2 – 79 µg/L) and 30 µg/L (7 – 121 µg/L) in nonsmokers. Smokers excreted approximately 4 times more AAMA and AAMA-sulfoxide and 3 times more GAMA than nonsmokers. Statistical evaluation showed that these differences were significant (p <0.001). It was concluded that AAMA-sulfoxide is a major metabolite of AA in humans, as 37% of the metabolites measured in urine could be assigned to this compound. In addition, cigarette smoke was identified as a major contributor to the overall exposure to AA in the general population. As a result, reducing the amount of cigarettes smoked would significantly reduce exposure to AA.

The background exposure to AA derived from the diet was determined in a human biomonitoring study. Six nonsmoking human subjects were asked to collect urine over a period of 72 days in intervals of 8 hours. Median concentrations in the urine samples (n = 54) were 24.0 µg/L (AAMA, 7.8 – 79.8 µg/L), 16.7 µg/L (AAMA-sulfoxide, 6.8 – 70.1 µg/L) and 3.82 µg/L (GAMA, 1.0 – 23.6 µg/L). As AA is rapidly excreted from the human organism and excretion was steady over the observation period, the amount excreted corresponds directly to the amount ingested. Accordingly, a median daily intake of 0.5 µg/kg b.w. AA (0.25 – 0.81 µg/kg b.w.) could be calculated, which is in good agreement with previous estimates. Additionally, significant (p <0.001) interindividual differences, probably due to variations in enzyme activity, were observed concerning the ratio GAMA : (AAMA + AAMA-sulfoxide).

Potential inter-species differences in AA-bioactivation and toxicokinetics were evaluated by single oral administration of doses similar to daily dietary exposure to rats and humans. Male Fischer 344 rats (n = 5/dose group) were administered 20 and 100 µg/kg b.w. $^{13}C_3$-AA in deionized water via oral gavage. Human subjects (n = 3/gender) were orally exposed to 0.5 and 20 µg/kg b.w. $^{13}C_3$-AA in drinking water. Urine samples were collected in intervals for 96 and 94 hours, respectively. Urinary concentrations of $^{13}C_3$-AAMA, $^{13}C_3$-GAMA and $^{13}C_3$-AAMA-sulfoxide were monitored by HILIC-MS/MS. $^{13}C_3$-AAMA-sulfoxide was not detected in rat urine. The recovered urinary metabolites accounted for 66.30% and 70.45% of a 20 and 100 µg/kg b.w. dose in rats and for 71.26% and 70.03% of

a 0.5 and 20 µg/kg b.w. dose in humans. In rats, $^{13}C_3$-AAMA accounted for 33.58% and 38.79% of dose. 32.72% and 31.66% of dose could be recovered as $^{13}C_3$-GAMA. In humans, $^{13}C_3$-AAMA, $^{13}C_3$-GAMA and $^{13}C_3$-AAMA-sulfoxide accounted for 51.74% and 49.16%, 6.32% and 6.41% and 13.20% and 14.46% of the applied dose, respectively.

The obtained data suggest that in humans AA is bioactivated to GA to a considerably smaller extent compared to rats. As a result, humans may be at a much lower risk for cancer mediated by AA than rodents.

10 Zusammenfassung

Die weitverbreitete Chemikalie Acrylamid (AA) wurde als möglicherweise krebserregend im Menschen eingestuft (*23, 24*). Diese Klassifizierung beruhte auf positiven Ergebnissen aus Kanzerogenitätsstudien in Nagern (*21, 22*) sowie einer Reihe von *in vitro* Mutagenitätstests (*16, 127, 242*). Im Jahr 2002 wurde entdeckt, dass AA während der Zubereitung von stärkehaltigen Nahrungsmitteln entsteht (*28, 29*). Nach den neuesten Expositionsabschätzungen der FDA (2006) wurde auf der Basis von AA-Gehalten in Lebensmitteln und Ernährungsgewohnheiten eine tägliche Aufnahme von etwa 0.4 µg/kg KG (Körpergewicht) errechnet. Die 90. Percentile lag bei 0.95 µg/kg KG (*176*). In Kindern und Heranwachsenden ist die tägliche AA Aufnahme jedoch um etwa Faktor 1.5 höher. Dies beruht auf einem vergleichsweise geringeren Körpergewicht und anderen Ernährungsvorlieben (*175*). Außer über die Nahrung können Menschen während der Produktion oder Verarbeitung von monomerem AA, über Rückstände in Polyacrylamiden und über Zigarettenrauch gegenüber AA exponiert sein (*1, 171*).

Nach oraler Gabe wird AA schnell resorbiert und im ganzen Organismus verteilt (*42, 43*). AA wird über das Cytochrom P450 Isoenzym CYP 2E1 in das reaktive Epoxid Glycidamid (GA) umgewandelt. Sowohl AA als auch GA binden an Glutathion. Nach enzymatischer Verstoffwechslung werden die Mercaptursäuren *N*-Acetyl-*S*-(2-carbamoylethyl)-*L*-cystein (AAMA) sowie die Regioisomere *N*-Acetyl-*S*-(2-carbamoyl-2-hydroxyethyl)-*L*-cystein (GAMA) und *N*-Acetyl-*S*-(1-carbamoyl-2-hydroxyethyl)-*L*-cystein (iso-GAMA) mit dem Urin ausgeschieden (*39*). Ein weiterer Weg für die metabolische Umwandlung von GA ist die durch Epoxidhydrolase katalysierte Hydrolyse zum Diol Glyceramid (*38, 39*). Nach der Verabreichung von AA an Menschen in Dosen, die die tägliche Aufnahme über die Nahrung um das 1000 bis 6000-fache überschritten, wurde ein neuer Metabolit im Urin entdeckt, der als das *S*-oxid von AAMA identifiziert werden konnte (*38*).

Im Allgemeinen werden Daten aus Tierstudien für die Risikobewertung von (möglichen) Kanzerogenen im Menschen verwendet. Spezies-Unterschiede bezüglich der Biotransformation können demzufolge zu Unter- oder Überbewertung des Risikos für den Menschen führen (*35*). Das Ziel dieser Arbeit war es, eine hochspezifische und empfindliche analytische Methode für die Quantifizierung der wichtigsten Metaboliten von AA im Urin zu entwickeln. Neben Messungen bezüglich der Hintergrundbelastung im Menschen sollten Biotransformation und Toxikokinetik von AA in Menschen und Ratten nach oraler Gabe von $^{13}C_3$-AA bestimmt werden. Die gewonnenen Daten sollten dazu beitragen, lineare Extrapolation ausgehend von Tiermodellen für zukünftige Risikoabschätzungen zu vermeiden.

Unter Verwendung einer zwitterionischen stationären Phase (Zic-HILIC) wurde eine HILIC-MS/MS Methode für die Quantifizierung der Mercaptursäuren von AA und GA sowie AAMA-sulfoxid entwickelt und validiert. Im Gegensatz zu Umkehrphasen führte die Anwendung von Zic-HILIC zu effizienter Retention und Trennung der hochpolaren Verbindungen. Vorhergehende Probenaufarbeitung wurde vermieden, indem eine Säulenschaltung über eine Stability BS-C17 Trapsäule in das System integriert wurde. Auf diesem Weg wurden Störeinflüsse durch die Urinmatrix minimiert.

Um die Praxistauglichkeit der Methode zu demonstrieren, wurden Spoturine von 67 Rauchern (22 männliche und 45 weibliche) und 67 Nichtrauchern (21 männliche und 46 weibliche) bezüglich der Gehalte an AAMA, GAMA und AAMA-sulfoxid analysiert. Die Konzentrationen waren in allen Proben oberhalb der Nachweisgrenze. Mittlere Konzentrationen für AAMA, GAMA und AAMA-sulfoxid betrugen 165 µg/L (14 – 1 018 µg/L), 25 µg/L (4 – 172 µg/L) und 121 µg/L (16 – 761 µg/L) bei Rauchern und 39 µg/L (6 – 283 µg/L), 9 µg/L (2 – 79 µg/L) und 30 µg/L (7 – 121 µg/L) bei Nichtrauchern. Raucher schieden ungefähr 4 mal mehr AAMA und AAMA-sulfoxid und 3 mal mehr GAMA aus. Die statistische Auswertung zeigte, dass diese Unterschiede signifikant waren (p <0.001). Aus den Ergebnissen wurde der Schluss gezogen, dass AAMA-sulfoxid mit 37% der gemessenen Metabolite im Urin ein Hauptmetabolit von AA im Menschen ist. Desweiteren wurde Zigarettenrauch als eine Hauptquelle von AA in der Allgemeinbevölkerung identifiziert und daraus gefolgert, dass eine Reduktion des Rauchens zu einer signifikanten Erniedrigung der AA Exposition führen würde.

Die Hintergrundbelastung durch AA in der Nahrung wurde in einer Human-Biomonitoring-Studie ermittelt. Sechs Nichtraucher wurden gebeten, über einen Zeitraum von 72 Stunden in Intervallen von 8 Stunden ihren Urin zu sammeln. Die mittleren Urinkonzentrationen (n = 54) betrugen 24.0 µg/L (AAMA, 7.8 – 79.8 µg/L), 16.7 µg/L (AAMA-sulfoxid, 6.8 – 70.1 µg/L) und 3.82 µg/L (GAMA, 1.0 – 23.6 µg/L). Da AA schnell aus dem menschlichen Organismus ausgeschieden wird und die Elimination über den gesamten Beobachtungszeitraum gleichmäßig war, korreliert die ausgeschiedene Menge mit der aufgenommenen Menge. Demzufolge wurde eine mittlere Aufnahme von 0.5 µg/kg KG AA (0.25 – 0.81 µg/kg KG) berechnet. Dieser Wert ist vergleichbar mit bestehenden Schätzungen. Außerdem wurden signifikante (p <0.001) interindividuelle Unterschiede bezüglich des Verhältnisses GAMA : (AAMA + AAMA-sulfoxid) beobachtet, die möglicherweise auf Variationen in der Enzymaktivität zurückzuführen sind.

Mögliche Speziesunterschiede im Bezug auf AA-Bioaktivierung und Toxikokinetik wurden nach einmaliger oraler Gabe von Dosen die der täglichen Aufnahme entsprechen

an Ratten und Menschen untersucht. Männlichen Fischer 344 Ratten (n = 5/Dosisgruppe) wurde per Schlundsonde 20 und 100 µg/kg KG $^{13}C_3$-AA in deionisiertem Wasser verabreicht. Menschlichen Probanden (3 männliche, 3 weibliche) wurde 0.5 und 20 µg/kg KG $^{13}C_3$-AA in Trinkwasser gegeben. Über 96 bzw. 94 Stunden wurde in Intervallen Urin gesammelt. Die Urinkonzentrationen von $^{13}C_3$-AAMA, $^{13}C_3$-GAMA und $^{13}C_3$-AAMA-sulfoxid wurden per HILIC-MS/MS bestimmt. In Rattenurinen konnte kein $^{13}C_3$-AAMA-sulfoxid gefunden werden. Insgesamt wurden 66.30% und 70.45% der 20, bzw. 100 µg/kg KG Dosis im Rattenurin wiedergefunden und 71.26% sowie 70.03% der 0.5, bzw. 20 µg/kg KG Dosis im menschlichen Urin. In den Ratten wurden 33.58% und 38.79% der jeweiligen Dosis als $^{13}C_3$-AAMA und 32.72% und 31.66% als $^{13}C_3$-GAMA ausgeschieden. Im Menschen machten $^{13}C_3$-AAMA, $^{13}C_3$-GAMA und $^{13}C_3$-AAMA-sulfoxid 51.74% und 49.16%, 6.32% und 6.41% sowie 13.20% und 14.46% der verabreichten Dosis aus.

Die gewonnenen Daten deuten darauf hin, dass AA im Menschen im Vergleich zur Ratte zu einem weitaus geringeren Anteil in GA umgewandelt wird. Daraus resultiert, dass das Krebsrisiko durch AA für den Menschen möglicherweise viel geringer ist als für den Nager.

11 References

1.   European Union, Risk Assessment Report-Acrylamide. *Office for Official Publications of the European Communities* **2002,** Luxembourg.

2.   King, D. J.; Noss, R. R., Toxicity of polyacrylamide and acrylamide monomer. *Rev. Environ. Health* **1989,** 8, (1-4), 3-16.

3.   Smith, E. A.; Oehme, F. W., Acrylamide and polyacrylamide: a review of production, use, environmental fate and neurotoxicity. *Rev. Environ. Health* **1991,** 9, (4), 215-28.

4.   Spencer, P. S.; Schaumburg, H. H., A review of acrylamide neurotoxicity. Part II. Experimental animal neurotoxicity and pathologic mechanisms. *Can. J. Neurol. Sci.* **1974,** 1, (3), 152-69.

5.   Spencer, P. S.; Schaumburg, H. H., A review of acrylamide neurotoxicity. Part I. Properties, uses and human exposure. *Can. J. Neurol. Sci.* **1974,** 1, (2), 143-50.

6.   LoPachin, R. M., Acrylamide neurotoxicity: neurological, morhological and molecular endpoints in animal models. *Adv. Exp. Med. Biol.* **2005,** 561, 21-37.

7.   Lopachin, R. M.; Gavin, T., Acrylamide-induced nerve terminal damage: relevance to neurotoxic and neurodegenerative mechanisms. *J. Agric. Food Chem.* **2008,** 56, (15), 5994-6003.

8.   Calleman, C. J.; Wu, Y.; He, F.; Tian, G.; Bergmark, E.; Zhang, S.; Deng, H.; Wang, Y.; Crofton, K. M.; Fennell, T.; Costa, L. G., Relationships between biomarkers of exposure and neurological effects in a group of workers exposed to acrylamide. *Toxicol. Appl. Pharmacol.* **1994,** 126, (2), 361-71.

9.   Goffeng, L. O.; Heier, M. S.; Kjuus, H.; Sjoholm, H.; Sorensen, K. A.; Skaug, V., Nerve conduction, visual evoked responses and electroretinography in tunnel workers previously exposed to acrylamide and N-methylolacrylamide containing grouting agents. *Neurotoxicol. Teratol.* **2008,** 30, (3), 186-94.

10.   Goffeng, L. O.; Kjuus, H.; Heier, M. S.; Alvestrand, M.; Ulvestad, B.; Skaug, V., Colour vision and light sensitivity in tunnel workers previously exposed to acrylamide and N-methylolacrylamide containing grouting agents. *Neurotoxicology* **2008,** 29, (1), 31-9.

11.   Burek, J. D.; Albee, R. R.; Beyer, J. E.; Bell, T. J.; Carreon, R. M.; Morden, D. C.; Wade, C. E.; Hermann, E. A.; Gorzinski, S. J., Subchronic toxicity of acrylamide administered to rats in the drinking water followed by up to 144 days of recovery. *J. Environ. Pathol. Toxicol.* **1980,** 4, (5-6), 157-82.

12.   Dearfield, K. L.; Douglas, G. R.; Ehling, U. H.; Moore, M. M.; Sega, G. A.; Brusick, D. J., Acrylamide: a review of its genotoxicity and an assessment of heritable genetic risk. *Mutat. Res.* **1995,** 330, (1-2), 71-99.

13.   Tyl, R. W.; Friedman, M. A., Effects of acrylamide on rodent reproductive performance. *Reprod. Toxicol.* **2003,** 17, (1), 1-13.

14.   Tyl, R. W.; Friedman, M. A.; Losco, P. E.; Fisher, L. C.; Johnson, K. A.; Strother, D. E.; Wolf, C. H., Rat two-generation reproduction and dominant lethal study of acrylamide in drinking water. *Reprod. Toxicol.* **2000,** 14, (5), 385-401.

15.   Tyl, R. W.; Marr, M. C.; Myers, C. B.; Ross, W. P.; Friedman, M. A., Relationship between acrylamide reproductive and neurotoxicity in male rats. *Reprod. Toxicol.* **2000,** 14, (2), 147-57.

16.   Hashimoto, K.; Tanii, H., Mutagenicity of acrylamide and its analogues in Salmonella typhimurium. *Mutat. Res.* **1985,** 158, (3), 129-33.

17.   Besaratinia, A.; Pfeifer, G. P., Genotoxicity of acrylamide and glycidamide. *J. Natl. Cancer Inst.* **2004,** 96, (13), 1023-9.

18.   Manjanatha, M. G.; Aidoo, A.; Shelton, S. D.; Bishop, M. E.; McDaniel, L. P.; Lyn-Cook, L. E.; Doerge, D. R., Genotoxicity of acrylamide and its metabolite glycidamide administered in drinking water to male and female Big Blue mice. *Environ. Mol. Mutagen.* **2006,** 47, (1), 6-17.

19.   Favor, J.; Shelby, M. D., Transmitted mutational events induced in mouse germ cells following acrylamide or glycidamide exposure. *Mutat. Res.* **2005,** 580, (1-2), 21-30.

20.   Ghanayem, B. I.; Witt, K. L.; El-Hadri, L.; Hoffler, U.; Kissling, G. E.; Shelby, M. D.; Bishop, J. B., Comparison of germ cell mutagenicity in male CYP2E1-null and wild-type mice treated with acrylamide: evidence supporting a glycidamide-mediated effect. *Biol. Reprod.* **2005,** 72, (1), 157-63.

21.   Johnson, K. A.; Gorzinski, S. J.; Bodner, K. M.; Campbell, R. A.; Wolf, C. H.; Friedman, M. A.; Mast, R. W., Chronic toxicity and oncogenicity study on acrylamide incorporated in the drinking water of Fischer 344 rats. *Toxicol. Appl. Pharmacol.* **1986,** 85, (2), 154-68.

22.   Friedman, M. A.; Dulak, L. H.; Stedham, M. A., A lifetime oncogenicity study in rats with acrylamide. *Fundam. Appl. Toxicol.* **1995,** 27, (1), 95-105.

23.   IARC, Monographs on the Evaluation of Carcinogenic Risk to Humans: Acrylamide. *International Agency for the Research on Cancer* **1986,** 39, 41-66.

24.   IARC, Monographs on the Evaluation of Carcinogenic Risk to Humans: Acrylamide. *International Agency for the Research on Cancer* **1994,** 60, pp. 389.

25.   Tornqvist, M., Acrylamide in food: the discovery and its implications: a historical perspective. *Adv. Exp. Med. Biol.* **2005,** 561, 1-19.

26.   Hagmar, L.; Tornqvist, M.; Nordander, C.; Rosen, I.; Bruze, M.; Kautiainen, A.; Magnusson, A. L.; Malmberg, B.; Aprea, P.; Granath, F.; Axmon, A., Health effects of occupational exposure to acrylamide using hemoglobin adducts as biomarkers of internal dose. *Scand. J. Work Environ. Health* **2001,** 27, (4), 219-26.

27.   Bergmark, E., Hemoglobin adducts of acrylamide and acrylonitrile in laboratory workers, smokers and nonsmokers. *Chem. Res. Toxicol.* **1997,** 10, (1), 78-84.

28.   Tareke, E.; Rydberg, P.; Karlsson, P.; Eriksson, S.; Tornqvist, M., Acrylamide: a cooking carcinogen? *Chem. Res. Toxicol.* **2000,** 13, (6), 517-22.

29.   Tareke, E.; Rydberg, P.; Karlsson, P.; Eriksson, S.; Tornqvist, M., Analysis of acrylamide, a carcinogen formed in heated foodstuffs. *J. Agric. Food Chem.* **2002,** 50, (17), 4998-5006.

30.   FAO/WHO, Consultation Report: Health Implications of Acrylamide in Food. *Summary report of a meeting held in Geneva, 25-27 June* **2002,** http://www.who.int/foodsafety/publications/chem/en/acrylamide_full.pdf.

31.   Segerback, D.; Calleman, C. J.; Schroeder, J. L.; Costa, L. G.; Faustman, E. M., Formation of N-7-(2-carbamoyl-2-hydroxyethyl)guanine in DNA of the mouse and the rat following intraperitoneal administration of [14C]acrylamide. *Carcinogenesis* **1995,** 16, (5), 1161-5.

32.   Poirier, M. C., Chemical-induced DNA damage and human cancer risk. *Nat. Rev. Cancer* **2004,** 4, (8), 630-7.

33.   Granath, F.; Ehrenberg, L.; Paulsson, B.; Tornqvist, M., Cancer risk from exposure to occupational acrylamide. *Occup. Environ. Med.* **2001,** 58, (9), 608-9.

34.   Dybing, E.; Sanner, T., Risk assessment of acrylamide in foods. *Toxicol. Sci.* **2003,** 75, (1), 7-15.

35.   European Commission, Technical Guidance Document on Risk Assessment. *European Commission Joint Research Centre* **2003,** Brussels.

36.   MSDS, Material Safety Data Sheet Acrylamide. **2005,** http://www.sciencelab.com/msdsList.php.

37.   Gallagher, S. R., One-dimensional SDS gel electrophoresis of proteins. *Curr. Protoc. Cell Biol.* **2007,** Chapter 6, Unit 6 1.

38.   Fennell, T. R.; Sumner, S. C.; Snyder, R. W.; Burgess, J.; Spicer, R.; Bridson, W. E.; Friedman, M. A., Metabolism and hemoglobin adduct formation of acrylamide in humans. *Toxicol. Sci.* **2005,** 85, (1), 447-59.

39.   Sumner, S. C.; MacNeela, J. P.; Fennell, T. R., Characterization and quantitation of urinary metabolites of [1,2,3-13C]acrylamide in rats and mice using 13C nuclear magnetic resonance spectroscopy. *Chem. Res. Toxicol.* **1992,** 5, (1), 81-9.

40.   Sumner, S. C.; Williams, C. C.; Snyder, R. W.; Krol, W. L.; Asgharian, B.; Fennell, T. R., Acrylamide: a comparison of metabolism and hemoglobin adducts in rodents following dermal, intraperitoneal, oral, or inhalation exposure. *Toxicol. Sci.* **2003,** 75, (2), 260-70.

41.   Doerge, D. R.; Twaddle, N. C.; Boettcher, M. I.; McDaniel, L. P.; Angerer, J., Urinary excretion of acrylamide and metabolites in Fischer 344 rats and B6C3F(1) mice administered a single dose of acrylamide. *Toxicol. Lett.* **2007,** 169, (1), 34-42.

42.   Edwards, P. M., The distribution and metabolism of acrylamide and its neurotoxic analogues in rats. *Biochem. Pharmacol.* **1975,** 24, (13-14), 1277-82.

43.   Miller, M. J.; Carter, D. E.; Sipes, I. G., Pharmacokinetics of acrylamide in Fisher-344 rats. *Toxicol. Appl. Pharmacol.* **1982,** 63, (1), 36-44.

44.   Hinchman, C. A.; Ballatori, N., Glutathione conjugation and conversion to mercapturic acids can occur as an intrahepatic process. *J. Toxicol. Environ. Health* **1994,** 41, (4), 387-409.

45.   Sumner, S. C.; Fennell, T. R.; Moore, T. A.; Chanas, B.; Gonzalez, F.; Ghanayem, B. I., Role of cytochrome P450 2E1 in the metabolism of acrylamide and acrylonitrile in mice. *Chem. Res. Toxicol.* **1999,** 12, (11), 1110-6.

46.   Settels, E.; Bernauer, U.; Palavinskas, R.; Klaffke, H. S.; Gundert-Remy, U.; Appel, K. E., Human CYP2E1 mediates the formation of glycidamide from acrylamide. *Arch. Toxicol.* **2008,** 82, (10), 717-27.

47.   Pearson, R. G.; Songstad, J., Application of the Principle of Hard and Soft Bases to Organic Chemistry. *J. Am. Chem. Soc.* **1967,** 89, (8), 1827-1836.

48.   Hashimoto, K.; Aldridge, W. N., Biochemical studies on acrylamide, a neurotoxic agent. *Biochem. Pharmacol.* **1970,** 19, (9), 2591-604.

49.   Dearfield, K. L.; Abernathy, C. O.; Ottley, M. S.; Brantner, J. H.; Hayes, P. F., Acrylamide: its metabolism, developmental and reproductive effects, genotoxicity, and carcinogenicity. *Mutat. Res.* **1988,** 195, (1), 45-77.

50.   Dixit, R.; Mukhtar, H.; Seth, P. K.; Murti, C. R., Conjugation of acrylamide with glutathione catalysed by glutathione-S-transferases of rat liver and brain. *Biochem. Pharmacol.* **1981,** 30, (13), 1739-44.

51.   Friedman, M., Chemistry, biochemistry, and safety of acrylamide. A review. *J. Agric. Food Chem.* **2003,** 51, (16), 4504-26.

52. Bailey, E.; Farmer, P. B.; Bird, I.; Lamb, J. H.; Peal, J. A., Monitoring exposure to acrylamide by the determination of S-(2-carboxyethyl)cysteine in hydrolyzed hemoglobin by gas chromatography-mass spectrometry. *Anal. Biochem.* **1986,** 157, (2), 241-8.

53. Calleman, C. J.; Bergmark, E.; Costa, L. G., Acrylamide is metabolized to glycidamide in the rat: evidence from hemoglobin adduct formation. *Chem. Res. Toxicol.* **1990,** 3, (5), 406-12.

54. Bergmark, E.; Calleman, C. J.; Costa, L. G., Formation of hemoglobin adducts of acrylamide and its epoxide metabolite glycidamide in the rat. *Toxicol. Appl. Pharmacol.* **1991,** 111, (2), 352-63.

55. Barber, D. S.; LoPachin, R. M., Proteomic analysis of acrylamide-protein adduct formation in rat brain synaptosomes. *Toxicol. Appl. Pharmacol.* **2004,** 201, (2), 120-36.

56. Sickles, D. W.; Sperry, A. O.; Testino, A.; Friedman, M., Acrylamide effects on kinesin-related proteins of the mitotic/meiotic spindle. *Toxicol. Appl. Pharmacol.* **2007,** 222, (1), 111-21.

57. Silvari, V.; Haglund, J.; Jenssen, D.; Golding, B. T.; Ehrenberg, L.; Tornqvist, M., Reaction-kinetic parameters of glycidamide as determinants of mutagenic potency. *Mutat. Res.* **2005,** 580, (1-2), 91-101.

58. Solomon, J. J.; Fedyk, J.; Mukai, F.; Segal, A., Direct alkylation of 2'-deoxynucleosides and DNA following in vitro reaction with acrylamide. *Cancer Res.* **1985,** 45, (8), 3465-70.

59. Testa, B.; Kramer, S. D., The biochemistry of drug metabolism--an introduction: Part 2. Redox reactions and their enzymes. *Chem. Biodivers.* **2007,** 4, (3), 257-405.

60. Lewis, D. F., On the recognition of mammalian microsomal cytochrome P450 substrates and their characteristics: towards the prediction of human p450 substrate specificity and metabolism. *Biochem. Pharmacol.* **2000,** 60, (3), 293-306.

61. Tanaka, E.; Terada, M.; Misawa, S., Cytochrome P450 2E1: its clinical and toxicological role. *J. Clin. Pharm. Ther.* **2000,** 25, (3), 165-75.

62. Novak, R. F.; Woodcroft, K. J., The alcohol-inducible form of cytochrome P450 (CYP 2E1): role in toxicology and regulation of expression. *Arch. Pharm. Res.* **2000,** 23, (4), 267-82.

63. Taubert, D.; Glockner, R.; Muller, D.; Schomig, E., The garlic ingredient diallyl sulfide inhibits cytochrome P450 2E1 dependent bioactivation of acrylamide to glycidamide. *Toxicol. Lett.* **2006,** 164, (1), 1-5.

64. Calleman, C. J.; Stern, L. G.; Bergmark, E.; Costa, L. G., Linear versus nonlinear models for hemoglobin adduct formation by acrylamide and its metabolite glycidamide: implications for risk estimation. *Cancer Epidemiol. Biomarkers Prev.* **1992,** 1, (5), 361-8.

65. Gamboa da Costa, G.; Churchwell, M. I.; Hamilton, L. P.; Von Tungeln, L. S.; Beland, F. A.; Marques, M. M.; Doerge, D. R., DNA adduct formation from acrylamide via conversion to glycidamide in adult and neonatal mice. *Chem. Res. Toxicol.* **2003,** 16, (10), 1328-37.

66. Bjellaas, T.; Olstorn, H. B.; Becher, G.; Alexander, J.; Knutsen, S. H.; Paulsen, J. E., Urinary metabolites as biomarkers of acrylamide exposure in mice following dietary crisp bread administration or subcutaneous injection. *Toxicol. Sci.* **2007,** 100, (2), 374-80.

67. Ingelman-Sundberg, M., Human drug metabolising cytochrome P450 enzymes: properties and polymorphisms. *Naunyn Schmiedebergs Arch Pharmacol* **2004,** 369, (1), 89-104.

68. Bartsch, H.; Nair, U.; Risch, A.; Rojas, M.; Wikman, H.; Alexandrov, K., Genetic polymorphism of CYP genes, alone or in combination, as a risk modifier of tobacco-related cancers. *Cancer Epidemiol. Biomarkers Prev.* **2000,** 9, (1), 3-28.

69. Danko, I. M.; Chaschin, N. A., Association of CYP2E1 gene polymorphism with predisposition to cancer development. *Exp. Oncol.* **2005,** 27, (4), 248-56.

70. Mandl, J.; Banhegyi, G.; Kalapos, M. P.; Garzo, T., Increased oxidation and decreased conjugation of drugs in the liver caused by starvation. Altered metabolism of certain aromatic compounds and acetone. *Chem. Biol. Interact.* **1995,** 96, (2), 87-101.

71. Lucas, D.; Farez, C.; Bardou, L. G.; Vaisse, J.; Attali, J. R.; Valensi, P., Cytochrome P450 2E1 activity in diabetic and obese patients as assessed by chlorzoxazone hydroxylation. *Fundam. Clin. Pharmacol.* **1998,** 12, (5), 553-8.

72. McCarver, D. G.; Byun, R.; Hines, R. N.; Hichme, M.; Wegenek, W., A genetic polymorphism in the regulatory sequences of human CYP2E1: association with increased chlorzoxazone hydroxylation in the presence of obesity and ethanol intake. *Toxicol. Appl. Pharmacol.* **1998,** 152, (1), 276-81.

73. Duale, N.; Bjellaas, T.; Alexander, J.; Becher, G.; Haugen, M.; Paulsen, J. E.; Frandsen, H.; Olesen, P. T.; Brunborg, G., Biomarkers of human exposure to acrylamide and relation to polymorphisms in metabolizing genes. *Toxicol. Sci.* **2009,** (Epub ahead of print).

74. Krueger, S. K.; Williams, D. E., Mammalian flavin-containing monooxygenases: structure/function, genetic polymorphisms and role in drug metabolism. *Pharmacol. Ther.* **2005,** 106, (3), 357-87.

75. Ziegler, D. M., Recent studies on the structure and function of multisubstrate flavin-containing monooxygenases. *Annu. Rev. Pharmacol. Toxicol.* **1993,** 33, 179-99.

76. Kramer, S. D.; Testa, B., The biochemistry of drug metabolism--an introduction: part 6. Inter-individual factors affecting drug metabolism. *Chem. Biodivers.* **2008,** 5, (12), 2465-578.

77. Mitchell, S. C., Flavin mono-oxygenase (FMO)--the 'other' oxidase. *Curr. Drug Metab.* **2008,** 9, (4), 280-4.

78. Ziegler, D. M., Flavin-containing monooxygenases: enzymes adapted for multisubstrate specificity. *Trends Pharmacol. Sci.* **1990,** 11, (8), 321-4.

79. Testa, B.; Kramer, S. D., The biochemistry of drug metabolism--an introduction: part 4. reactions of conjugation and their enzymes. *Chem. Biodivers.* **2008,** 5, (11), 2171-336.

80. Hayes, J. D.; Strange, R. C., Glutathione S-transferase polymorphisms and their biological consequences. *Pharmacology* **2000,** 61, (3), 154-66.

81. Heuner, A.; Dekant, W.; Schwegler, J. S.; Silbernagl, S., Localization and capacity of the last step of mercapturic acid biosynthesis and the reabsorption and acetylation of cysteine S-conjugates in the rat kidney. *Pflugers Arch.* **1991,** 417, (5), 523-7.

82. Anttila, S.; Hirvonen, A.; Husgafvel-Pursiainen, K.; Karjalainen, A.; Nurminen, T.; Vainio, H., Combined effect of CYP1A1 inducibility and GSTM1 polymorphism on histological type of lung cancer. *Carcinogenesis* **1994,** 15, (6), 1133-5.

83. Kihara, M.; Noda, K., Risk of smoking for squamous and small cell carcinomas of the lung modulated by combinations of CYP1A1 and GSTM1 gene polymorphisms in a Japanese population. *Carcinogenesis* **1995,** 16, (10), 2331-6.

84. Hengstler, J. G.; Van der Burg, B.; Steinberg, P.; Oesch, F., Interspecies differences in cancer susceptibility and toxicity. *Drug Metab. Rev.* **1999,** 31, (4), 917-70.

85. Paulsson, B.; Rannug, A.; Henderson, A. P.; Golding, B. T.; Tornqvist, M.; Warholm, M., In vitro studies of the influence of glutathione transferases and epoxide hydrolase on the detoxification of acrylamide and glycidamide in blood. *Mutat. Res.* **2005,** 580, (1-2), 53-9.

86. Testa, B.; Kramer, S. D., The biochemistry of drug metabolism--an introduction: part 3. Reactions of hydrolysis and their enzymes. *Chem. Biodivers.* **2007,** 4, (9), 2031-122.

87. Morisseau, C.; Hammock, B. D., Epoxide hydrolases: mechanisms, inhibitor designs, and biological roles. *Annu. Rev. Pharmacol. Toxicol.* **2005,** 45, 311-33.

88.   Arand, M.; Cronin, A.; Adamska, M.; Oesch, F., Epoxide hydrolases: structure, function, mechanism, and assay. *Methods Enzymol.* **2005,** 400, 569-88.

89.   Benhamou, S.; Reinikainen, M.; Bouchardy, C.; Dayer, P.; Hirvonen, A., Association between lung cancer and microsomal epoxide hydrolase genotypes. *Cancer Res.* **1998,** 58, (23), 5291-3.

90.   Zusterzeel, P. L.; Peters, W. H.; Visser, W.; Hermsen, K. J.; Roelofs, H. M.; Steegers, E. A., A polymorphism in the gene for microsomal epoxide hydrolase is associated with pre-eclampsia. *J. Med. Genet.* **2001,** 38, (4), 234-7.

91.   Lee, W. J.; Brennan, P.; Boffetta, P.; London, S. J.; Benhamou, S.; Rannug, A.; To-Figueras, J.; Ingelman-Sundberg, M.; Shields, P.; Gaspari, L.; Taioli, E., Microsomal epoxide hydrolase polymorphisms and lung cancer risk: a quantitative review. *Biomarkers* **2002,** 7, (3), 230-41.

92.   Lancaster, J. M.; Brownlee, H. A.; Bell, D. A.; Futreal, P. A.; Marks, J. R.; Berchuck, A.; Wiseman, R. W.; Taylor, J. A., Microsomal epoxide hydrolase polymorphism as a risk factor for ovarian cancer. *Mol. Carcinog.* **1996,** 17, (3), 160-2.

93.   Joos, L., COPD and genetics--what's new? *Swiss Med. Wkly.* **2004,** 134, (31-32), 437-9.

94.   Miller, M. S.; Spencer, P. S., The mechanisms of acrylamide axonopathy. *Annu. Rev. Pharmacol. Toxicol.* **1985,** 25, 643-66.

95.   Crofton, K. M.; Padilla, S.; Tilson, H. A.; Anthony, D. C.; Raymer, J. H.; MacPhail, R. C., The impact of dose rate on the neurotoxicity of acrylamide: the interaction of administered dose, target tissue concentrations, tissue damage, and functional effects. *Toxicol. Appl. Pharmacol.* **1996,** 139, (1), 163-76.

96.   Satchell, P. M., Baroreceptor dysfunction in acrylamide axonal neuropathy. *Brain* **1990,** 113 (Pt 1), 167-76.

97.   Abelli, L.; Ferri, G. L.; Astolfi, M.; Conte, B.; Geppetti, P.; Parlani, M.; Dahl, D.; Polak, J. M.; Maggi, C. A., Acrylamide-induced visceral neuropathy: evidence for the involvement of capsaicin-sensitive nerves of the rat urinary bladder. *Neuroscience* **1991,** 41, (1), 311-21.

98.   Calleman, C. J., The metabolism and pharmacokinetics of acrylamide: implications for mechanisms of toxicity and human risk estimation. *Drug. Metab. Rev.* **1996,** 28, (4), 527-90.

99.   Costa, L. G.; Deng, H.; Calleman, C. J.; Bergmark, E., Evaluation of the neurotoxicity of glycidamide, an epoxide metabolite of acrylamide: behavioral, neurochemical and morphological studies. *Toxicology* **1995,** 98, (1-3), 151-61.

100.   LoPachin, R. M.; Balaban, C. D.; Ross, J. F., Acrylamide axonopathy revisited. *Toxicol. Appl. Pharmacol.* **2003,** 188, (3), 135-53.

101.   Sickles, D. W.; Brady, S. T.; Testino, A.; Friedman, M. A.; Wrenn, R. W., Direct effect of the neurotoxicant acrylamide on kinesin-based microtubule motility. *J. Neurosci. Res.* **1996,** 46, (1), 7-17.

102.   Lopachin, R. M.; Barber, D. S.; Geohagen, B. C.; Gavin, T.; He, D.; Das, S., Structure-toxicity analysis of type-2 alkenes: in vitro neurotoxicity. *Toxicol. Sci.* **2007,** 95, (1), 136-46.

103.   Smith, M. K.; Zenick, H.; Preston, R. J.; George, E. L.; Long, R. E., Dominant lethal effects of subchronic acrylamide administration in the male Long-Evans rat. *Mutat. Res.* **1986,** 173, (4), 273-7.

104.   Zenick, H.; Hope, E.; Smith, M. K., Reproductive toxicity associated with acrylamide treatment in male and female rats. *J. Toxicol. Environ. Health* **1986,** 17, (4), 457-72.

105.   Adler, I. D.; Baumgartner, A.; Gonda, H.; Friedman, M. A.; Skerhut, M., 1-Aminobenzotriazole inhibits acrylamide-induced dominant lethal effects in spermatids of male mice. *Mutagenesis* **2000,** 15, (2), 133-6.

106.   Sublet, V. H.; Zenick, H.; Smith, M. K., Factors associated with reduced fertility and implantation rates in females mated to acrylamide-treated rats. *Toxicology* **1989,** 55, (1-2), 53-67.

107.   Costa, L. G.; Deng, H.; Gregotti, C.; Manzo, L.; Faustman, E. M.; Bergmark, E.; Calleman, C. J., Comparative studies on the neuro- and reproductive toxicity of acrylamide and its epoxide metabolite glycidamide in the rat. *Neurotoxicology* **1992,** 13, (1), 219-24.

108.   Sobel, W.; Bond, G. G.; Parsons, T. W.; Brenner, F. E., Acrylamide cohort mortality study. *Br. J. Ind. Med.* **1986,** 43, (11), 785-8.

109.   Collins, J. J.; Swaen, G. M.; Marsh, G. M.; Utidjian, H. M.; Caporossi, J. C.; Lucas, L. J., Mortality patterns among workers exposed to acrylamide. *J. Occup. Med.* **1989,** 31, (7), 614-7.

110.   Marsh, G. M.; Lucas, L. J.; Youk, A. O.; Schall, L. C., Mortality patterns among workers exposed to acrylamide: 1994 follow up. *Occup. Environ. Med.* **1999,** 56, (3), 181-90.

111.   Swaen, G. M.; Haidar, S.; Burns, C. J.; Bodner, K.; Parsons, T.; Collins, J. J.; Baase, C., Mortality study update of Acrylamide workers. *Occup. Environ. Med.* **2007,** 64, (6), 396-401.

112. Marsh, G. M.; Youk, A. O.; Buchanich, J. M.; Kant, I. J.; Swaen, G., Mortality patterns among workers exposed to acrylamide: updated follow up. *J. Occup. Environ. Med.* **2007,** 49, (1), 82-95.

113. Mucci, L. A.; Dickman, P. W.; Steineck, G.; Adami, H. O.; Augustsson, K., Dietary acrylamide and cancer of the large bowel, kidney, and bladder: absence of an association in a population-based study in Sweden. *Br. J. Cancer* **2003,** 88, (1), 84-9.

114. Mucci, L. A.; Adami, H. O.; Wolk, A., Prospective study of dietary acrylamide and risk of colorectal cancer among women. *Int. J. Cancer* **2006,** 118, (1), 169-73.

115. Pelucchi, C.; Galeone, C.; Levi, F.; Negri, E.; Franceschi, S.; Talamini, R.; Bosetti, C.; Giacosa, A.; La Vecchia, C., Dietary acrylamide and human cancer. *Int. J. Cancer* **2006,** 118, (2), 467-71.

116. Pelucchi, C.; Galeone, C.; Maso, L. D.; Talamini, R.; Montella, M.; Ramazzotti, V.; Negri, E.; Franceschi, S.; Vecchia, C. L., Dietary acrylamide and renal cell cancer. *Int. J. Cancer* **2007,** 120, (6), 1376-7.

117. Olesen, P. T.; Olsen, A.; Frandsen, H.; Frederiksen, K.; Overvad, K.; Tjonneland, A., Acrylamide exposure and incidence of breast cancer among postmenopausal women in the Danish Diet, Cancer and Health Study. *Int. J. Cancer.* **2008,** 122, (9), 2094-100.

118. Hogervorst, J. G.; Schouten, L. J.; Konings, E. J.; Goldbohm, R. A.; van den Brandt, P. A., Dietary acrylamide intake and the risk of renal cell, bladder, and prostate cancer. *Am. J. Clin. Nutr.* **2008,** 87, (5), 1428-38.

119. Hogervorst, J. G.; Schouten, L. J.; Konings, E. J.; Goldbohm, R. A.; van den Brandt, P. A., Dietary acrylamide intake is not associated with gastrointestinal cancer risk. *J. Nutr.* **2008,** 138, (11), 2229-36.

120. Hogervorst, J. G.; Schouten, L. J.; Konings, E. J.; Goldbohm, R. A.; van den Brandt, P. A., A prospective study of dietary acrylamide intake and the risk of endometrial, ovarian, and breast cancer. *Cancer Epidemiol. Biomarkers Prev.* **2007,** 16, (11), 2304-13.

121. Bull, R. J.; Robinson, M.; Laurie, R. D.; Stoner, G. D.; Greisiger, E.; Meier, J. R.; Stober, J., Carcinogenic effects of acrylamide in Sencar and A/J mice. *Cancer Res.* **1984,** 44, (1), 107-11.

122. Erdreich, L. S.; Friedman, M. A., Epidemiologic evidence for assessing the carcinogenicity of acrylamide. *Regul. Toxicol. Pharmacol.* **2004,** 39, (2), 150-7.

123. Dourson, M.; Hertzberg, R.; Allen, B.; Haber, L.; Parker, A.; Kroner, O.; Maier, A.; Kohrman, M., Evidence-based dose-response assessment for thyroid tumorigenesis from acrylamide. *Regul. Toxicol. Pharmacol.* **2008,** 52, (3), 264-89.

124.   Bowyer, J. F.; Latendresse, J. R.; Delongchamp, R. R.; Muskhelishvili, L.; Warbritton, A. R.; Thomas, M.; Tareke, E.; McDaniel, L. P.; Doerge, D. R., The effects of subchronic acrylamide exposure on gene expression, neurochemistry, hormones, and histopathology in the hypothalamus-pituitary-thyroid axis of male Fischer 344 rats. *Toxicol. Appl. Pharmacol.* **2008,** 230, (2), 208-15.

125.   Maniere, I.; Godard, T.; Doerge, D. R.; Churchwell, M. I.; Guffroy, M.; Laurentie, M.; Poul, J. M., DNA damage and DNA adduct formation in rat tissues following oral administration of acrylamide. *Mutat. Res.* **2005,** 580, (1-2), 119-29.

126.   Moore, M. M.; Amtower, A.; Doerr, C.; Brock, K. H.; Dearfield, K. L., Mutagenicity and clastogenicity of acrylamide in L5178Y mouse lymphoma cells. *Environ. Mutagen.* **1987,** 9, (3), 261-7.

127.   Adler, I. D.; Ingwersen, I.; Kliesch, U.; el Tarras, A., Clastogenic effects of acrylamide in mouse bone marrow cells. *Mutat. Res.* **1988,** 206, (3), 379-85.

128.   Tsuda, H.; Shimizu, C. S.; Taketomi, M. K.; Hasegawa, M. M.; Hamada, A.; Kawata, K. M.; Inui, N., Acrylamide; induction of DNA damage, chromosomal aberrations and cell transformation without gene mutations. *Mutagenesis* **1993,** 8, (1), 23-9.

129.   Baum, M.; Fauth, E.; Fritzen, S.; Herrmann, A.; Mertes, P.; Merz, K.; Rudolphi, M.; Zankl, H.; Eisenbrand, G., Acrylamide and glycidamide: genotoxic effects in V79-cells and human blood. *Mutat. Res.* **2005,** 580, (1-2), 61-9.

130.   Shipp, A.; Lawrence, G.; Gentry, R.; McDonald, T.; Bartow, H.; Bounds, J.; Macdonald, N.; Clewell, H.; Allen, B.; Van Landingham, C., Acrylamide: review of toxicity data and dose-response analyses for cancer and noncancer effects. *Crit. Rev. Toxicol.* **2006,** 36, (6-7), 481-608.

131.   Mei, N.; Hu, J.; Churchwell, M. I.; Guo, L.; Moore, M. M.; Doerge, D. R.; Chen, T., Genotoxic effects of acrylamide and glycidamide in mouse lymphoma cells. *Food Chem. Toxicol.* **2008,** 46, (2), 628-36.

132.   Doerge, D. R.; da Costa, G. G.; McDaniel, L. P.; Churchwell, M. I.; Twaddle, N. C.; Beland, F. A., DNA adducts derived from administration of acrylamide and glycidamide to mice and rats. *Mutat. Res.* **2005,** 580, (1-2), 131-41.

133.   Yousef, M. I.; El-Demerdash, F. M., Acrylamide-induced oxidative stress and biochemical perturbations in rats. *Toxicology* **2006,** 219, (1-3), 133-41.

134.   Slupphaug, G.; Kavli, B.; Krokan, H. E., The interacting pathways for prevention and repair of oxidative DNA damage. *Mutat. Res.* **2003,** 531, (1-2), 231-51.

135. Annola, K.; Karttunen, V.; Keski-Rahkonen, P.; Myllynen, P.; Segerback, D.; Heinonen, S.; Vahakangas, K., Transplacental transfer of acrylamide and glycidamide are comparable to that of antipyrine in perfused human placenta. *Toxicol. Lett.* **2008,** 182 (1-3), 50-56.

136. Annola, K.; Keski-Rahkonen, P.; Vahakangas, K.; Lehtonen, M., Simultaneous determination of acrylamide, its metabolite glycidamide and antipyrine in human placental perfusion fluid and placental tissue by liquid chromatography-electrospray tandem mass spectrometry. *J. Chromatogr. B Analyt. Technol. Biomed. Life Sci.* **2008,** 876, (2), 191-197.

137. Schettgen, T.; Kutting, B.; Hornig, M.; Beckmann, M. W.; Weiss, T.; Drexler, H.; Angerer, J., Trans-placental exposure of neonates to acrylamide--a pilot study. *Int. Arch. Occup. Environ. Health* **2004,** 77, (3), 213-6.

138. Sorgel, F.; Weissenbacher, R.; Kinzig-Schippers, M.; Hofmann, A.; Illauer, M.; Skott, A.; Landersdorfer, C., Acrylamide: increased concentrations in homemade food and first evidence of its variable absorption from food, variable metabolism and placental and breast milk transfer in humans. *Chemotherapy* **2002,** 48, (6), 267-74.

139. Tareke, E.; Lyn-Cook, B.; Robinson, B.; Ali, S. F., Acrylamide: a dietary carcinogen formed in vivo? *J. Agric. Food Chem.* **2008,** 56, (15), 6020-3.

140. Tornqvist, M.; Kautiainen, A.; Gatz, R. N.; Ehrenberg, L., Hemoglobin adducts in animals exposed to gasoline and diesel exhausts. 1. Alkenes. *J. Appl. Toxicol.* **1988,** 8, (3), 159-70.

141. Vesper, H. W.; Ospina, M.; Meyers, T.; Ingham, L.; Smith, A.; Gray, J. G.; Myers, G. L., Automated method for measuring globin adducts of acrylamide and glycidamide at optimized Edman reaction conditions. *Rapid Commun. Mass Spectrom.* **2006,** 20, (6), 959-64.

142. Bergmark, E.; Calleman, C. J.; He, F.; Costa, L. G., Determination of hemoglobin adducts in humans occupationally exposed to acrylamide. *Toxicol. Appl. Pharmacol.* **1993,** 120, (1), 45-54.

143. Erickson, B. E., Finding acrylamide. *Anal. Chem.* **2004,** 76, (13), 247A-248A.

144. Tornqvist, M.; Fred, C.; Haglund, J.; Helleberg, H.; Paulsson, B.; Rydberg, P., Protein adducts: quantitative and qualitative aspects of their formation, analysis and applications. *J. Chromatogr. B Analyt. Technol. Biomed. Life Sci.* **2002,** 778, (1-2), 279-308.

145. Boettcher, M. I.; Schettgen, T.; Kutting, B.; Pischetsrieder, M.; Angerer, J., Mercapturic acids of acrylamide and glycidamide as biomarkers of the internal exposure to acrylamide in the general population. *Mutat. Res.* **2005,** 580, (1-2), 167-76.

146.   Boettcher, M. I.; Angerer, J., Determination of the major mercapturic acids of acrylamide and glycidamide in human urine by LC-ESI-MS/MS. *J. Chromatogr. B Analyt. Technol. Biomed. Life Sci.* **2005,** 824, (1-2), 283-94.

147.   Fennell, T. R.; Sumner, S. C.; Snyder, R. W.; Burgess, J.; Friedman, M. A., Kinetics of Elimination of Urinary Metabolites of Acrylamide in Humans. *Toxicol. Sci.* **2006,** 93, (2), 256-267.

148.   Urban, M.; Kavvadias, D.; Riedel, K.; Scherer, G.; Tricker, A. R., Urinary mercapturic acids and a hemoglobin adduct for the dosimetry of acrylamide exposure in smokers and nonsmokers. *Inhal. Toxicol.* **2006,** 18, (10), 831-9.

149.   Kellert, M.; Scholz, K.; Wagner, S.; Dekant, W.; Volkel, W., Quantitation of mercapturic acids from acrylamide and glycidamide in human urine using a column switching tool with two trap columns and electrospray tandem mass spectrometry. *J. Chromatogr. A* **2006,** 1131, ((1-2)), 58-66.

150.   Bjellaas, T.; Stolen, L. H.; Haugen, M.; Paulsen, J. E.; Alexander, J.; Lundanes, E.; Becher, G., Urinary acrylamide metabolites as biomarkers for short-term dietary exposure to acrylamide. *Food Chem. Toxicol.* **2007,** 45, (6), 1020-6.

151.   Heudorf, U.; Hartmann, E.; Angerer, J., Acrylamide in children - exposure assessment via urinary acrylamide metabolites as biomarkers. *Int. J. Hyg. Environ. Health* **2009,** 212, (2), 135-41.

152.   Hartmann, E. C.; Boettcher, M. I.; Schettgen, T.; Fromme, H.; Drexler, H.; Angerer, J., Hemoglobin adducts and mercapturic acid excretion of acrylamide and glycidamide in one study population. *J. Agric. Food Chem.* **2008,** 56, (15), 6061-8.

153.   Fuhr, U.; Boettcher, M. I.; Kinzig-Schippers, M.; Weyer, A.; Jetter, A.; Lazar, A.; Taubert, D.; Tomalik-Scharte, D.; Pournara, P.; Jakob, V.; Harlfinger, S.; Klaassen, T.; Berkessel, A.; Angerer, J.; Sorgel, F.; Schomig, E., Toxicokinetics of acrylamide in humans after ingestion of a defined dose in a test meal to improve risk assessment for acrylamide carcinogenicity. *Cancer Epidemiol. Biomarkers Prev.* **2006,** 15, (2), 266-71.

154.   Boettcher, M. I.; Bolt, H. M.; Drexler, H.; Angerer, J., Excretion of mercapturic acids of acrylamide and glycidamide in human urine after single oral administration of deuterium-labelled acrylamide. *Arch. Toxicol.* **2006,** 80, (2), 55-61.

155.   Schettgen, T.; Broding, H. C.; Angerer, J.; Drexler, H., Hemoglobin adducts of ethylene oxide, propylene oxide, acrylonitrile and acrylamide-biomarkers in occupational and environmental medicine. *Toxicol. Lett.* **2002,** 134, (1-3), 65-70.

156.   Schettgen, T.; Weiss, T.; Drexler, H.; Angerer, J., A first approach to estimate the internal exposure to acrylamide in smoking and non-smoking adults from Germany. *Int. J. Hyg. Environ. Health* **2003,** 206, (1), 9-14.

157. Paulsson, B.; Athanassiadis, I.; Rydberg, P.; Tornqvist, M., Hemoglobin adducts from glycidamide: acetonization of hydrophilic groups for reproducible gas chromatography/tandem mass spectrometric analysis. *Rapid Commun. Mass Spectrom.* **2003,** 17, (16), 1859-65.

158. Schettgen, T.; Rossbach, B.; Kutting, B.; Letzel, S.; Drexler, H.; Angerer, J., Determination of haemoglobin adducts of acrylamide and glycidamide in smoking and non-smoking persons of the general population. *Int. J. Hyg. Environ. Health* **2004,** 207, (6), 531-9.

159. Hagmar, L.; Wirfalt, E.; Paulsson, B.; Tornqvist, M., Differences in hemoglobin adduct levels of acrylamide in the general population with respect to dietary intake, smoking habits and gender. *Mutat. Res.* **2005,** 580, (1-2), 157-65.

160. Chevolleau, S.; Jacques, C.; Canlet, C.; Tulliez, J.; Debrauwer, L., Analysis of hemoglobin adducts of acrylamide and glycidamide by liquid chromatography-electrospray ionization tandem mass spectrometry, as exposure biomarkers in French population. *J. Chromatogr. A* **2007,** 1167, (2), 125-34.

161. Bjellaas, T.; Olesen, P. T.; Frandsen, H.; Haugen, M.; Stolen, L. H.; Paulsen, J. E.; Alexander, J.; Lundanes, E.; Becher, G., Comparison of Estimated Dietary Intake of Acrylamide with Haemoglobin Adducts of Acrylamide and Glycidamide. *Toxicol. Sci.* **2007,** 98, (1), 110-7.

162. Vesper, H. W.; Bernert, J. T.; Ospina, M.; Meyers, T.; Ingham, L.; Smith, A.; Myers, G. L., Assessment of the relation between biomarkers for smoking and biomarkers for acrylamide exposure in humans. *Cancer Epidemiol. Biomarkers Prev.* **2007,** 16, (11), 2471-8.

163. Wilson, K. M.; Vesper, H. W.; Tocco, P.; Sampson, L.; Rosen, J.; Hellenas, K. E.; Tornqvist, M.; Willett, W. C., Validation of a food frequency questionnaire measurement of dietary acrylamide intake using hemoglobin adducts of acrylamide and glycidamide. *Cancer Causes Control* **2009,** 20, (3), 269-78.

164. SCF, Opinion of the Scientific Committee on Food on new findings regarding the presence of acrylamide in food. **2002,** http://www.ec.europa.eu/food/fs/sc/scf/out131_en.pdf.

165. DFG/MAK Commission, The MAK Collection for Occupational Health and Safety: Acrylamide. **2007,** http://www.dfg.de/dfg_im_profil/struktur/gremien/senat/kommissionen_ausschuess e/senatskommission_pruefung_arbeitsstoffe/.

166. OSHA, Regulations (Standards - 29 CFR), Table Z-1 Limits for Air Contaminants **2006,** U.S. Department of Labor: Occupational Safety & Health Administration. http://www.osha.gov/pls/oshaweb/owadisp.show_document?p_table=STANDARD S&p_id=9992,

167.   HSE/COSHH, List of approved workplace exposure limits. *Health and Safety Executive: Control of Substances Hazardous to Health* **2007,** http://www.hse.gov.uk/coshh/table1.pdf.

168.   Pantusa, V. P.; Stock, T. H.; Morandi, M. T.; Harrist, R. B.; Afshar, M., Inhalation exposures to acrylamide in biomedical laboratories. *AIHA J. (Fairfax, Va)* **2002,** 63, (4), 468-73.

169.   CIR, Cosmetic Ingredient Review Expert Panel: Amended final report on the safety assessment of polyacrylamide and acrylamide residues in cosmetics. *Int. J. Toxicol.* **2005,** 24 Suppl 2, 21-50.

170.   Schumacher, J. N.; Green, C. R.; Best, F. W.; Newell, M. P., Smoke composition. An extensive investigation of the water-soluble portion of cigarette smoke. *J. Agric. Food Chem.* **1977,** 25, (2), 310-20.

171.   Smith, C. J.; Perfetti, T. A.; Rumple, M. A.; Rodgman, A.; Doolittle, D. J., "IARC group 2A Carcinogens" reported in cigarette mainstream smoke. *Food Chem. Toxicol.* **2000,** 38, (4), 371-83.

172.   Kutting, B.; Uter, W.; Drexler, H., The association between self-reported acrylamide intake and hemoglobin adducts as biomarkers of exposure. *Cancer Causes Control* **2008,** 19, (3), 273-81.

173.   Petersen, B. J.; Tran, N., Exposure to acrylamide: placing exposure in context. *Adv. Exp. Med. Biol.* **2005,** 561, 63-76.

174.   Dybing, E.; Farmer, P. B.; Andersen, M.; Fennell, T. R.; Lalljie, S. P.; Muller, D. J.; Olin, S.; Petersen, B. J.; Schlatter, J.; Scholz, G.; Scimeca, J. A.; Slimani, N.; Tornqvist, M.; Tuijtelaars, S.; Verger, P., Human exposure and internal dose assessments of acrylamide in food. *Food Chem. Toxicol.* **2005,** 43, (3), 365-410.

175.   Mosbach-Schulz, O.; Seiffert, I.; Sommerfeld, C., Abschätzung der Acrylamid-Aufnahme durch hochbelastete Nahrungsmittel in Deutschland (in German). **2003,** Bundesinstitut für Risikobewertung (BfR), Berlin, Germany http://www.bfr.bund.de/cm/208/abschaetzung_der_acrylamid_aufnahme_durch_ho chbelastete_nahrungsmittel_in_deutschland_studie.pdf,

176.   U.S. FDA/CFSAN; DiNovi, M., The 2006 Exposure Assessment for Acrylamide. **2006,** http://www.cfsan.fda.gov/~dms/acryexpo.html.

177.   Svensson, K.; Abramsson, L.; Becker, W.; Glynn, A.; Hellenas, K. E.; Lind, Y.; Rosen, J., Dietary intake of acrylamide in Sweden. *Food Chem. Toxicol.* **2003,** 41, (11), 1581-6.

178.   Boon, P. E.; de Mul, A.; van der Voet, H.; van Donkersgoed, G.; Brette, M.; van Klaveren, J. D., Calculations of dietary exposure to acrylamide. *Mutat. Res.* **2005,** 580, (1-2), 143-55.

179.   Swedish National Food Administration, Analytical methodology and survey results for acrylamide in foods. **2002,** http://www.slv.se/templates/SLV_Page.aspx?id=15879&epslanguage=EN-GB.

180.   Stadler, R. H.; Blank, I.; Varga, N.; Robert, F.; Hau, J.; Guy, P. A.; Robert, M. C.; Riediker, S., Acrylamide from Maillard reaction products. *Nature* **2002,** 419, (6906), 449-50.

181.   BVL, Acrylamide: Signalvalues 7th Evaluation (in German). **2008,** Bundesamt für Verbraucherschutz und Lebensmittelsicherheit, Germany. http://www.bvl.bund.de/cln_007/nn_493422/DE/01__Lebensmittel/03__UnerwStof feUndOrganismen/04__Acrylamid/05__Signalwerte/signalwerte__node.html__nnn =true,

182.   Mottram, D. S.; Wedzicha, B. L.; Dodson, A. T., Acrylamide is formed in the Maillard reaction. *Nature* **2002,** 419, (6906), 448-9.

183.   Zyzak, D. V.; Sanders, R. A.; Stojanovic, M.; Tallmadge, D. H.; Eberhart, B. L.; Ewald, D. K.; Gruber, D. C.; Morsch, T. R.; Strothers, M. A.; Rizzi, G. P.; Villagran, M. D., Acrylamide formation mechanism in heated foods. *J. Agric. Food Chem.* **2003,** 51, (16), 4782-7.

184.   Yaylayan, V. A.; Wnorowski, A.; Perez Locas, C., Why asparagine needs carbohydrates to generate acrylamide. *J. Agric. Food Chem.* **2003,** 51, (6), 1753-7.

185.   Stadler, R. H.; Robert, F.; Riediker, S.; Varga, N.; Davidek, T.; Devaud, S.; Goldmann, T.; Hau, J.; Blank, I., In-depth mechanistic study on the formation of acrylamide and other vinylogous compounds by the maillard reaction. *J. Agric. Food Chem.* **2004,** 52, (17), 5550-8.

186.   Yaylayan, V. A.; Locas, C. P.; Wnorowski, A.; O'Brien, J., The role of creatine in the generation of N-methylacrylamide: a new toxicant in cooked meat. *J. Agric. Food Chem.* **2004,** 52, (17), 5559-65.

187.   Ehling, S.; Hengel, M.; Shibamoto, T., Formation of acrylamide from lipids. *Adv. Exp. Med. Biol.* **2005,** 561, 223-33.

188.   Casado, F. J.; Montano, A., Influence of Processing Conditions on Acrylamide Content in Black Ripe Olives. *J. Agric. Food Chem.* **2008,** 56, (6), 2021-7.

189.   Granvogl, M.; Koehler, P.; Latzer, L.; Schieberle, P., Development of a stable isotope dilution assay for the quantitation of glycidamide and its application to foods and model systems. *J. Agric. Food Chem.* **2008,** 56, (15), 6087-92.

190. Tritscher, A. M., Human health risk assessment of processing-related compounds in food. *Toxicol. Lett.* **2004,** 149, (1-3), 177-86.

191. Friedman, M.; Levin, C. E., Review of methods for the reduction of dietary content and toxicity of acrylamide. *J. Agric. Food Chem.* **2008,** 56, (15), 6113-40.

192. Surdyk, N.; Rosen, J.; Andersson, R.; Aman, P., Effects of asparagine, fructose, and baking conditions on acrylamide content in yeast-leavened wheat bread. *J. Agric. Food Chem.* **2004,** 52, (7), 2047-51.

193. FAO/WHO, Summary and Conclusions from the 64th meeting of the Joint FAO/WHO Expert Committee on Food Additives (JECFA). **2005,** http://www.who.int/entity/ipcs/food/jecfa/summaries/summary_report_64_final.pdf

194. Barlow, S.; Renwick, A. G.; Kleiner, J.; Bridges, J. W.; Busk, L.; Dybing, E.; Edler, L.; Eisenbrand, G.; Fink-Gremmels, J.; Knaap, A.; Kroes, R.; Liem, D.; Muller, D. J.; Page, S.; Rolland, V.; Schlatter, J.; Tritscher, A.; Tueting, W.; Wurtzen, G., Risk assessment of substances that are both genotoxic and carcinogenic report of an International Conference organized by EFSA and WHO with support of ILSI Europe. *Food Chem. Toxicol.* **2006,** 44, (10), 1636-50.

195. Kroes, R.; Renwick, A. G.; Cheeseman, M.; Kleiner, J.; Mangelsdorf, I.; Piersma, A.; Schilter, B.; Schlatter, J.; van Schothorst, F.; Vos, J. G.; Wurtzen, G., Structure-based thresholds of toxicological concern (TTC): guidance for application to substances present at low levels in the diet. *Food Chem Toxicol* **2004,** 42, (1), 65-83.

196. EFSA, Opinion of the Scientific Committee on a request from the European Food Safety Authority (EFSA) related to a harmonized approach for risk assessment of substances which are both genotoxic and carcinogenic (Request No. EFSA-Q-2004-020). **2005,** http://www.efsa.europa.eu/EFSA/Scientific_Opinion/sc_op_ej282_gentox_en3.pdf.

197. Sanner, T.; Dybing, E.; Willems, M. I.; Kroese, E. D., A simple method for quantitative risk assessment of non-threshold carcinogens based on the dose descriptor T25. *Pharmacol. Toxicol.* **2001,** 88, (6), 331-41.

198. Ruden, C., Acrylamide and cancer risk--expert risk assessments and the public debate. *Food Chem. Toxicol.* **2004,** 42, (3), 335-49.

199. Ghanayem, B. I.; Witt, K. L.; Kissling, G. E.; Tice, R. R.; Recio, L., Absence of acrylamide-induced genotoxicity in CYP2E1-null mice: evidence consistent with a glycidamide-mediated effect. *Mutat. Res.* **2005,** 578, (1-2), 284-97.

200. Paulsson, B.; Grawe, J.; Tornqvist, M., Hemoglobin adducts and micronucleus frequencies in mouse and rat after acrylamide or N-methylolacrylamide treatment. *Mutat. Res.* **2002,** 516, (1-2), 101-11.

201. Paulsson, B.; Kotova, N.; Grawe, J.; Henderson, A.; Granath, F.; Golding, B.; Tornqvist, M., Induction of micronuclei in mouse and rat by glycidamide, genotoxic metabolite of acrylamide. *Mutat. Res.* **2003,** 535, (1), 15-24.

202. NTP, Report on Carcinogens, Eleventh Edition: Acrylamide CAS No. 79-06-1. **2005,** http://www.ntp.niehs.nih.gov/ntp/roc/eleventh/profiles/s003acry.pdf.

203. Ruden, C., Principles and practices of health risk assessment under current EU regulations. *Regul. Toxicol. Pharmacol.* **2006,** 44, (1), 14-23.

204. Dybing, E.; O'Brien, J.; Renwick, A. G.; Sanner, T., Risk assessment of dietary exposures to compounds that are genotoxic and carcinogenic--an overview. *Toxicol. Lett.* **2008,** 180, (2), 110-7.

205. O'Brien, J.; Renwick, A. G.; Constable, A.; Dybing, E.; Muller, D. J.; Schlatter, J.; Slob, W.; Tueting, W.; van Benthem, J.; Williams, G. M.; Wolfreys, A., Approaches to the risk assessment of genotoxic carcinogens in food: a critical appraisal. *Food Chem Toxicol* **2006,** 44, (10), 1613-35.

206. USEPA, Assessment of Health Risks from Exposure to Acrylamide. *US Environmental Protection Agency* **1985,** Washington DC: Office of Toxic Substances.

207. WHO, Acrylamide. Environmental Health Criteria 49. **1985,** World Health Organization, Geneva.

208. van Welie, R. T.; van Dijck, R. G.; Vermeulen, N. P.; van Sittert, N. J., Mercapturic acids, protein adducts, and DNA adducts as biomarkers of electrophilic chemicals. *Crit Rev Toxicol* **1992,** 22, (5-6), 271-306.

209. Needham, L. L.; Calafat, A. M.; Barr, D. B., Uses and issues of biomonitoring. *Int. J. Hyg. Environ. Health.* **2007,** 210, (3-4), 229-38.

210. Calafat, A. M.; Needham, L. L., Factors affecting the evaluation of biomonitoring data for human exposure assessment. *Int. J. Androl.* **2008,** 31, (2), 139-43.

211. Fennell, T. R.; Friedman, M. A., Comparison of acrylamide metabolism in humans and rodents. *Adv. Exp. Med. Biol.* **2005,** 561, 109-16.

212. Linden, J. C.; Lawhead, C. L., Liquid Chromatography of Saccharides. *J. Chrom.* **1975,** 105, (1), 125-133.

213. Palmer, J. K., A Versatile for Sugar Analysis via Liquid Chromatography. *Anal. Lett.* **1975,** 8, (3), 215-224.

214. Hemstrom, P.; Irgum, K., Hydrophilic interaction chromatography. *J. Sep. Sci.* **2006,** 29, (12), 1784-821.

215. Cubbon, S.; Bradbury, T.; Wilson, J.; Thomas-Oates, J., Hydrophilic interaction chromatography for mass spectrometric metabonomic studies of urine. *Anal. Chem.* **2007,** 79, (23), 8911-8.

216. Idborg, H.; Zamani, L.; Edlund, P. O.; Schuppe-Koistinen, I.; Jacobsson, S. P., Metabolic fingerprinting of rat urine by LC/MS Part 1. Analysis by hydrophilic interaction liquid chromatography-electrospray ionization mass spectrometry. *J. Chromatogr. B Analyt. Technol. Biomed. Life Sci.* **2005,** 828, (1-2), 9-13.

217. Boersema, P. J.; Mohammed, S.; Heck, A. J., Hydrophilic interaction liquid chromatography (HILIC) in proteomics. *Anal. Bioanal. Chem.* **2008,** 391, (1), 151-9.

218. Lindegardh, N.; Hanpithakpong, W.; Wattanagoon, Y.; Singhasivanon, P.; White, N. J.; Day, N. P., Development and validation of a liquid chromatographic-tandem mass spectrometric method for determination of oseltamivir and its metabolite oseltamivir carboxylate in plasma, saliva and urine. *J. Chromatogr. B Analyt. Technol. Biomed. Life Sci.* **2007,** 859, (1), 74-83.

219. Qin, F.; Zhao, Y. Y.; Sawyer, M. B.; Li, X. F., Hydrophilic Interaction Liquid Chromatography-Tandem Mass Spectrometry Determination of Estrogen Conjugates in Human Urine. *Anal. Chem.* **2008,** 80, (9), 3404-3411.

220. Alpert, A. J., Hydrophilic-interaction chromatography for the separation of peptides, nucleic acids and other polar compounds. *J. Chromatogr.* **1990,** 499, 177-96.

221. Guo, Y.; Gaiki, S., Retention behavior of small polar compounds on polar stationary phases in hydrophilic interaction chromatography. *J. Chromatogr. A* **2005,** 1074, (1-2), 71-80.

222. Maisch, A., Sability BS-C23 - eine spezielle C18-Phase mit positiver Ladung (in German). *GIT-Fachz. Lab.* **2001,** 21, (4), 370-371.

223. Wang, X.; Li, W.; Rasmussen, H. T., Orthogonal method development using hydrophilic interaction chromatography and reversed-phase high-performance liquid chromatography for the determination of pharmaceuticals and impurities. *J. Chromatogr. A* **2005,** 1083, (1-2), 58-62.

224. Cech, N. B.; Enke, C. G., Practical implications of some recent studies in electrospray ionization fundamentals. *Mass. Spectrom. Rev.* **2001,** 20, (6), 362-87.

225. Scholz, K.; Dekant, W.; Volkel, W.; Pahler, A., Rapid detection and identification of N-acetyl-L-cysteine thioethers using constant neutral loss and theoretical multiple reaction monitoring combined with enhanced product-ion scans on a linear ion trap mass spectrometer. *J. Am. Soc. Mass Spectrom.* **2005,** 16, (12), 1976-84.

226. Sugiyama, S.; Ohigashi, S.; Sawa, R.; Hayashi, H., Selective preparation of 2,3-epoxypropanamide and ist facile conversion to 2,3-dihydroxypropanamide with acidic resins. *Bull. Chem. Soc. Jpn.* **1989,** 62, 3202-3206.

227. Werner, M.; Birner, G.; Dekant, W., Sulfoxidation of mercapturic acids derived from tri- and tetrachloroethene by cytochromes P450 3A: a bioactivation reaction in addition to deacetylation and cysteine conjugate beta-lyase mediated cleavage. *Chem. Res. Toxicol.* **1996,** 9, (1), 41-9.

228. Adam, W.; Bialas, J.; Hadjiarapoglou, L., A Convenient Preparation of Acetone Solutions of Dimethyldioxirane. *Chem. Ber.* **1991,** 124, (10), 2377.

229. Li, W.; Cohen, L. H., Quantitation of endogenous analytes in biofluid without a true blank matrix. *Anal. Chem.* **2003,** 75, (21), 5854-9.

230. Boersema, P. J.; Divecha, N.; Heck, A. J.; Mohammed, S., Evaluation and optimization of ZIC-HILIC-RP as an alternative MudPIT strategy. *J. Proteome Res.* **2007,** 6, (3), 937-46.

231. Bjellaas, T.; Janak, K.; Lundanes, E.; Kronberg, L.; Becher, G., Determination and quantification of urinary metabolites after dietary exposure to acrylamide. *Xenobiotica* **2005,** 35, (10-11), 1003-18.

232. Besaratinia, A.; Pfeifer, G. P., A review of mechanisms of acrylamide carcinogenicity. *Carcinogenesis* **2007,** 28, ((3)), 519-28.

233. Hopkins, J. M.; Evans, H. J., Cigarette smoke-induced DNA damage and lung cancer risks. *Nature* **1980,** 283, (5745), 388-90.

234. Dekant, W.; Volkel, W., Human exposure to bisphenol A by biomonitoring: methods, results and assessment of environmental exposures. *Toxicol. Appl. Pharmacol.* **2008,** 228, (1), 114-34.

235. Doerge, D. R.; Young, J. F.; McDaniel, L. P.; Twaddle, N. C.; Churchwell, M. I., Toxicokinetics of acrylamide and glycidamide in Fischer 344 rats. *Toxicol. Appl. Pharmacol.* **2005,** 208, (3), 199-209.

236. Twaddle, N. C.; McDaniel, L. P.; Gamboa da Costa, G.; Churchwell, M. I.; Beland, F. A.; Doerge, D. R., Determination of acrylamide and glycidamide serum toxicokinetics in B6C3F1 mice using LC-ES/MS/MS. *Cancer Lett.* **2004,** 207, (1), 9-17.

237. Dekant, W.; Vamvakas, S., Toxikologie - Eine Einführung für Chemiker, Biologen und Pharmazeuten. *2nd Edition* **2005,** Elsevier, Spektrum Akademischer Verlag, Heidelberg, Germany, (in German), pp. 79.

238.   Hashmi, M.; Vamvakas, S.; Anders, M. W., Bioactivation mechanism of S-(3-oxopropyl)-N-acetyl-L-cysteine, the mercapturic acid of acrolein. *Chem. Res. Toxicol.* **1992,** 5, (3), 360-5.

239.   Lash, L. H.; Sausen, P. J.; Duescher, R. J.; Cooley, A. J.; Elfarra, A. A., Roles of cysteine conjugate beta-lyase and S-oxidase in nephrotoxicity: studies with S-(1,2-dichlorovinyl)-L-cysteine and S-(1,2-dichlorovinyl)-L-cysteine sulfoxide. *J. Pharmacol. Exp. Ther.* **1994,** 269, (1), 374-83.

240.   Ramu, K.; Fraiser, L. H.; Mamiya, B.; Ahmed, T.; Kehrer, J. P., Acrolein mercapturates: synthesis, characterization, and assessment of their role in the bladder toxicity of cyclophosphamide. *Chem. Res. Toxicol.* **1995,** 8, (4), 515-24.

241.   Sheffels, P.; Schroeder, J. L.; Altuntas, T. G.; Liggitt, H. D.; Kharasch, E. D., Role of cytochrome P4503A in cysteine S-conjugates sulfoxidation and the nephrotoxicity of the sevoflurane degradation product fluoromethyl-2,2-difluoro-1-(trifluoromethyl)vinyl ether (compound A) in rats. *Chem. Res. Toxicol.* **2004,** 17, (9), 1177-89.

242.   Shelby, M. D.; Cain, K. T.; Cornett, C. V.; Generoso, W. M., Acrylamide: induction of heritable translocation in male mice. *Environ. Mutagen.* **1987,** 9, (4), 363-8.

Acknowledgments

First of all, I would like to thank Prof. Dr. Wolfgang Dekant for offering the fascinating topic of my PhD thesis, the opportunity to present the results of my work at the SOT meeting in Seattle, and for his continuing support.

I would like to thank Prof. Dr. Ulrike Holzgrabe for supervising my PhD thesis on behalf of the Faculty for Chemistry and Pharmacy.

PD Dr. Angela Mally, thank you for many constructive comments concerning my dissertation.

Financial support by the DFG (Deutsche Forschungsgemeinschaft) is thankfully acknowledged.

Silvia Baumann and Silvia Wagner, thank you for kindly providing the student urine samples for background measurements.

Kay Ansorg, thank you for your help with the syntheses of the standards and the NMR-measurements.

Dr. Ute Schauer, Ursula Tatsch and Heike Keim-Heusler, thank you for your assisstance with the animal and human studies.

Nataly Bittner, lots of thanks for your patience during my HILIC measurements.

Maximilian Sieber and Dr. Marco Kellert, thanks for many fruitful discussions on all sorts of chemical (and other) issues, the valuable tips for the syntheses and your help with the NMR-interpretation.

Paul Wanek, thank you for your help with innumerable computer problems.

All my colleagues from the work groups of Prof. Dekant, PD Dr. Mally and Prof. Lutz, thanks for a great working atmosphere.

Karo, Andi, Marco, Silvia, Max, Paul, Ute, Ursula, Heike, Hannelore and Nataly, thank you for 3 ½ unforgettable years, lots of fun during diverse roof parties, boat trips and evenings at the bowling center, and for your friendship.

Special thanks go to my family for always believing in me.

Finally, Robert, thank you for your great support and encouragement during the last years.

B

Publications

Kopp E.K., Dekant W.

Toxicokinetics of acrylamide in rats and humans following single oral administration of low doses.

Toxicol. Appl. Pharmacol. **2009,** 235, (2), 135-42.

Kopp E.K., Sieber M., Kellert M., Dekant, W.

Rapid and sensitive HILIC-ESI-MS/MS quantitation of polar metabolites of acrylamide in human urine using column switching with an online trap column.

J. Agric. Food Chem. **2008,** 56, (21), 9828-34.

Abstracts

Kopp E.K., Dekant W.

Acrylamide: Toxicokinetics in humans.

The Toxicologist **2008**, 102, (1), 479

SOT **2008**, Seattle, USA

Scholz K., Kopp E.K., Paehler A., Voelkel W.

Detection of reactive intermediates as thioethers generated by neutrophils and microsomes using a specific constant neutral loss scan combined with product ion scans.

ASMS **2006**, Seattle, USA